F^{19} NUCLEAR SPIN-LATTICE RELAXATION IN LIQUIDS

Thesis by

Thomas Edmund Burke

In Partial Fulfillment of the Requirements

For the Degree of

Doctor of Philosophy

California Institute of Technology

Pasadena, California

1969

(Submitted October 16, 1968)

To Ann

ACKNOWLEDGMENTS

I wish to express my sincere appreciation to Professor Sunney I. Chan for his assistance and encouragement during all phases of this work.

I am indebted to Dr. Alan S. Dubin for his many contributions to the instrumental and computational aspects of this Thesis and for his continued willingness to help "thresh out" ideas.

Financial support from the following sources is gratefully acknowledged: the California Institute of Technology, E. I. Du Pont de Nemours & Co., the National Science Foundation, and the Shell Companies Foundation.

Finally, I especially wish to thank my wife Ann for her continued encouragement and empathy throughout the course of my graduate education.

ABSTRACT

A magnetic nucleus located on an internal rotor is coupled not only to the rotational magnetic field generated by the end-over-end rotation of the molecule but also to the magnetic field produced by the internal rotation of the top relative to the frame. Although the importance of the nuclear-spin—internal-rotation coupling as a nuclear spin-lattice relaxation mechanism has been established, the nature of the stochastic processes which modulate the interaction and are thereby responsible for the coupling between the nuclear spin system and the lattice has yet to be determined.

In order to elucidate the nature of the dynamical processes that provide the coupling between the nuclear spins and the lattice, both the temperature and viscosity dependence of the fluorine spin-lattice relaxation times for benzotrifluoride have been examined. The viscosity dependence of the fluorine spin-lattice relaxation times for hexafluorobutyne-2 has also been investigated.

It is concluded that the rotational magnetic fields generated by overall and internal rotation are fluctuating independently and that each field is described by a distinct correlation time. It is also concluded that, contrary to previous proposals, the nuclear-spin—internal-rotation interaction contributes significantly to the spin-lattice relaxation of the methyl group protons in molecules such as toluene.

The effect of solvents on the relaxation of rigid molecules has also been investigated. The fluorine spin-lattice relaxation times of CF_3CH_2Cl, CF_3CH_2Br, CF_3CH_2I, and CF_3CCl_3 have been measured as a function of concentration in various solvents, both polar and non-polar. The intramolecular contributions to relaxation, arising from the intramolecular dipolar and spin—overall-rotation interactions, were analyzed in terms of various correlation time models. It is found that the Hill[1] model for molecular reorientation provides the only satisfactory explanation for all the results; it is also found that, in general, the efficacy of the Hill model is dependent upon the mutual viscosity.

---

(1) N. E. Hill, Proc. Phys. Soc. (London) B67, 149 (1954).

TABLE OF CONTENTS

I. GENERAL INTRODUCTION

In Part I we discuss the basic elements of nuclear spin-lattice relaxation: the theory of relaxation, relaxation mechanisms, correlation times, and the measurement of relaxation times. The discussion of the theory of relaxation is of a cursory nature because the subject has been exhaustively treated by numerous authors including Abragam[1] and Slichter.[2]

1. The Theory of Nuclear Spin-Lattice Relaxation

When a macroscopic system containing a large number N of nuclear spins is placed in a static magnetic field $\vec{H}_0 = H_0\vec{k}$, it acquires an equilibrium magnetization $\vec{M}_0$ that is directed along the field axis

$$\vec{M}_0 = \frac{N\gamma^2\hbar^2 I(I+1)\vec{H}_0}{3kT} \tag{1}$$

The motion of the magnetization in a time-dependent magnetic field $\vec{H}(t) = H_0\vec{k} + \vec{H}_1(t)$ can be described by the Bloch equation[3]

$$\frac{d\vec{M}}{dt} = \gamma\vec{M}\times\vec{H}(t) - \frac{(M_x\vec{i} + M_y\vec{j})}{T_2} - \frac{(M_z - M_0)\vec{k}}{T_1} \tag{2}$$

The term $\gamma\vec{M}\times\vec{H}(t)$ is the equation of motion of the magnetization for an ensemble of free spins. The second and third terms are damping terms which describe the tendency of $\vec{M}$ to return to the thermal

equilibrium value: in the absence of $\vec{H}_1(t)$ the x- and y-components of $\vec{M}$ vanish exponentially with a time constant T_2, the transverse relaxation time; the z-component approaches $\vec{M}_0$ exponentially with a time constant T_1, the longitudinal, or "spin-lattice", relaxation time.

Bloembergen, Purcell, and Pound[4] have proposed that nuclear spin-lattice relaxation is caused by the fluctuating magnetic and electric fields that are associated with random molecular motions. Relaxation occurs when the Fourier spectra of the fluctuating fields contain non-vanishing components at the frequency corresponding to a transition between two levels of the nuclear spin system: these transitions serve to bring the spin system into thermal equilibrium with the "lattice". Thus spin-lattice relaxation times are directly related to transition probabilities. Slichter[2] has presented a very detailed treatment of the calculation of transition probabilities by the density matrix method. The results are summarized here.

A non-stationary perturbation $\mathcal{H}_1(t)$ causes transitions between the states k and m at a rate

$$W_{km} = \hbar^{-2} \int_{-\infty}^{\infty} \overline{\langle m|\mathcal{H}_1(t+\tau)|k\rangle \langle k|\mathcal{H}_1(t)|m\rangle} e^{-i\omega_{mk}\tau} d\tau \qquad (3)$$

where $\omega_{mk} = \hbar^{-1}(E_m - E_k)$ and the bar denotes an ensemble average. The integral, customarily represented by $J_{mk}(\omega)$, is the Fourier transform of the autocorrelation function

$$\overline{\langle m|\mathcal{H}_1(t+\tau)|k\rangle \langle k|\mathcal{H}_1(t)|m\rangle} \equiv G_{mk}(\tau)$$

of the randomly fluctuating Hamiltonian and is the spectral energy density of the fluctuation at the transition frequency ω_{mk}. Equation (3) may be written

$$W_{km} = \hbar^{-2} J_{mk}(\omega) = \hbar^{-2} \int_{-\infty}^{\infty} G_{mk}(\tau) e^{-i\omega_{mk}\tau} d\tau \qquad (4)$$

The calculation of W_{km} requires information on the physical basis of the field fluctuation and on the form of the autocorrelation function $G_{mk}(\tau)$. When the fluctuation can be described by a one-dimensional Markoffian process, as is generally assumed, the autocorrelation function has an exponential time dependence[5]

$$G_{mk}(\tau) = \overline{|\langle m|\mathcal{H}_1(0)|k\rangle|^2}\, e^{-|\tau|/\tau_c} \qquad (5)$$

where the correlation time τ_c is a "characteristic time" for the fluctuation and $G_{mk}(\tau)$ is a measure of its persistence. There are several realistic models which lead to an exponential autocorrelation function of the form of Eq. (5) and which correspond to situations frequently encountered in practice. Rotational Brownian motion in the limit of viscous damping will have this property.[6] Any two-valued randomly jumping function will also lead to an exponentially decaying autocorrelation function.[7]

For spin-$\frac{1}{2}$ systems, the rate of longitudinal relaxation $(1/T_1) = 2W_{km}$ is given by

$$(1/T_1) = \frac{1}{\hbar^2} \left| \langle m \left| \mathcal{H}_1(0) \right| k \rangle \right|^2 \frac{4\tau_c}{1 + \omega_{mk}^2 \tau_c^2} \qquad (6)$$

Thus the rate of relaxation is proportional to the matrix elements of the perturbing Hamiltonian and to the time scale of the fluctuations.

2. Relaxation Mechanisms

Various interactions can give rise to the fluctuating perturbations that are manifested as relaxation mechanisms. Several examples are the tensor dipolar interactions, the spin-rotational interaction, the electric quadrupole coupling, and the anisotropic chemical shift. The first two examples, the only relaxation mechanisms relevant to the experiments described in this Thesis, are discussed in Section II. 2.

3. Correlation Times[8,9]

The response of a macroscopic system to a time-dependent perturbation is often a manifestation of the dynamics of the system at the molecular level. A number of macroscopic phenomena can be interpreted in terms of correlation times which are characteristic times for fluctuations of the dynamical variables of the system. In this section we shall give several examples of applications of correlation times and then we shall discuss some of the models used for their calculation.

The first example, of prime importance because of a wealth of experimental data, is dielectric relaxation. The response of a

dipolar liquid to a time-dependent electric field $\vec{E} = \vec{E}_0 \cos(\omega t)$ is related to the complex dielectric constant $\epsilon^*(\omega)$:

$$\epsilon^*(\omega) = \epsilon_\infty + \frac{\epsilon_0 - \epsilon_\infty}{1 + i\omega\tau_M} \tag{7}$$

where ϵ_0 and ϵ_∞ are, respectively, the static and high-frequency (optical) dielectric constants; τ_M, the macroscopic relaxation time, is the time required for the macroscopic polarization of the dielectric to decrease to 1/e of its initial value. The macroscopic relaxation is related to molecular relaxation by the expression

$$\tau_M = F\tau_\mu \tag{8}$$

where $F(1 \lesssim F \lesssim 2)$ is an internal-field factor[10] and τ_μ is the correlation time which characterizes the fluctuations in the orientation of the dipole vector $\vec{\mu}$.

The second example that we shall consider is light scattering. When polarized light is scattered from molecules having non-spherical polarizability, the Raman spectrum contains a broad, depolarized component known as the Rayleigh "wing".[11] The depolarized component arises from thermal fluctuations in the orientation of the anisotropic polarizability tensor α. It has been shown that the normalized intensity distribution $I(\Delta\omega)$ of the Rayleigh "wing" is

$$I(\Delta\omega) = \frac{1}{1 + (\Delta\omega)^2 \tau_\alpha^2} \tag{9}$$

where $\Delta\omega$ is the frequency shift and τ_α is the correlation time associated with fluctuations in the orientation of $\underset{\sim}{\alpha}$.[12]

The concept of correlation times has also been applied to such problems as, for example, the analysis of infra-red band shapes[13] and the absorption and dispersion of ultrasonic waves;[14] however, we shall not delve into these particular problems. As our final example we shall consider nuclear spin relaxation. The rate of longitudinal relaxation due to the dipolar interaction between two identical nuclei on the same molecule is

$$(1/T_1) = A\left[\frac{\tau_2}{1 + \omega^2 \tau_2^2} + \frac{4\tau_2}{1 + 4\omega^2 \tau_2^2}\right] \tag{10}$$

where A is related to the properties of the nuclei, and τ_2 is the correlation time characterizing the reorientation of the dipolar coupling tensor.[4]

The above phenomena are related in the sense that molecular rotation is involved in each case. Thus it is not unreasonable that the correlation times τ_α, τ_μ, and τ_2 are related. For the particular case where the Debye model is valid (vide infra), the correlation time associated with the reorientation of an ℓ-rank tensor is[4]

$$\tau = \frac{8\pi a^3 \eta}{\ell(\ell + 1)\, kT} \tag{11}$$

Since the dipole moment vector is a first-rank tensor and the polarizability and dipolar coupling tensors are second-rank, Eq. (11) gives

$$\tau_2 = \tau_\alpha = \tfrac{1}{3}\tau_\mu \tag{12}$$

When molecular reorientation proceeds by large-angle jumps instead of by the Brownian rotational diffusion of the Debye model, the above relations [Eq. (11) and (12)] are not valid:[15] instead

$$\tau_2 = \tau_\alpha = \tau_\mu \tag{13}$$

However, Powles[16] has pointed out that many liquids, including highly associated liquids such as water, reorient by small-angle jumps (viz., Brownian rotational diffusion) and that $\tau_\mu/\tau_2 \approx 3$.

Since most studies of rotational relaxation have been effected by dielectric relaxation techniques, most of the literature of correlation times pertains directly to τ_μ and only indirectly to τ_2. In what follows we shall exercise care to distinguish between the two. For our use we shall assume that $\tau_2 \equiv \tfrac{1}{3}\tau_\mu$.

3. 1. Molecular Reorientation

The reorientation of polar molecules in solution is influenced by randomly fluctuating torques and by the viscous damping of the solvent. Cole[17] has presented a particularly simple analysis of the

problem: we shall describe his analysis here. The equation of motion for θ--the angle through which the dipole turns--is assumed to be

$$I\ddot{\theta} = -\xi\dot{\theta} + N(t) \tag{14}$$

where I is the moment of inertia, ξ is the rotational friction coefficient, and N(t) represents the randomly fluctuating torques. Multiplying by θ and substituting $\theta\ddot{\theta} = d(\theta\dot{\theta})/dt - \dot{\theta}^2$ and $\theta\dot{\theta} = d(\frac{1}{2}\theta^2)/dt$ gives

$$I\frac{d^2}{dt^2}(\tfrac{1}{2}\theta^2) + \xi\frac{d}{dt}(\tfrac{1}{2}\theta^2) = I\dot{\theta}^2 + \theta N(t) \tag{15}$$

Introducing the equilibrium distribution function f_0 and taking an average over ensembles leads to

$$I\frac{d^2}{dt^2}\langle\tfrac{1}{2}\theta^2 f_0\rangle + \xi\frac{d}{dt}\langle\tfrac{1}{2}\theta^2 f_0\rangle = \langle I\dot{\theta}^2 f_0\rangle + \langle\theta N(t) f_0\rangle \tag{16}$$

where $\langle\frac{1}{2}f_0\theta^2\rangle$ represents the mean square angular displacement. Cole neglects the average over $\theta N(t)$ and replaces the average kinetic energy $\frac{1}{2}I\dot{\theta}^2$ by kT. The resulting differential equation has the following solution for the initial conditions $\theta = \dot{\theta} = 0$ at $t = 0$:

$$\langle\tfrac{1}{2}f_0\theta^2\rangle = \frac{2kT}{\xi}\left\{t - \frac{I}{\xi}\left[1 - \exp(-\xi t/I)\right]\right\} \tag{17}$$

In the limit where the time is short or the rotational friction coefficient ξ is small, $\langle\frac{1}{2}\theta^2 f_0\rangle \approx (kT/I)t^2$: the reorientation is independent of the surrounding media and is dynamically coherent. In

the limit where the time is long or ξ is large, $\langle \frac{1}{2}\theta^2 f_0 \rangle \approx (2kT/\xi)t$: the reorientation is dominated by viscous damping.

Since the correlation time τ_μ is the time per unit angular displacement, the correlation time in the "inertial limit" is

$$\tau_\mu \approx (I/kT)^{\frac{1}{2}} \tag{18}$$

which, except for a numerical factor, is the same as the result obtained by Steele.[18, 19] The correlation time at the other extreme--the "Debye limit"--is

$$\tau_\mu \approx \xi/2kT \tag{19}$$

which is precisely Debye's result.[20]

3. 2. Correlation Times in the Debye Limit

Since the rotational friction coefficient is related to the total potential V acting on a molecule[18]

$$\xi^2 = (2I/\pi) \langle \partial^2 V/\partial\theta^2 \rangle \tag{20}$$

the evaluation of ξ is an intractable problem. Debye interpreted ξ by assuming that the polar molecules behave as spheres of radius a in a hydrodynamic fluid of macroscopic viscosity η. Stokes' law of classical hydrodynamics leads to

$$\xi = 8\pi a^3 \eta \tag{21}$$

and therefore

$$\tau_\mu = \frac{4\pi a^3 \eta}{kT} \tag{22}$$

Thus the correlation time is proportional to the molecular size and to the macroscopic viscosity.

Meakins[21] has studied the effect of the relative sizes of the polar solute and the non-polar solvent upon the applicability of the Debye equation [Eq. (22)]. He has concluded that the Debye formula gives good agreement with experimental correlation times when the volume of the solute molecule is at least three times larger than that of the solvent molecule. When the solute and solvent volumes are more nearly equal, the calculated value of τ_μ is much greater than the experimental value.

The expected proportionality between τ_μ and the viscosity does not always hold. Smyth[22] has presented examples where a 500-fold increase of viscosity causes less than a 2-fold change in the correlation time. Numerous results support the contention that viscosity effects are important only when rotational motion causes a displacement of solvent molecules.

Although the Debye model for the molecular relaxation time τ_μ has proved to be useful, in many cases it is inadequate. There have been two general approaches to the shortcomings of the Debye model: attempts have been made to account for deviations of molecular shape from spherical symmetry; there have been efforts to

redefine the viscous interaction in terms of the properties of both the solute and solvent molecules.

Symmetry Corrections. -- For the general case of a non-spherical molecule there is a correlation time associated with reorientation about each of the principal inertial axes:

$$(\tau_\mu)_i = \frac{4\pi abc\,\eta f_i}{kT} \qquad i = a, b, c \tag{23}$$

where a, b, and c are the dimensions of the rotational ellipsoid and f_i is a numerical factor that is a function of the orientation of the molecular dipole with respect to the particular axis.[23]

Viscosity Corrections. -- Wirtz and co-workers[24, 25] have attempted to account for the finite size of the solvent molecules. They consider that the spherical solute molecule, of radius a_2, creates a hydrodynamic disturbance which propagates through concentric layers of solvent molecules, of radius a_1. Because of what amounts to "slippage" between adjacent layers, the rotational friction coefficient ξ is reduced by a factor f:

$$f = \left[(6a_1/a_2) + (1 + a_1/a_2)^{-3}\right]^{-1} \tag{24}$$

Thus the dipolar correlation time is

$$\tau_\mu = \frac{4\pi a_2^{\,3}\eta}{kT}\left[(6a_1/a_2) + (1 + a_1/a_2)^{-3}\right]^{-1} \tag{25}$$

Hill[26] has proposed that the dipolar correlation time should

not be related to the viscosity of the solvent, but rather to a mutual viscosity which is a measure of the interaction between the solute and solvent. The mutual viscosity η_{12} can be obtained from the viscosity η_m of a solution composed of liquids whose viscosities are η_1 and η_2 (subscripts 1 and 2 refer, respectively, to the solvent and the solute):

$$\eta_m = x_1^2 \eta_1 \frac{\sigma_1}{\sigma_m} + x_2^2 \eta_2 \frac{\sigma_2}{\sigma_m} + 2x_1 x_2 \eta_{12} \frac{\sigma_{12}}{\sigma_m} \qquad (26)$$

where the σ's are intermolecular distances and the x's are mole fractions. For a dilute solution of a polar molecule in a non-polar solvent, the Hill theory gives

$$\tau_\mu = 3\left[\frac{I_{12} I_2}{I_{12} + I_2}\right]\left[\frac{m_1 + m_2}{m_1 m_2}\right] \frac{\eta_{12} \sigma_{12}}{kT} \qquad (27)$$

where I_2 is the moment of inertia of the polar solute molecule, I_{12} is the moment of inertia of the solvent molecule about the center of mass of the solute molecule at the instant of collision, and the m's are the molecular masses.

Meakins[27] has tested the validity of the Hill equation for dilute solutions and has concluded that, particularly for small solute molecules, the agreement between experiment and theory is better for the Hill equation than for the Debye equation. However, the agreement between the Hill theory and experiment vanishes rapidly as the sizes of the solute and solvent molecules deviate from equality; the

agreement is also dependent upon the symmetry of the rotational ellipsoid of the solute molecule: the Hill equation works best when the rotational ellipsoid is reasonably symmetrical ($I_A \approx I_B \approx I_C$).[28]

Hase[29] has developed a microscopic-viscosity expression that is dependent upon the molecular volumes of the solvent and solute (V_1 and V_2, respectively):

$$\eta_{micro} = \eta \exp(-A V_1/V_2) \tag{28}$$

where A is an empirical parameter. Thus

$$\tau_\mu = \frac{4\pi a_2^3 \eta}{kT} \exp(-A V_1/V_2) \tag{29}$$

Illinger[9] has pointed out that the relative values of the molecular volumes V_1 and V_2 serve as a useful classification scheme. For $V_2 \gg V_1$, the solvent may be considered to be a continuous medium and, therefore, the Debye equation [Eq. (22)] or the Fischer equation [Eq. (23)] may be expected to hold for, respectively, spherical and ellipsoidal molecules. As V_2 approaches V_1, but with V_2 larger than V_1, the coarse-grained nature of the solvent must be considered, but a hydrodynamic model is still applicable. Illinger suggests that the Wirtz equation could be valid in this case. When $V_2 \approx V_1$ the hydrodynamic model is clearly unacceptable and a detailed picture of the solute-solvent interaction must be considered. If this interaction is adequately described by the mutual viscosity, Hill's equation might

be valid in this range. Illinger has cautioned that such a classification is a broad generalization and that the detailed assessment of the validity of the various models is highly tenuous.

3.3. Correlation Times in the Inertial Limit

Equation (20) shows that the rotational friction coefficient goes to zero when the potential energy V is independent of the angle. Thus the reorientation is dynamically coherent and the correlation time depends only on the moment of inertia I and the absolute temperature T. Steele[18, 19] has shown that in the inertial limit the correlation time for nuclear-spin relaxation is given by

$$\tau_2 = \tfrac{1}{2}(\pi I/3kT)^{\frac{1}{2}} \qquad (30)$$

Equation (30) predicts that the intramolecular dipolar contribution to relaxation is independent of the molecular environment. Although the inertial model might be expected to hold for specific examples such as CH_4, CF_4, and the internal motion of the CF_3 top in benzotrifluoride, there is a considerable body of experimental evidence that indicates that the inertial model is not usually applicable. For example, the correlation times τ_2 for benzene and cyclohexane--two of the examples cited by Steele in support of his theory--have been shown to be dependent upon the solvent[30] and also upon the hydrostatic pressure[31]: clearly, the inertial model cannot account for either observation.

3. 4. Relaxation as a Rate Process

Kauzmann[32] has questioned the validity of the concept of a rotational friction coefficient based on a diffusion model of infinitesimal reorientations. He has argued that the temperature dependence observed in dielectric relaxation indicates that at some stage of the reorientation process a molecule is forced to wait until it has acquired, by thermal fluctuations, a considerable amount of energy in excess of the average thermal energy of the medium. In other words, reorientation most likely proceeds by discrete jumps between stable orientations separated by a potential barrier. The correlation time, equal to the reciprocal of the jump frequency, is given by

$$\tau_\mu = (h/kT) \exp (\Delta G^{\neq}/RT) \qquad (31)$$

where $\Delta G^{\neq}$ is the free energy of activation. The reaction rate theory of molecular reorientation has not been extensively utilized because, as was previously pointed out, comparisons of τ_2 and τ_μ indicate that many liquids, including highly associated liquids such as water, reorient by Brownian rotational motion.

4. Pulsed Nuclear Magnetic Resonance[33]

4. 1. The Rotating Coordinate System[34]

The equation of motion for a nuclear moment $\vec{\mu}$ in a static

magnetic field $\vec{H}_0$ is

$$\vec{\mu} \times \vec{H}_0 = \gamma \hbar \vec{I} \times \vec{H}_0 = \hbar \frac{d\vec{I}}{dt} \tag{32}$$

It is both convenient and customary to transform the equation of motion from the laboratory fixed reference frame to a coordinate system rotating with an angular velocity $\vec{\omega}$. If $\partial/\partial t$ represents differentiation with respect to the rotating coordinate system, the rate of change of $\vec{I}$ with respect to the fixed coordinate system is

$$\frac{d\vec{I}}{dt} = \frac{\partial \vec{I}}{\partial t} + \vec{\omega} \times \vec{I} \tag{33}$$

Rearranging Eq. (33) gives

$$\frac{\partial \vec{I}}{\partial t} = \gamma \vec{I} \times (\vec{H}_0 + \vec{\omega}/\gamma) = \gamma \vec{I} \times \vec{H}_r \tag{34}$$

where $\vec{H}_r$ is the effective magnetic field in the rotating coordinate system.

In a typical nuclear magnetic resonance experiment a circularly polarized magnetic field $\vec{H}_1$, perpendicular to the static field $\vec{H}_0$, rotates about H_0 with an angular frequency ω. Since $\vec{H}_1$ appears as a constant field in the rotating coordinate system, the axes of the rotating frame can be selected such that

$$\vec{H}_0 = H_0 \vec{k}' \qquad \vec{\omega} = -\omega \vec{k}' \qquad \vec{H}_1 = H_1 \vec{i}' \tag{35}$$

Then in the rotating coordinate system

$$\vec{H}_r = (H_0 - \frac{\omega}{\gamma})\vec{k}' + H_1\vec{i}' = \frac{1}{\gamma}(\omega_0 - \omega)\vec{k}' + H_1\vec{i}' \tag{36}$$

At resonance $\omega = \omega_0$; therefore

$$\vec{H}_r = H_1\vec{i}' \tag{37}$$

and the equation of motion of the nuclear moment in the rotating frame becomes

$$\frac{\partial \vec{I}}{\partial t} = \gamma H_1 \vec{I} \times \vec{i}' \tag{38}$$

The nuclear moment precesses about the x′-axis with an angular frequency $\omega = \gamma H_1$. Since the total magnetic moment $\vec{M}$ of the sample is the vector sum of all the individual nuclear moments, $\vec{M}$ behaves similarly: i. e., at resonance

$$\frac{\partial \vec{M}}{\partial t} = \gamma H_1 \vec{M} \times \vec{i}' \tag{39}$$

The preceding treatment is somewhat artificial because it was based on the assumption that the static magnetic field can be described by a single value H_0. In fact, the magnetic field is best described in terms of a normalized distribution function f(H) centered at $H = H_0$. The field deviation may be described by $\Delta H = H - H_0$; σ, the root mean

square deviation, is a measure of the width of the distribution. The vector sum of all the nuclear moments in the incremental region H to H + dH, an isochromat, is M(H)dH. We shall represent the isochromats by $M(\Delta\omega)$ in order to emphasize the distribution of precessional frequencies imposed by the field distribution.

Introducing these concepts, the effective field in the rotating coordinate system becomes

$$\vec{H}_r = (\Delta H + H_0 - \frac{\omega}{\gamma})\vec{k}' + H_1 \vec{i}' = \frac{1}{\gamma}(\Delta\omega + \omega_0 - \omega)\vec{k}' + H_1 \vec{i}' \qquad (40)$$

At resonance

$$\vec{H}_r = \Delta H \vec{k}' + H_1 \vec{i}' \qquad (41)$$

and the equation of motion for the isochromats is

$$\frac{\partial \vec{M}(\Delta\omega)}{\partial t} = \gamma \Delta H \vec{M}(\Delta\omega) \times \vec{k}' + \gamma H_1 \vec{M}(\Delta\omega) \times \vec{i}' \qquad (42)$$

In a pulsed nuclear magnetic resonance experiment, the magnitude of the radio-frequency field is large ($H_1 \gg \sigma$) and the duration of the rf pulse t_w is short ($t_w \ll 1/\gamma\sigma$); therefore, Eq. (42) gives

$$\frac{\partial \vec{M}(\Delta\omega)}{\partial t} = \gamma H_1 \vec{M}(\Delta\omega) \times \vec{i}' \qquad (43)$$

The motion of the isochromats is identical to the motion of the total magnetic moment: precession about the x′-axis with an angular

frequency $\omega = \gamma H_1$.

In a time t_w the total magnetic moment will precess through an angle $\theta = \gamma H_1 t_w$. A "90° pulse" ($\gamma H_1 t_w = \frac{\pi}{2}$) turns the total magnetic moment through 90° from the z'-axis to the y'-axis; a "180° pulse" ($\gamma H_1 t_w = \pi$) inverts the total magnetization aligning it along the -z'-axis. Pulsed nuclear magnetic resonance experiments are performed with combinations of 90° and 180° pulses.

4. 2. Free Induction Decay

A 90° pulse applied to a system initially at thermal equilibrium aligns the total magnetic moment along the y'-axis. Since the y'-axis is rotating with an angular frequency $\omega_o = \gamma H_o$ with respect to the laboratory coordinates, a signal is induced in the receiver coil of the spectrometer. The frequency of the signal is ω_o, and the amplitude of the signal is proportional to $M_{y'}$, the component of magnetization along the y'-axis. As viewed in the rotating coordinate system, the isochromats begin to fan out

$$\frac{\partial \vec{M}}{\partial t} (\Delta\omega) = \gamma \Delta H \vec{M}(\Delta\omega) \times \vec{k}' \qquad (44)$$

with some leading the y'-axis and others lagging. Consequently, $M_{y'}$ decreases with time (Figure 1). This phenomenon is commonly referred to as the free induction decay.

If, for example, the frequency distribution is described by an error function, the free induction decay envelope has the form

FIGURE 1

The formation of a free induction decay as viewed from the rotating reference frame. Initially the net magnetization is in its equilibrium position (A) parallel to the direction of the static magnetic field H_0. The pulsed rf field H_1 causes the magnetization to rotate (B) rapidly about H_1. At the end of the 90° pulse the net magnetic moment is in the equatorial plane (C). Following the removal of H_1, the variations in H_0 over the sample cause the isochromats to slowly fan out (D).

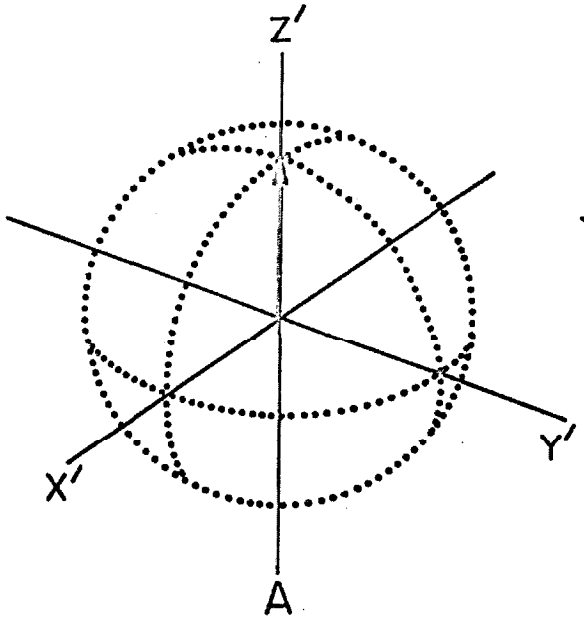
Z′
X′
Y′
A

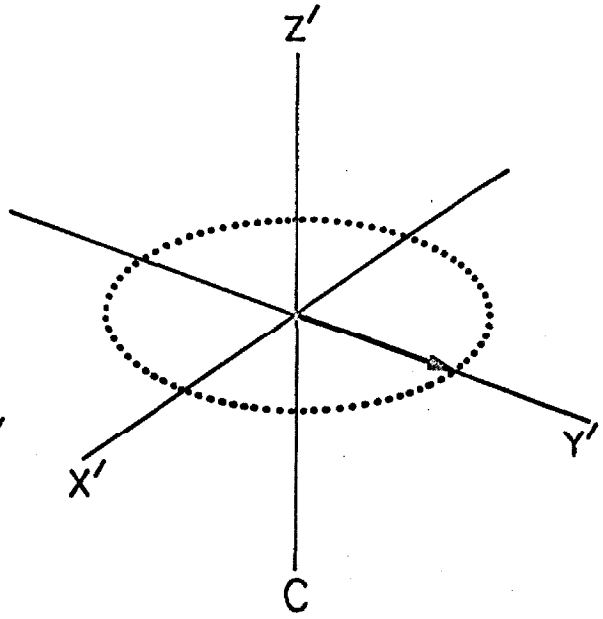
Z′
X′
Y′
C

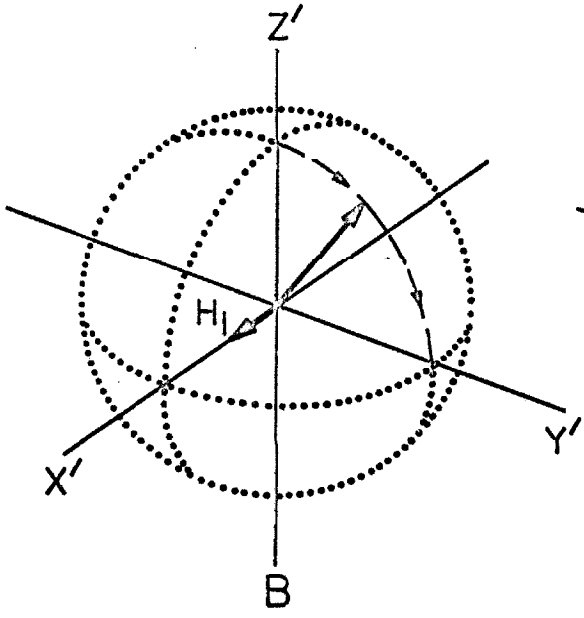
Z′
H
X′
Y′
B

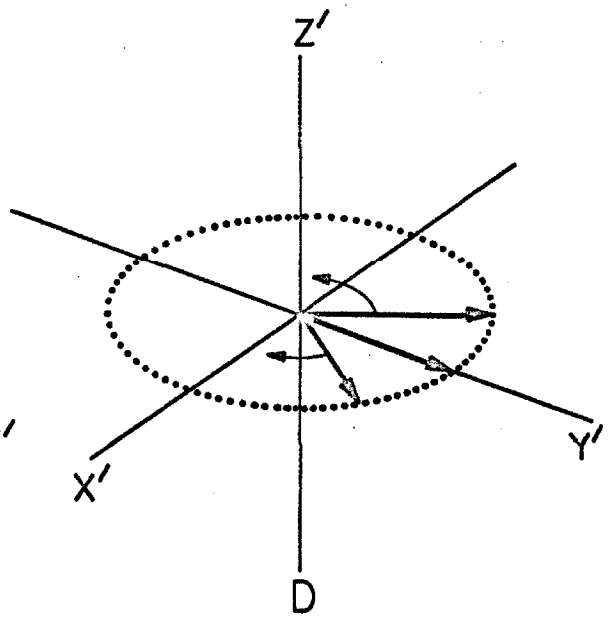
Z′
X′
Y′
D

$$V(t) \propto M_{y'} = M_0 \exp(-\sigma^2\gamma^2t^2/2) \tag{45}$$

The time required for $M_{y'}$, and consequently the induced signal, to decay to e^{-1} of its original value is T_2^*. This may be regarded as the characteristic time for the isochromats to lose phase coherence. For the error function frequency distribution

$$T_2^* = \frac{\sqrt{2}}{\gamma\sigma} \tag{46}$$

It should be noted that there is no free induction decay following a 180° pulse because there is no component of the total magnetic moment along the y'-axis.

4. 3. Measurement of the Longitudinal Relaxation Time

The measurement of the longitudinal or spin-lattice relaxation time is initiated by a 180° pulse which inverts the total magnetic moment. Due to interactions of the spin system with the "lattice" the magnetization begins to return to its equilibrium value. If, after a time t_1, a 90° pulse is applied, the residual magnetization $M_Z(t_1)$ is rotated into the x'y'-plane where it induces a signal (again assuming an error function frequency distribution)

$$V(t) \propto M_{y'} = M_Z(t_1) \exp(-\gamma^2\sigma^2t^2/2) \tag{47}$$

i. e. , the initial amplitude of the free induction decay signal is proportional to the residual magnetization at time t_1. The spin system is allowed to equilibrate, and the process is repeated with a delay t_2. The induced signal is

$$V(t) \propto M_{y'} = M_z (t_2) \exp (-\gamma^2 \sigma^2 t^2/2) \tag{48}$$

If the process is repeated many times and the results are superimposed, one obtains a "multiple exposure" as in Figure 2. The initial amplitudes of the free induction decays are the loci of a curve

$$M_z(t) = M_0[1 - 2 \exp (-t/T_1)] \tag{49}$$

where T_1 is the characteristic time for spin-lattice relaxation. When $M_z(t) = 0$, $t = \tau_{null}$, there is no free induction decay. τ_{null} is customarily determined in a "T_1" experiment, but the two times are related

$$\tau_{null} = T_1 \ell n 2 \tag{50}$$

FIGURE 2

A "multiple exposure" of a sequence of T_1 experiments.

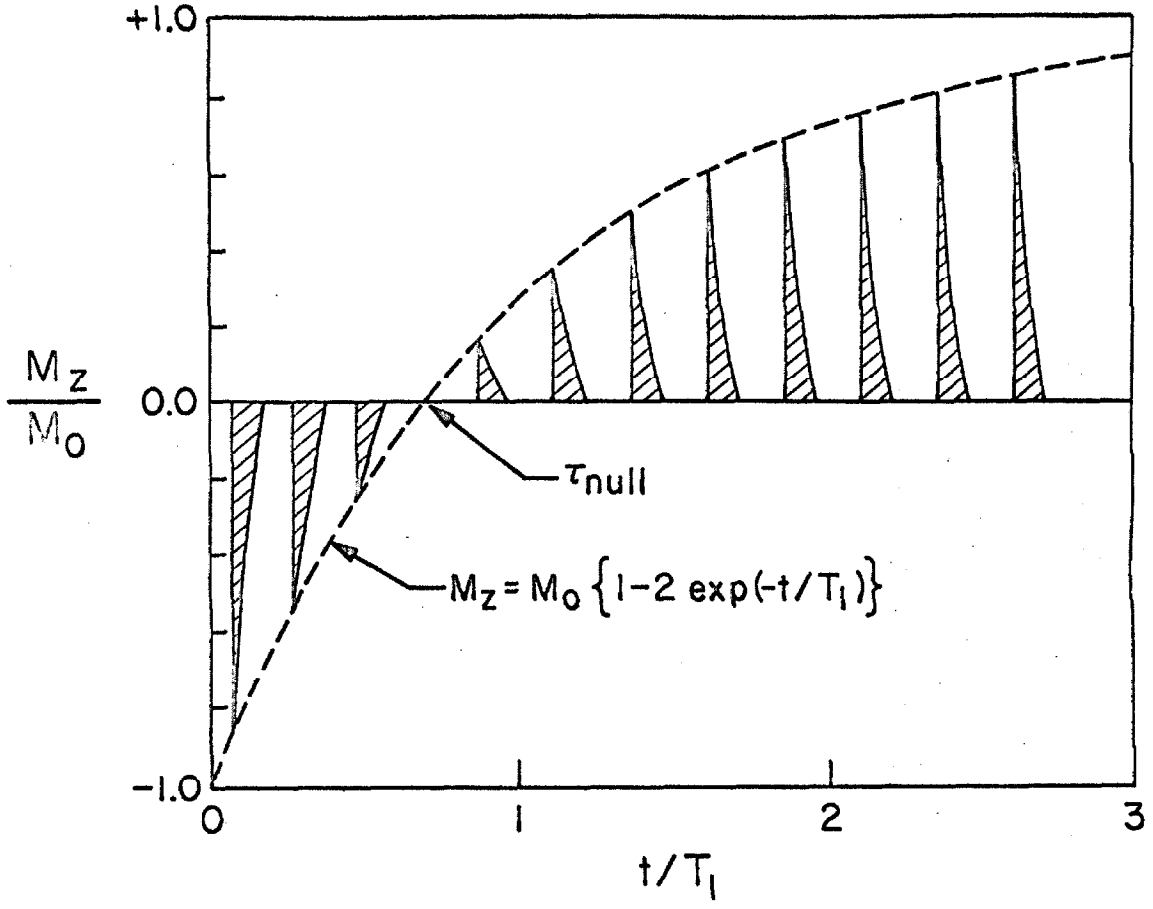
+1.0
0.0
-1.0
$\frac{M_z}{M_0}$
τ_{null}
$M_z = M_0\{1-2\exp(-t/T_1)\}$
0
1
2
3
t/T_1

REFERENCES

(1) A. Abragam, The Principles of Nuclear Magnetism (Oxford University Press, London, 1961), Chap. VIII.

(2) C. P. Slichter, Principles of Magnetic Resonance (Harper & Row, New York, 1963).

(3) F. Bloch, Phys. Rev. 70, 460 (1946).

(4) N. Bloembergen, E. M. Purcell, and R. V. Pound, Phys. Rev. 73, 679 (1948).

(5) J. L. Doob, Ann. Math. Statistics 15, 229 (1944).

(6) P. S. Hubbard, Phys. Rev. 109, 1153 (1958).

(7) Slichter, Appendix C.

(8) Vera V. Daniel, Dielectric Relaxation (Academic Press, New York, 1967).

(9) K. H. Illinger, "Absorption and Dispersion of Microwaves in Gases and Liquids," in Progress in Dielectrics, ed. by J. B. Birks (Academic Press, New York, 1962), Vol. 4.

(10) R. C. Miller and C. P. Smyth, J. Am. Chem. Soc. 79, 3310 (1957).

(11) Immanuel L. Fabelinski, Molecular Scattering of Light (Plenum Press, New York, 1968).

(12) M. Leontovich, J. Phys. USSR 4, 449 (1941).

(13) H. Shimizu, J. Chem. Phys. 43, 2453 (1965).

(14) K. F. Herzfeld and T. A. Litovitz, Absorption and Dispersion of Ultrasonic Waves (Academic Press, New York, 1959).

(15) E. N. Ivanov, Soviet Phys.--JETP 18, 1041 (1964).

(16) J. G. Powles, "The Relaxation of Molecular Orientation in Liquids," in Molecular Relaxation Processes (Academic Press, New York, 1966), p. 127.

(17) R. H. Cole, J. Chem. Phys. 42, 637 (1965).

(18) W. A. Steele, J. Chem. Phys. 38, 2404 (1963); 38, 2411 (1963).

(19) W. B. Moniz, W. A. Steele, and J. A. Dixon, J. Chem. Phys. 38, 2418 (1963).

(20) P. Debye, Polar Molecules (Chemical Catalog Co., New York, 1929).

(21) R. J. Meakins, Trans. Faraday Soc. 54, 1160 (1958).

(22) A. J. Curtis, P. L. McGeer, G. B. Rathmann, and C. P. Smyth, J. Am. Chem. Soc. 74, 644 (1952).

(23) A. Budo, E. Fischer, S. Miyamoto, Phys. Z. 40, 337 (1939).

(24) A. Spernal and K. Wirtz, Z. Naturforsch. 8a, 522 (1953).

(25) A. Gierer and K. Wirtz, Z. Naturforsch. 8a, 532 (1953).

(26) N. E. Hill, Proc. Phys. Soc. (London) B67, 149 (1954).

(27) R. J. Meakins, Proc. Phys. Soc. (London) 72, 283 (1958).

(28) D. A. Pitt and C. P. Smyth, J. Am. Chem. Soc. 81, 783 (1959).

(29) H. Hase, Z. Naturforsch. 8a, 695 (1953).

(30) R. W. Mitchell and M. Eisner, J. Chem. Phys. 33, 86 (1960).

(31) B. D. Boss and E. O. Stejskal, J. Chem. Phys. 45, 81 (1966).

(32) W. Kauzmann, Rev. Mod. Phys. 14, 12 (1942).

(33) E. L. Hahn, Phys. Rev. 80, 580 (1950).

(34) I. I. Rabi, N. F. Ramsey, and J. Schwinger, Rev. Mod. Phys. 26, 167 (1954).

II. NUCLEAR SPIN RELAXATION IN THE PRESENCE OF INTERNAL ROTATION

1. Introduction

A nuclear spin can interact with the magnetic field produced by overall molecular rotation. This interaction, commonly called the spin-rotation interaction, is described by the following Hamiltonian:

$$h^{-1}\mathcal{H}_{SR} = -\vec{I} \cdot \underset{\sim}{C} \cdot \vec{J} \qquad (1)$$

where $\underset{\sim}{C}$ is the spin-rotational coupling tensor and $\vec{I}$ and $\vec{J}$ are, respectively, the nuclear spin and molecular rotation vectors. The effect of this interaction on the stationary states of molecules can be detected by molecular beam resonance experiments[1] and as fine structure in microwave rotational spectra.[2] From such experiments the spin-rotational constants of, for example, HF,[3] SF_6,[3] CH_4,[4,5] CF_4,[6] and fluorobenzene[7] have been determined.

In gases at high pressures and in liquids, the spin-rotational interaction is time dependent since molecular collisions cause frequent changes in the orientation and the magnitude of the angular momentum vector. Since the fluctuating Hamiltonian couples the nuclear spin system to the lattice, it can induce nuclear spin relaxation.[8] The importance of this relaxation mechanism has been discussed by a number of authors including Gutowsky,[9,10] Powles,[11] and Waugh.[12,13] A theoretical treatment, valid for the case of spherical

molecules in the liquid state, has been described by Hubbard.[14] Unfortunately, the spin-rotational tensors are known for only a few relatively simple molecules; even then, frequently, all the components of the tensor are not known. This has greatly handicapped the interpretation of relaxation measurements. Even in the few cases where the spin-rotational tensors have been uniquely determined, methane and fluorobenzene for example, the interpretation of the relaxation data is complicated because of a lack of knowledge about the detailed nature of the fluctuations that determine the power spectrum.

Recently there has been considerable interest in the interpretation of the spin-lattice relaxation of molecules containing internal rotors. Green and Powles[11] have studied the spin-lattice relaxation of the fluorine nuclei in benzotrifluoride and have found T_1 to be unusually short and strongly temperature dependent. They have interpreted their results in terms of a spin–overall-rotation interaction modulated by the Brownian motion of the molecule; Faulk and Eisner[15] have reached a similar conclusion. Green and Powles have also found that the high temperature behavior of the methyl group protons of toluene, para-fluorotoluene, para-xylene, and mesitylene indicates a spin-rotational contribution to relaxation, although it is not nearly so pronounced as for fluorine nuclei. However, Dubin and Chan[16] have recently shown that when the nuclei under investigation are situated on a top that is undergoing internal reorientation with respect to the remainder of the molecule, it is necessary to modify the spin-rotational Hamiltonian to account for the interaction of the nuclear

spins with the magnetic field produced by internal rotation. They have derived the complete spin-rotational Hamiltonian for molecules such as benzotrifluoride that consist of a symmetric internal top attached to a frame with at least two planes of symmetry and have indicated the effect of the nuclear-spin–internal-rotation coupling in the limit of low and high barriers. To confirm their predictions they examined the fluorine spin-lattice relaxation of halogen substituted benzotrifluorides. They found that, while meta and para substitution have essentially no effect on the relaxation time, ortho substitution drastically increases T_1. Their interpretation is that ortho substituents change the symmetry and increase the height of the barrier to internal rotation thereby quenching the spin–internal-rotation interaction. In view of their results, it is appropriate to reinterpret the work of Green and Powles, Faulk and Eisner, and Pritchard and Richards[17] because benzotrifluoride and some of the methyl substituted benzenes have such low barriers to internal rotation that the tops may be considered to be free rotors.

Although Dubin and Chan have shown that the nuclear-spin–internal-rotation coupling can lead to relaxation, neither the nature

nor the time scale of the fluctuations that make the Hamiltonian time dependent have been ascertained. Intuitively we might expect one of two alternative situations: the total angular momentum of the internal top $\vec{j}'$ can be made time dependent by hard collisions which cause $\Delta j'$ transitions between the states of the internal rotor; alternatively, the overall tumbling motion of the molecule can cause $\Delta m_{j'}$ transitions by changing the projection of $\vec{j}'$ on the laboratory axes. The time scale of the former should be related to the mean time between hard collisions, and the latter, to the correlation time for overall reorientation.

In this paper we shall reexamine the fluorine spin-lattice relaxation of benzotrifluoride in terms of the spin–internal-rotation mechanism. The observed viscosity and temperature dependences of the relaxation will be examined in order to elucidate the nature of the fluctuations responsible for the observed time modulation of this interaction. We have also investigated the spin-lattice relaxation of the fluorine nuclei in hexafluorobutyne-2. Here, in contrast to benzotrifluoride where the barrier to internal rotation has sixfold symmetry, the barrier has threefold symmetry. However, the height of the barrier is expected to be low so that in this molecule the nuclear-spin–internal-rotation interaction is expected to be operative. We shall present the results of relaxation measurements as a function of viscosity in two solvents of varying viscosity. Finally, we shall show that the nuclear-spin–internal-rotation coupling contributes significantly to the relaxation of the methyl group protons in the methyl substituted benzenes.

2. Experimental

2. 1. Instrumentation

The spin-lattice relaxation times were measured by standard pulsed nuclear magnetic resonance techniques (180° pulse - 90° pulse)[18] with a phase-coherent spectrometer similar to Clark's.[19]

A voltage-to-frequency converter and gated counter were used, as described by Stejskal,[20] to sample a portion of the detected free induction decay signal. The digital output of the counter, the time integral of a portion of the free induction decay, is proportional to the initial amplitude of the free induction decay and to $M_z(t)$. Typically, the first 2 msec of a 5 msec free induction decay were sampled. A time-interval counter was used to measure the delay between the 180° pulse and the 90° pulse.

2. 2. Data Analysis

The various noise sources (saturation of the preamplifier and receiver due to transmitter pulses, preamplifier shot noise, radio-frequency and 60 Hz pickup, etc.) produce, in effect, a dc offset voltage that causes an apparent increase in the magnitude of $M_z(t)$. Furthermore, although the detection system is phase sensitive, the data acquisition system indicates only the magnitude of $M_z(t)$ but not its phase. In order to compensate for these effects we write the Bloch equation for the z-component for the magnetization:

$$M'_Z = -M'_0 + 2\delta + 2(M'_0 - \delta)\exp(-t/T_1) \qquad t \leq T_1 \ell n 2$$

$$M'_Z = M'_0 - 2(M'_0 - \delta)\exp(-t/T_1) \qquad t \geq T_1 \ell n 2 \tag{2}$$

where δ denotes the root mean square noise and the primes ($'$) denote experimental values: e. g., $M'_Z = |M_Z| + \delta$. Figure 1 illustrates the behavior of Eq. (2) and, for comparison, the Bloch equation for the z-component of the magnetization.

The experimental data, $M'_Z(t_i)$ and t_i, are fit to Eq. (2) by using T_1, M'_0, and δ as parameters and requiring that

$$\frac{1}{n}\sum_{i=1}^{n}\left\{M'_Z(t_i) - \begin{bmatrix} -M'_0 + 2\delta + 2(M'_0 - \delta)\exp(-t/T_1) \\ \\ M'_0 - 2(M'_0 - \delta)\exp(-t/T_1) \end{bmatrix}\right\}^2 \tag{3}$$

be a minimum: i. e., T_1 is extracted from the data by a least squares analysis.

The data acquisition system also provides a convenient method for signal averaging. It is well known that, for a series of repeated measurements, the signals add coherently and the noise adds randomly: the noise tends to cancel.[21] For a signal with "white noise", the apparent signal/noise ratio increases as the square root of the number of repetitions of the experiment

$$(S/N)_m = (S/N)_0 (m)^{\frac{1}{2}} \tag{4}$$

FIGURE 1

A comparison of the temporal behavior of Equation 2 and the Bloch equation for the z-component of the magnetization.

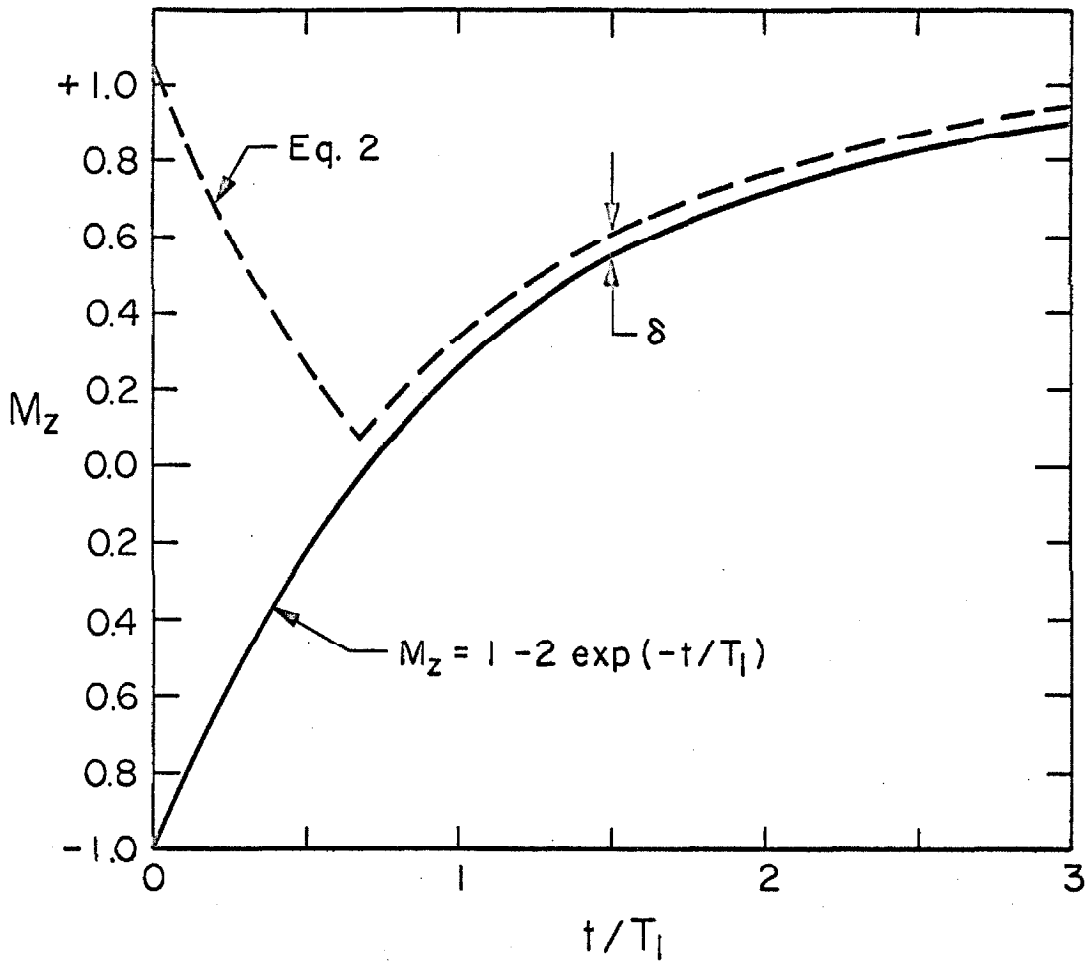
+1.0
0.8
0.6
0.4
0.2
0.0
0.2
0.4
0.6
0.8
-1.0
M_z
Eq. 2
δ
$M_z = 1 - 2 \exp(-t/T_1)$
0
1
2
3
t/T_1

where $(S/N)_i$ is the signal/noise ratio after i repetitions. This fact provides the raison d'être for devices such as computers of average transients ("CAT's") and boxcar integrators. This technique can be implemented by measuring $M'_z(t_i)$ m times, calculating the mean value $\overline{M'_z(t_i)}$, and using it in place of $M'_z(t_i)$ in the least squares analysis [Eq. (7)]. In principle, m is infinite whereas in a computer of average transients it is limited by the capacity of the memory elements, and in a boxcar integrator, by the leakage rate of the integrating capacitor.

In a typical experiment we measure $M'_z(t_i)$ five times at each t_i; the number of t_i's varies from 25 to 50 in the range $0 < t_i \lesssim 3T_1$. The arithmetic means are computed and the results are then subjected to an unweighted, non-linear least squares analysis. Typical relaxation curves (Figures 2 and 3) indicate that the experimental data are in excellent agreement with the single exponential model and that the relaxation can be described by a single relaxation time.

2. 3. Materials

The hexafluorobutyne-2 and benzotrifluoride (φCF_3) were obtained from, respectively, the Pierce and Aldrich Chemical Companies and were distilled prior to use. The solvents, spectral grade reagents, were used without further purification. The samples were degassed by the freeze-pump-thaw technique and were sealed under their own vapor pressure.

FIGURE 2

Relaxation curve for pure hexafluorobutyne-2 (T_1 = 1.84 sec).

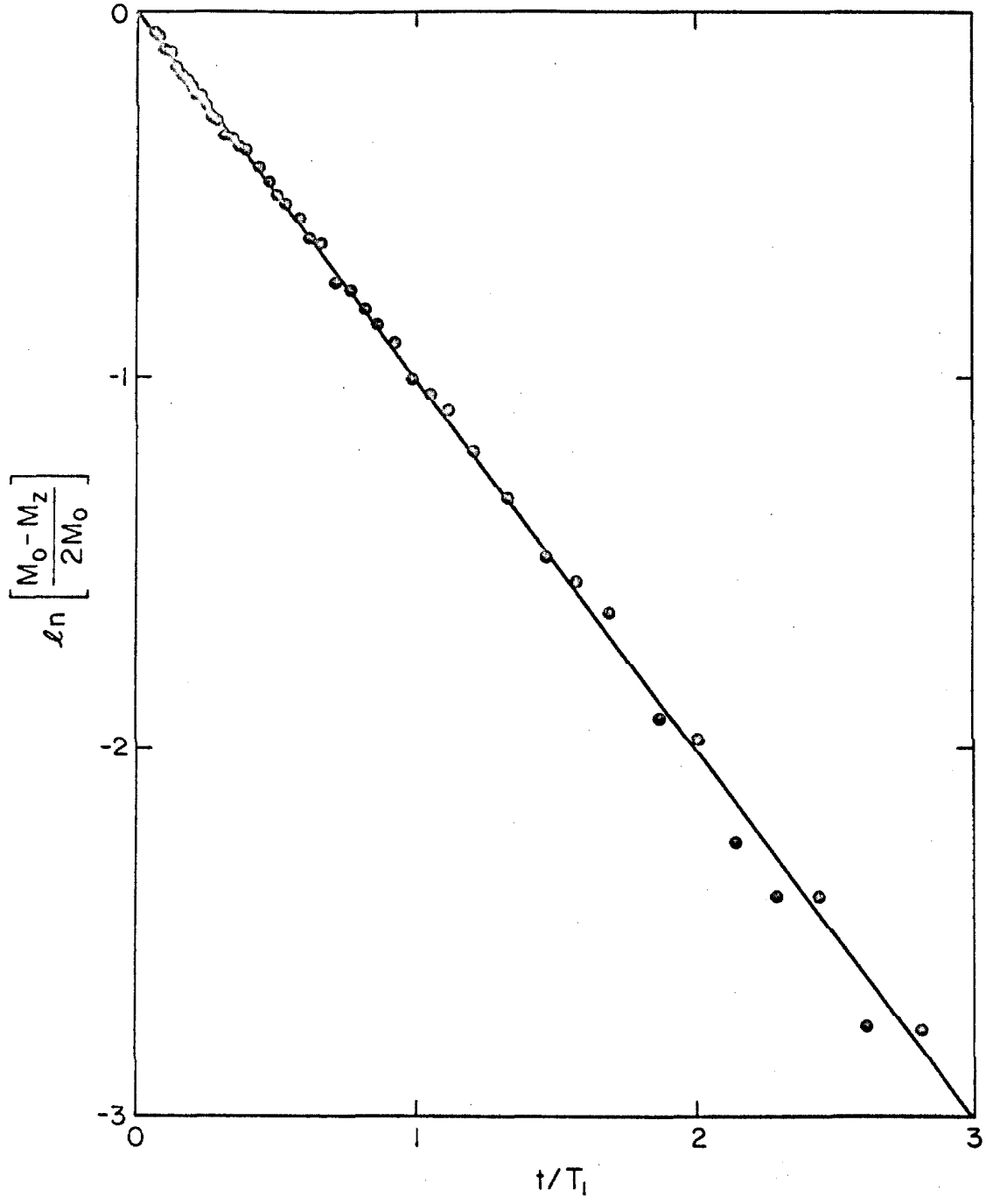
0
-1
-2
-3
0
1
2
3
$\ell n \left[\frac{M_o - M_z}{2M_o}\right]$
t/T_1

FIGURE 3

Relaxation curve for pure benzotrifluoride (T_1 = 2.56 *sec*).

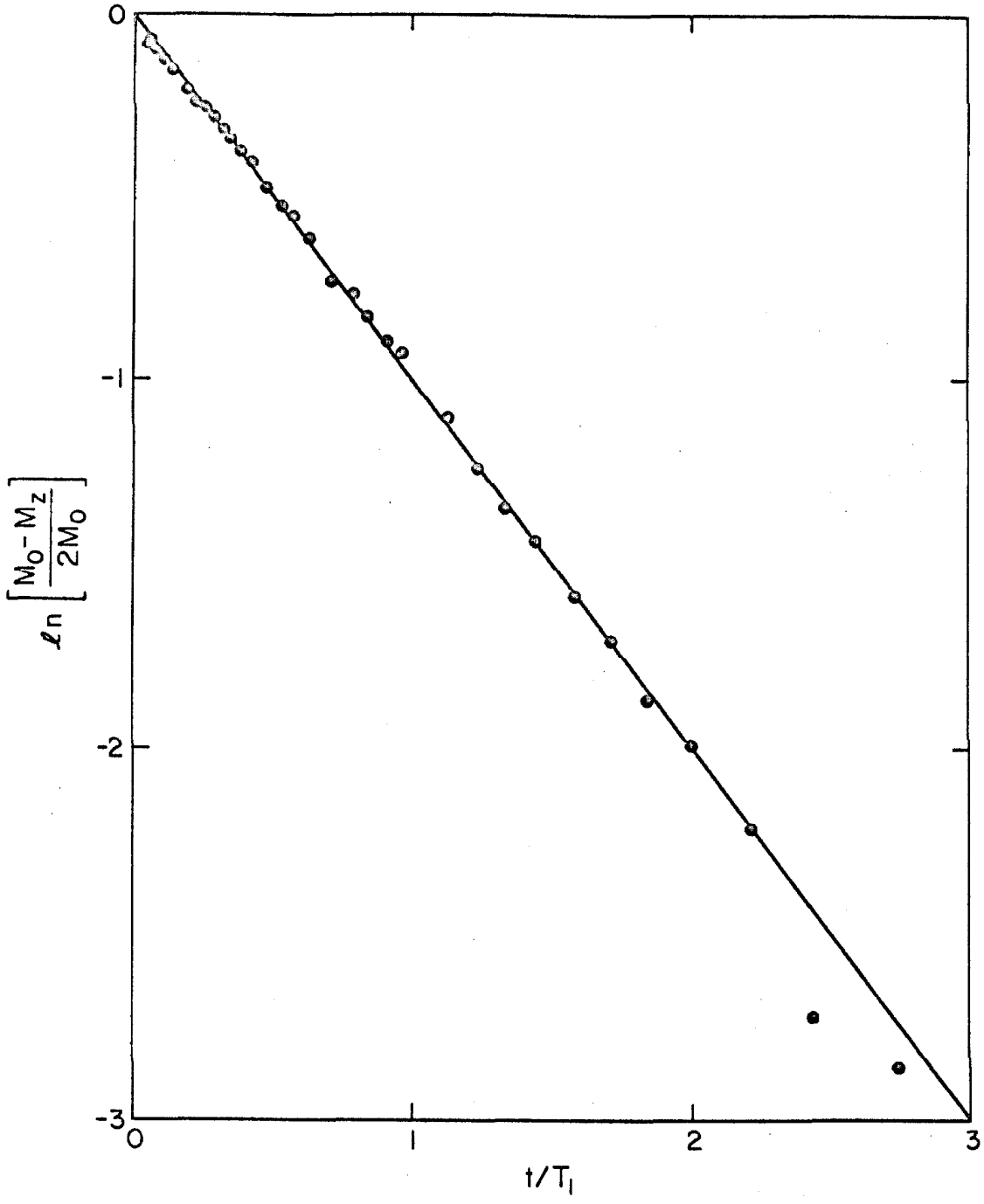
0
-1
-2
-3
0
1
2
3
$\ell n \left[\frac{M_0 - M_z}{2M_0}\right]$
t/T_1

3. Results

The rate of longitudinal relaxation $(1/T_1)$ of hexafluorobutyne-2 was measured as a function of concentration in diethyl ether and CCl_4. Attempts were made to observe the concentration dependence of $(1/T_1)$ in other solvents, but hexafluorobutyne-2 was found to be insoluble in CS_2, CH_3CN, and $HCCl_3$.

The experiments were performed at 25°C at a Larmor frequency of 12.3 MHz. Several experiments at 8.8 MHz showed no detectable difference thus indicating (1) that the anisotropic chemical shift mechanism[22, 23] does not contribute measurably to relaxation at field strengths of 3 kG, and (2) that the experiments were performed in the limit of extreme narrowing $(1 \gg \omega_0^2 \tau_c^2)$.

Figure 4 shows the concentration dependence of the relaxation rate: each point represents the average of two or more experiments; the error bars correspond to a precision of ± 2%; the solid lines represent expansions of the rates in terms of the mole fractions of the solute and are used to extrapolate the rates to infinite dilution.

The fluorine spin-lattice relaxation rates have been determined for benzotrifluoride as a function of concentration in CS_2. The experimental conditions were the same as for hexafluorobutyne-2. The data are also depicted in Figure 4.

4. Relaxation Mechanisms

The total rate of relaxation is due to the additive contributions of the various relaxation mechanisms: $(1/T_1) = R_A + R_B + R_C + \ldots$,

FIGURE 4

Spin-lattice relaxation rates of hexafluorobutyne-2 and benzotrifluoride as a function of concentration.

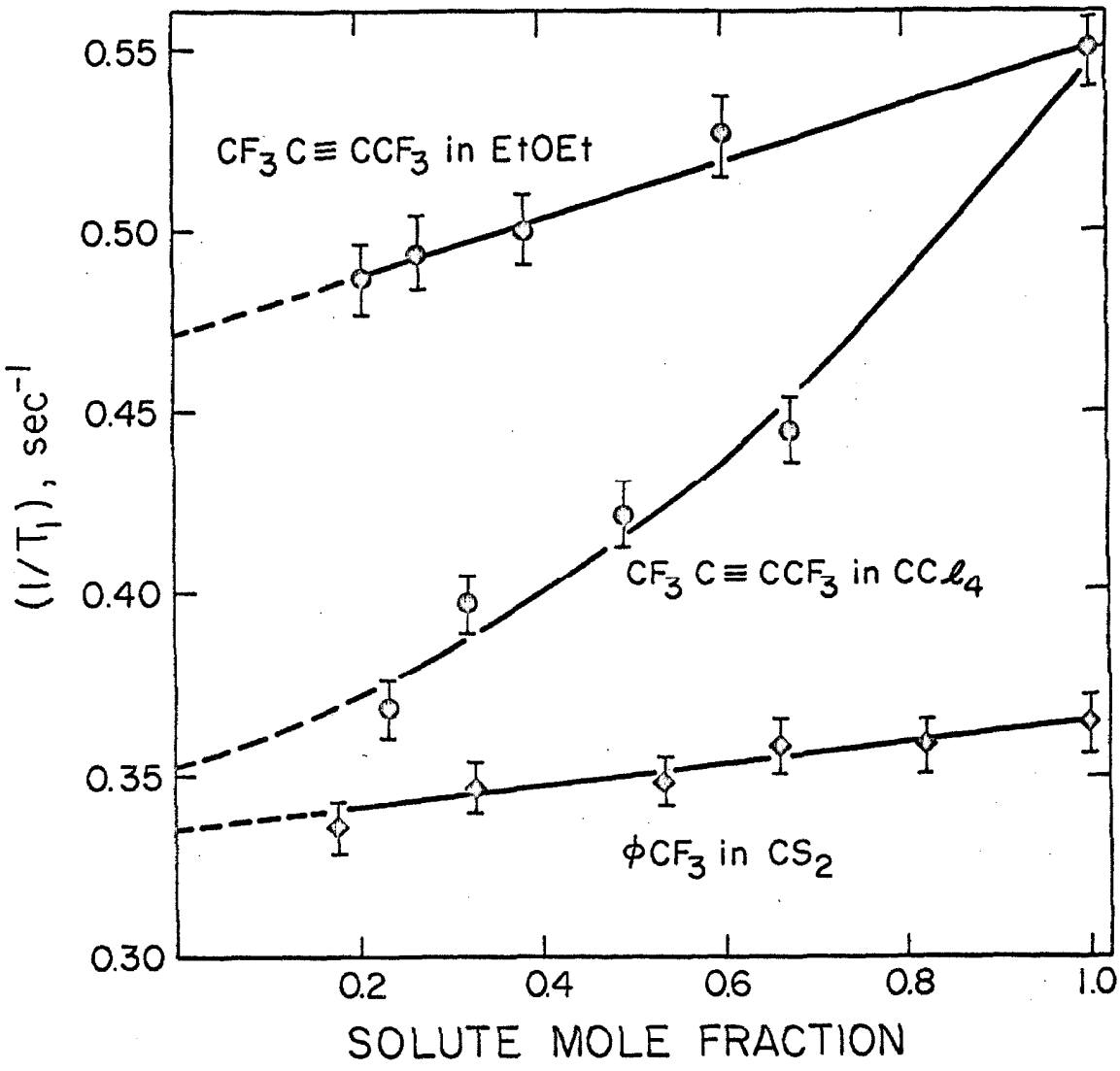
0.55
0.50
0.45
0.40
0.35
0.30
$(1/T_1)$, sec^{-1}
$CF_3C \equiv CCF_3$ in EtOEt
$CF_3C \equiv CCF_3$ in CCl_4
ϕCF_3 in CS_2
0.2
0.4
0.6
0.8
1.0
SOLUTE MOLE FRACTION

where R_A represents the rate due to those mechanisms, such as the intramolecular dipolar and quadrupolar interactions, which transform under molecular rotations as the second-order spherical harmonics $Y_2^m(\Omega)$; R_B represents the intermolecular dipolar interaction; and R_C represents the spin-rotational interaction which transforms as the angular momentum vector $\vec{J}$. We shall only be concerned with the intramolecular dipolar, the intermolecular dipolar, and the spin-rotational interactions. Other relaxation mechanisms can be excluded on physical or experimental grounds. Thus R_A and R_C depend on the dynamical variables (orientation and angular velocity, respectively) of the molecules under investigation and they may be categorized as intramolecular effects. Since the intramolecular relaxation mechanisms are of primary interest, it is necessary to separate the intra- and intermolecular contributions to relaxation. Thus

$$(1/T_1)_{intra} = R_A + R_C = (1/T_1) - R_B \tag{5}$$

4. 1. Intermolecular Dipolar Relaxation[8]

The relaxation rate due to intermolecular dipolar coupling between indentical spin-$\frac{1}{2}$ nuclei is

$$R_B \approx \frac{6\pi^2\hbar^2\gamma_I^4\eta}{5kT}\left[\frac{n_I\rho N_0}{M}\right] \tag{6}$$

where η, ρ, and M are, respectively, the viscosity, density and

molecular weight; the term in brackets is the nuclear spin density (spins per cm^3) expressed in terms of n_I, the number of I nuclei per molecule. The contribution to relaxation due to intermolecular dipolar coupling between dissimilar spin-$\frac{1}{2}$ nuclei I and S is given by an analogous expression:

$$R_B \approx \frac{4\pi^2 \hbar^2 \gamma_I^2 \gamma_S^2 \eta}{5kT} \left[\frac{n_S \rho N_0}{M}\right] \qquad (7)$$

The only appreciable intermolecular contributions to the relaxation of a fluorine nucleus are due to dipolar coupling with other fluorine nuclei and with protons. Thus, with the substitution of F for I and H for S, Equations (6) and (7) describe the intermolecular dipolar contributions to ^{19}F relaxation.

The validity of Eq. (6) can be tested by a comparison of calculated and experimental values of R_B. Zeidler,[24] for example, has investigated the proton relaxation of various organic molecules as a function of concentration in their perdeuterated analogues and has separated the intra- and intermolecular contributions by extrapolation of the relaxation rates to infinite dilution. In Table I, several of Zeidler's experimental results are compared with values calculated from Eq. (6).

It is necessary to specify the temperature dependences of both ρ and η in order to evaluate R_B at different temperatures. The temperature dependence of the density may be represented by the expression[25]

TABLE I. The Intermolecular Dipolar Contribution to Relaxation: A Comparison of Experimental and Calculated Values

	R_B, (sec^{-1})	
	experimental[a]	calculated[b]
CH_3CN	0. 018	0. 019
acetone	0. 029	0. 025
benzene	0. 044	0. 039

[a]M. D. Zeidler, Ber. Bunsenges. physik. Chem. 69, 659 (1965).

[b]Equation (6).

$$\rho_T = \rho_{T_0} \exp\left[-\int_{T_0}^{T} \alpha \, dT\right] \tag{8}$$

where α, the thermal coefficient of expansion, is

$$\alpha = \frac{1}{V}\left(\frac{dV}{dT}\right) = a + 2bT + 3cT^2 + \cdots \tag{9}$$

Rutledge and Smith's[26] density data have been used to determine α for benzotrifluoride

$$\alpha = 107 \times 10^{-5} + 0.400 \times 10^{-5} (T - 273) \tag{10}$$

Thus the density of benzotrifluoride at temperature T is

$$\rho_T = 1.1772 \exp\left\{-107 \times 10^{-5} (T - 298) - 0.400 \times 10^{-5} \times \left[(T^2 - 298^2) - 273 (T - 298)\right]\right\} \tag{11}$$

The viscosity is strongly temperature dependent and may be represented by the expression[27]

$$\eta_T = A \rho_T \exp(\Delta \tilde{G}_0^{\ddagger}/RT) \tag{12}$$

where A is a constant and $\Delta \tilde{G}_0^{\ddagger}$ is the molar "free energy of activation." Equation (12) indicates that the viscosity decreases exponentially with temperature which is in agreement with the observed behavior of most

liquids.[28] Faulk and Eisner have measured the viscosity of φCF_3 at various temperatures from 253°K to 333°K.[15] From their results we have determined that $\Delta\tilde{G}_0^{\ddagger}/R = 967°K$. Therefore, for φCF_3,

$$\eta_T = 1.83 \times 10^{-4} \rho_T \exp(967/T) \tag{13}$$

where ρ_T is given by Eq. (11).

The values of $(1/T_1)$, R_B, and $(1/T_1)_{intra}$ used in this discussion are presented in Tables II - IV.

4. 2. Intramolecular Dipolar Relaxation[8]

The contribution to relaxation caused by the dipolar interaction between two identical nuclei on a molecule which is undergoing isotropic reorientation with a correlation time τ_2 is

$$R_A = \frac{2\hbar^2\gamma_I^4 I(I+1)\tau_2}{r^6} \tag{14}$$

The extension to a system with n identical spins, each nuclei interacting with the remaining n - 1 nuclei, is complex because the motions of the n - 1 internuclear vectors are not independent. A number of semi-classical density matrix calculations pertaining to three and four spin systems with differing degrees of symmetry have shown that the decay of $(M_Z - M_0)$ is not exponential; rather, it is described by more complex functions such as sums of exponentials.[29-33] Since the predicted deviations from exponentiality are small, the decay of $(M_Z - M_0)$ can be described, to a good approximation, by a single

TABLE II

The Effect of Solvents on Hexafluorobutyne-2 Relaxation

	$1/T_1$[a]	R_B[a]	$(1/T_1)_{intra}$
	sec^{-1}	sec^{-1}	sec^{-1}
diethyl ether	0.472 ± 0.03[b]	0.012	0.460
CCl_4	0.352 ± 0.04[b]	0.0	0.352

[a]Infinite dilution value. [b]Estimated uncertainty.

TABLE III

The Effect of Solvents on Benzotrifluoride Relaxation

	$1/T_1$[a]	R_B[a]	$(1/T_1)_{intra}$
	sec^{-1}	sec^{-1}	sec^{-1}
CS_2	0.335	0.0	0.335
toluene	0.351[b]	0.024	0.327
p-xylene	0.351[b]	0.029	0.322
o-xylene	0.351[b]	0.037	0.314
$HCBr_3$	0.286[b]	0.021	0.265

[a]Infinite dilution value. [b]A. S. Dubin, Ph. D. thesis, California Institute of Technology, 1967 (unpublished).

TABLE IV

The Effect of Temperature on Benzotrifluoride Relaxation

T, °K[a]	$1/T_1$[a]	R_B	$(1/T_1)_{intra}$
	sec^{-1}	sec^{-1}	sec^{-1}
242	0.292	0.078	0.214
253	0.308	0.060	0.248
278	0.316	0.035	0.281
294	0.325	0.025	0.300
308	0.350	0.019	0.331
333	0.379	0.013	0.366
353	0.418	0.009	0.409
379	0.500	0.006	0.494
389	0.572	0.005	0.567
412	0.598	0.004	0.594
442	0.700	0.002	0.698
472	0.877	0.002	0.875
505	1.22	0.001	1.22
535	1.58	0.001	1.58
542	1.66	0.001	1.66

[a]D. K. Green and J. G. Powles, Proc. Phys. Soc. (London) 85, 87 (1965).

exponential with a rate constant

$$R_A = \frac{1}{n} \sum_{i<j} (R_A)_{ij} \tag{15}$$

where n is the number of interacting nuclei; $(R_A)_{ij}$, given by Eq. (14), is the contribution to relaxation due to the interactions of spins i and j; and the summation is over pairs of nuclei. The effect of interactions between dissimilar nuclei can be approximately accounted for by adding to Eq. (15) additional pairwise interaction terms, each multiplied by a factor of 2/3 to correct for the decreased efficiency of hetero-nuclear dipolar interactions.[34] Thus a general expression for the intramolecular dipolar contribution to the relaxation of a fluorine nucleus is

$$R_A = \hbar^2 \gamma_F^2 \left[\frac{3}{2} \gamma_F^2 \sum_{F'} r_{FF'}^{-6} + \frac{4}{3} \sum_i I_i (I_i + 1) \gamma_i^2 r_{Fi}^{-6} \right] \tau_2 \tag{16}$$

where the first summation is over the remaining fluorine nuclei and the second summation is over the non-fluorine nuclei.

An analysis of the intramolecular dipolar contribution to relaxation becomes exceedingly difficult when the molecule is not spherically symmetric and/or there is internal rotation because more than one correlation time is required to describe the motions of the molecule. The effects of anisotropic reorientation will not be considered because the works of both Woessner[35] and Shimizu[36] indicate that the effects will be small for the molecules considered here. On the other hand, the effects of internal rotation cannot be dismissed. For a molecule

with correlation times τ_2 for overall reorientation and τ_2^{int} for internal rotation, Woessner[37] has shown that the effective correlation time for nuclei on the internal rotor is

$$\tau_2^{eff} = \frac{3}{4}\left[\frac{1}{3}(3\cos^2\theta - 1)^2\tau_2 + (\sin^2 2\theta)\tau_2' + (\sin^4\theta)\tau_2''\right] \qquad (17)$$

where θ is the angle between the spin-spin vector and the internal rotation axis and τ_2' and τ_2'' are functions of τ_2 and τ_2^{int}. For the particular case in which the spin-spin vector is perpendicular to the internal rotation axis and the internal reorientation proceeds by infinitesimal steps, Eq. (17) reduces to

$$\tau_2^{eff} = \frac{3}{4}\left[\frac{1}{3} + \frac{\tau_2^{int}}{4\tau_2 + \tau_2^{int}}\right]\tau_2 \qquad (18)$$

Consequently $\frac{1}{4}\tau_2 \leq \tau_2^{eff} \leq \tau_2$: the lower limit represents the extreme where internal rotation is much more rapid than overall reorientation and the upper limit pertains to a rigid molecule. Thus any internal motion reduces the effectiveness of the intramolecular dipolar interaction.

The structure of hexafluorobutyne-2 has been determined by electron diffraction.[38] The bond lengths, bond angles, and the distances between pairs of fluorine nuclei are presented in Table V. Because of the strong dependence of internuclear separation, the interaction between fluorine nuclei on different carbon atoms is very weak (a 0.5% effect) and may be neglected. Thus Eq. (16) reduces to

TABLE V

Structural Parameters of Hexafluorobutyne-2

r_{C-F}	=	1.34 Å
r_{C-C}	=	1.46_5 Å
$r_{C\equiv C}$	=	1.22 Å
$\angle FCF$	=	$107.5° \pm 1°$
r_{F-F}	=	2.16 Å
$r_{F-F'}$	=	5.1 Å

$$R_A = \frac{3\hbar^2\gamma_F{}^4\tau_2{}^{eff}}{r_{FF}{}^6} = 1.32\times10^{10}\ \tau_2{}^{eff} \qquad (19)$$

In benzotrifluoride, the interaction between the fluorine nuclei and the ortho protons produces an added contribution to relaxation:

$$R_A \approx 1.47\times10^{10}\ \tau_2{}^{eff} \qquad (20)$$

The effect of the meta and para protons may be neglected.

4.3. Spin-Rotational Relaxation

The basic elements of the theory of spin-rotational relaxation in liquids were developed by Brown, Gutowsky, and Shimomura[10] who realized that the statistical properties of the spin-rotational Hamiltonian may be considerably different from those of the orientation dependent processes. They proposed a transient rotation model in which the molecules jump from one orientation to another at random times; the spin-rotational interaction is assumed to operate only during the jumps. The statistical properties of the model lead to the following expression for the spin-rotational contribution to the relaxation of nucleus I

$$R_C = \frac{1}{3}\gamma_I{}^2\langle H_{SR}{}^2\rangle_{av}\ \Delta^2/\tau_j \qquad (21)$$

where $\langle H_{SR}{}^2\rangle_{av}$ is the mean-squared magnitude of the magnetic field generated at nucleus I during a reorientation, Δ is the duration of the

spin-rotation impulse, and $\tau_j = \tau_j^\circ \exp(E_j/RT)$ is the average time between jumps. Equation (21) is in qualitative agreement with the temperature dependence of $1/T_{1F}$ for $CHFCl_2$ and, in the limit where $\Delta = \tau_j$, correctly describes the spin-rotation interaction in gases. Unfortunately, $\langle H_{SR}^2 \rangle_{av}$ and Δ were not evaluated.

Hubbard[14] has shown, using the semi-classical form of the density operator theory of relaxation, that the contribution of the spin-rotational interaction to the relaxation of identical spin-$\frac{1}{2}$ nuclei at equivalent positions in spherical molecules in the liquid state is

$$R_C = 2J_1(\omega_0) \tag{22}$$

$J_1(\omega_0)$, the spectral energy density of the fluctuations at the Larmor frequency, is

$$J_1(\omega_0) = \frac{4\pi^2 IkT}{9\hbar^2} \left[\frac{(2C_\perp + C_{||})^2 \tau_1}{1 + \omega_0^2 \tau_1^2} + \frac{2(C_\perp - C_{||})^2 \tau_{12}}{1 + \omega_0^2 \tau_{12}^2} \right] \tag{23}$$

where $C_\perp$ and $C_{||}$ are, respectively, the perpendicular and parallel components of the spin-rotational coupling tensor in units of Hz, and where τ_{12} is defined by

$$\frac{1}{\tau_{12}} \equiv \frac{1}{\tau_1} + \frac{1}{\tau_2} \tag{24}$$

τ_1 is the time constant describing the exponential decay of the angular velocity autocorrelation functions and τ_2 is the correlation time for

molecular reorientation. Because the derivation of Eq. (23) is based on the assumption that the orientation of the molecule is independent of the angular velocity, it is only valid in the limits where $\tau_1 \ll \tau_2$ or $\tau_1 \gg \tau_2$.

In the limit of extreme narrowing and where $\tau_1 \ll \tau_2$, which is probably the case in strongly interacting liquid systems, the rate of relaxation is

$$R_C = \frac{8\pi^2 I k T (2 C_\perp^2 + C_\parallel^2) \tau_1}{3\hbar^2} \tag{25}$$

When the reorientation of the molecule is due to isotropic Brownian motion τ_1 can be related to the more familiar τ_2:

$$\tau_1 = I/6kT\tau_2 \tag{26}$$

Green and Powles[11] have obtained essentially the same results as Hubbard using a less rigorous, more physically descriptive approach and have shown that Equations (21) and (25) are equivalent. Therefore the spin-rotational relaxation mechanism is insensitive to the details of molecular reorientation. As Green and Powles have pointed out, this is reasonable because the details of the reorientational motion depend on very short times ($\sim 10^{-13}$ sec) whereas T_1 is directly sensitive only to much longer times ($\sim 10^{-7}$ sec).

Dubin and Chan[16] have shown, and here we closely follow their treatment, that for nuclei located on an internal rotor that is under-

going reorientation with respect to the molecular frame it is necessary to consider the spin–internal-rotation coupling. For nuclei on a symmetric rotor attached to a frame with at least two planes of symmetry, the Hamiltonian is

$$h^{-1}\mathcal{H}_{SR} = -\sum_k \left[\vec{I}_k \cdot \mathcal{C}(k) \cdot \vec{J} + C_\alpha (1 - I_\alpha/I_{aa}) \vec{I}_k \cdot \vec{j}\right] \qquad (27)$$

where $\vec{J}$ is the total angular momentum vector, $\vec{j}$ is the angular momentum of the top relative to the frame, C_α is the spin–internal-rotation coupling constant, and I_α and I_{aa} are the moments of inertia of the top and the whole molecule about the top axis. It is convenient, in the limit of low barriers, to rewrite Eq. (27) in terms of $\vec{j}'$, the total angular momentum of the top:

$$h^{-1}\mathcal{H}_{SR} = -\sum_k \left[\vec{I}_k \cdot \mathcal{C}(k) \cdot \vec{J} - C_\alpha (I_\alpha/I_{aa}) I_{ka} J_a + C_\alpha \vec{I}_k \cdot \vec{j}'\right] \qquad (28)$$

Expanding Eq. (28) and combining similar terms gives

$$h^{-1}\mathcal{H}_{SR} \approx -\sum_k \left[C_{bb}^{(k)} I_{kb} J_b + C_{cc}^{(k)} I_{kc} J_c + C_\alpha I_{ka} J'_\alpha\right] \qquad (29)$$

since, to a good approximation, $C_{aa} = C_\alpha (I_\alpha/I_{aa})$. With the reasonable assumption that $C_{\alpha\alpha}^2 \gg C_{bb}^2 \sim C_{cc}^2$, the spin-rotational interaction is dominated by fluctuations of j′:

$$R_C \approx \frac{8\pi^2 kT I_\alpha C_\alpha^2 \tau_{j'}}{3\hbar^2} \qquad (30)$$

where $\tau_{j'}$ is the correlation time associated with fluctuations of $\vec{j}'$.

5. Spin-Rotational Coupling Constants

Although the spin-rotational contributions to relaxation are important, very little information is presently available about the coupling constants. Consequently, we shall briefly digress to discuss them, focusing our attention on hexafluorobutyne-2.

The components of the spin-rotation tensor of hexafluorobutyne-2 are not known, but it is possible to make a reasonable estimate of their magnitude on the basis of chemical shift data since the high-frequency part of the nuclear shielding constant is related to the spin-rotational constants.[39] The absolute shielding constant σ_N for nucleus N is given by

$$\sigma_N = \frac{e^2}{3mc^2}\left[\langle\psi_0|\sum_k r_{Nk}^{-1}|\psi_0\rangle - \sum_{N'\neq N}\frac{Z_{N'}}{R_{NN'}} + \frac{h}{4Mg_N\mu_N^2}\sum_i C_{ii}I_{ii}\right] \tag{31}$$

where the subscripts k and N' denote, respectively, the electrons and the nuclei. M is the proton mass; g_N, the nuclear g-value of the nucleus under investigation; and μ_N, the nuclear magneton. The I_{ii}'s are the principal components of the inertial tensor and the C_{ii}'s are the diagonal components of the spin-rotation tensor in the principal inertial frame.

The sum of the first two terms in Eq. (31) is proportional to the total electrostatic potential at the nucleus under consideration. For fluorine nuclei, this potential is relatively insensitive to the chemical

environment of the atom since it is primarily determined by the core electrons and the non-bonded valence electrons. Chan and Dubin[7] have assigned a value of (+470 ± 10) parts per million (ppm) to the sum of the first two terms. Thus

$$\sigma_N \approx 470 \times 10^{-6} + (\sigma^{CI})_{av} \tag{32}$$

The chemical shift of hexafluorobutyne-2 is +483 ppm with respect to F_2.[40] Since the absolute nuclear shielding constant of F_2 is -210 ppm,[41] the absolute nuclear shielding constant of hexafluorobutyne-2 is +273 ppm and $(\sigma^{CI})_{av} = -197$ ppm.

In general, nuclear shielding is anisotropic and must be described by a shielding tensor with diagonal components

$$(\sigma_N)_{ii} = \frac{e^2}{2mc^2}\left[\langle\psi_0|\sum_k \frac{r_{Nk}^2 - (r_{Nk})_i^2}{r_{Nk}^3}|\psi_0\rangle - \sum_{N'\neq N}\frac{R_{NN'}^2 - (R_{NN'})_i^2}{R_{NN'}^3}\right] + \frac{e^2}{mc^2}\,\frac{h}{4Mg_N\mu_N^2}\,C_{ii}\,I_{ii} \tag{33}$$

Typically, both the first and the second terms are anisotropic, but to a good approximation their sum is isotropic. Thus

$$(\sigma_N)_{ii} \approx 470 \times 10^{-6} + 0.20812 \times 10^{-6}\, C_{ii}\, I_{ii} \tag{34}$$

where I_{ii} is in units of 10^{-40} g cm^2 and C_{ii}, in kHz. For hexafluoro-

butyne-2

$$(\sigma^{CI})_{av} = -197 \times 10^{-6} = \frac{0.20812 \times 10^{-6}}{3} \sum_i C_{ii} I_{ii} \qquad (35)$$

or

$$C_{aa}I_{aa} + 2C_{bb}I_{bb} = -2840 \qquad (36)$$

Meyer[42] et al. have studied the anisotropy of the F^{19} chemical shift of HCF_3 oriented in a β-quinol clathrate. The principal components of the shielding tensor are $\sigma_\alpha = \sigma_\gamma = 264$ ppm and $\sigma_\beta = 369$ ppm; the α-axis is perpendicular to the H-C-F plane and the β-axis is parallel to the C-F bond. Although it is not explicitly stated, the values are apparently absolute since $\frac{1}{3}(\sigma_\alpha + \sigma_\beta + \sigma_\gamma) = 299$ ppm which is in agreement with the experimental value of σ_N.[43] Since the shielding tensor and the inertial tensor are not diagonal in the same coordinate system, it is necessary to transform $\mathfrak{g}$ from the α, β, γ coordinate system into the inertial coordinate system. The coordinate systems are depicted in Figure 5. The transformation can be represented as a matrix equation

$$\mathfrak{g}^i = \mathfrak{R}^{-1} \cdot \mathfrak{g}^P \cdot \mathfrak{R} \qquad (37)$$

where $\mathfrak{g}^i$ and $\mathfrak{g}^P$ are the second rank shielding tensors in, respectively, the intertial and principal axis systems and $\mathfrak{R}^{-1}$ and $\mathfrak{R}$ are rotational operators. Since the transformation is equivalent to a rotation about the α-axis, $\mathfrak{R}$ takes the form

FIGURE 5

The principal coordinate systems for the inertial tensor (x, y, and z) and the shielding tensor (α, β, and γ) of HCF_3 where $\theta = 20.1°$. The axes x and α are directed out of the plane of the paper.

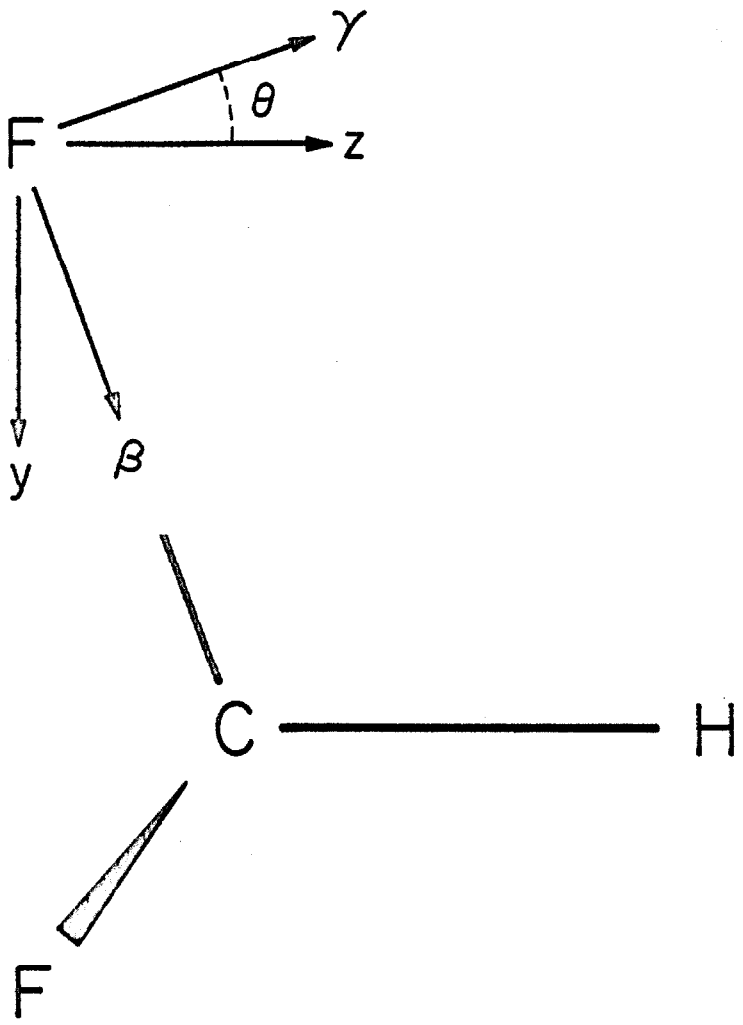
γ
θ
F
z
y
β
C
H
F

$$\mathcal{R} = \begin{pmatrix} 1 & 0 & 0 \\ 0 & \cos\theta & \sin\theta \\ 0 & -\sin\theta & \cos\theta \end{pmatrix} \tag{38}$$

and $\theta = 20.1°$. Thus

$$\sigma^{i} = \begin{pmatrix} 264 & 0 & 0 \\ 0 & 357 & 34 \\ 0 & 34 & 276 \end{pmatrix} \quad \text{ppm} \tag{39}$$

Correcting for the electrostatic contribution to shielding gives

$(\sigma^{CI})_{xx} \approx -206$ ppm, $(\sigma^{CI})_{yy} \approx -113$ ppm, and $(\sigma^{CI})_{zz} \approx -194$ ppm.

Thus

$$(\sigma^{CI})_{||} \equiv (\sigma^{CI})_{zz} = -194 \times 10^{-6} = 0.20812 \times 10^{-6}\ C_{||}I_{||} \tag{40}$$

$$2(\sigma^{CI})_{\perp} \equiv (\sigma^{CI})_{xx} + (\sigma^{CI})_{yy} = -319 \times 10^{-6}$$

$$= 2 \times 0.20812 \times 10^{-6}\ C_{\perp}I_{\perp} \tag{41}$$

The principal moments of inertia of HCF_3 are $I_{||} = 148 \times 10^{-40}$ g cm^2 and $I_{\perp} = 81.1 \times 10^{-40}$ g cm^2. Therefore, the spin-rotational constants for HCF_3 are $C_{||} = -6.30$ kHz and $C_{\perp} = -9.48$ kHz.

We can now equate $C_{||} = -6.30$ kHz with C_{α} for hexafluorobutyne-2. Since $C_{\alpha}I_{\alpha} = C_{aa}I_{aa}$, Eq. (36) gives $C_{bb} = C_{cc} \approx -0.69$ kHz. The same technique can be applied to benzotrifluoride. In Table VI we present the chemical shifts, the components of the inertial tensor, and the calculated components of the spin-rotational coupling tensor for both hexafluorobutyne-2 and benzotrifluoride.

TABLE VI

The Spin-Rotational and Inertial Constants of Hexafluorobutyne-2 and Benzotrifluoride

		Hexafluorobutyne-2	Benzotrifluoride
δ_{FCCl_3}		+57[a]	+64[b]
δ_{F_2}	ppm	+483	+490
C_{aa}		-3.15	-3.14
C_{bb}	kHz	-0.69	-0.98
C_{cc}		-0.69	-0.85
I_{aa}		296	295
I_{bb}	10^{-40} g cm^2	1385	895
I_{cc}		1385	1043
I_α	10^{-40} g cm^2	148	
C_α	kHz	-6.30	

[a]N. Muller and D. T. Carr, J. Phys. Chem. 67, 112 (1963).

[b]G. Filipovich and G. V. D. Tiers, J. Phys. Chem. 63, 761 (1959).

Ramsey and co-workers[4, 5] have determined the components of the spin-rotational tensor for methane. In order to apply their results to the nuclear-spin–internal-rotation coupling in toluene, it is necessary to transform their results into the principal inertial axis system of the CH_3 top. Using an expression analogous to Eq. (37) with $\theta = 19.5°$ we find

$$\mathfrak{C}^i = \mathfrak{R}^{-1} \cdot \mathfrak{C}^P \cdot \mathfrak{R} = \begin{pmatrix} 16.5 & 0 & 0 \\ 0 & 0.3 & 5.7 \\ 0 & 5.7 & 14.4 \end{pmatrix} \text{ kHz} \qquad (42)$$

and $C_\alpha = C_{zz} = 14.4$ kHz. Unfortunately, lack of information about the components of the shielding tensor prevents further elaboration.

6. Discussion of Results

6.1. Benzotrifluoride and Hexafluorobutyne-2

The barrier to internal rotation in hexafluorobutyne-2 is not known, but it can be argued that it is small. The barrier to CH_3 rotation decreases from 2.87 kcal/mole in ethane[44] to less than 30 cal/mole in butyne-2.[45] The barrier to CF_3 rotation in hexafluorobutyne-2 should reflect a comparable change from the value of 4.45 kcal/mole in hexafluoroethane.[46] It is reasonable that the barriers in butyne-2 and hexafluorobutyne-2 should be comparable. The internal rotation in benzotrifluoride has been shown to be nearly free.[47]

In the low barrier limit, the internal reorientation of the top may

be considered to be dynamically coherent and the correlation time for internal rotation can be calculated from Steele's inertial model.[48, 49] For a CF_3 top at 25°C

$$\tau_2^{int} \approx \tfrac{1}{2}\left[\frac{\pi I_\alpha}{3kT}\right]^{\frac{1}{2}} = 3.1 \times 10^{-13} \text{ sec} \qquad (43)$$

Calculations of the correlation time for overall rotation τ_2 are often based on the Debye equation for the dipolar correlation time τ_μ of a spherical molecule of radius a in a hydrodynamic fluid with macroscopic viscosity η[51, 52]:

$$\tau_2 = \tfrac{1}{3}\tau_\mu = \frac{4\pi a^3 \eta}{3kT} \qquad (44)$$

It is well known that dielectric relaxation times calculated from the Debye equation are frequently too large by a factor of from five to ten.[52] This can be ascribed to the fact that the viscosity, a bulk property, is not representative of the interactions at the molecular level. Gierer and Wirtz[53] have pointed out that the introduction of a microviscosity correction factor for rotational diffusion improves the agreement between the experimental and the calculated correlation times:

$$f = \left[6\, a_1/a_2 + (1 + a_1/a_2)^{-3}\right]^{-1} \qquad (45)$$

where a_1 and a_2 are, respectively, the radii of the solvent and solute molecules. This concept has been successfully applied to problems

of nuclear and dielectric relaxation and we shall use it here. Thus

$$\tau_2 \approx \frac{4\pi a_2^{\,3}\eta}{3kT}\left[6\, a_1/a_2 + (1 + a_1/a_2)^{-3}\right]^{-1} \tag{46}$$

The molecular radii $a \equiv (a_x a_y a_z)^{\frac{1}{3}}$, the a_i's being the molecular semiaxes, have been determined from measurements on CPK space-filling molecular models.

The intramolecular dipolar contribution to the relaxation of the fluorine nuclei may be obtained from Equations (18), (19), (20), (43), (46), and, where appropriate, (13). For pure φCF_3 at 240°K

$$R_A \approx 0.029 \text{ sec}^{-1} \tag{47}$$

which is of the order of 10% of $(1/T_1)_{intra}$; R_A is much smaller, both absolutely and relative to $(1/T_1)_{intra}$, at temperatures greater than 240°K. R_A is also very small for φCF_3 and hexafluorobutyne-2 at infinite dilution in various solvents at 298°K. Consequently the intramolecular dipolar contribution to relaxation may be neglected and

$$(1/T_1)_{intra} \approx R_C \tag{48}$$

<u>viz.</u>, the intramolecular contribution is due to the spin-rotational interaction. Since the internal rotation is essentially free, the spin-rotation contribution to relaxation R_C is dominated by the spin–internal-rotation coupling. Thus

$$(1/T_1)_{intra} \approx \frac{8\pi^2 kT I_\alpha C_\alpha^2 \tau_{j'}}{3\hbar^2} \qquad (49)$$

We have attempted to explain the various experimental results with Eq. (49) and various models for $\tau_{j'}$. The experimental data cannot be explained by assuming that, for example, $\tau_{j'}$ is proportional to τ_1. Such an approach fails to account for the rapid relaxation of both benzotrifluoride and hexafluorobutyne-2 at 298°K (i. e., $\tau_1 \ll \tau_{j'}$) and predicts a temperature dependence of $(1/T_1)_{intra}$ for φCF_3 that is much different from that observed experimentally. Furthermore, it predicts that, because of the viscosity dependence, the rate of relaxation of hexafluorobutyne-2 should be four times greater in diethyl ether than in CCl_4 whereas the observed difference is about 30%. Similar analyses can also show that $\tau_{j'}$ is not proportional to either an inverse combination of τ_1 and τ_2 [e. g., Eq. (24)] or an inverse collision frequency calculated from the kinetic theory of gases.[54] Thus we are forced to conclude that Eq. (49) is not applicable and/or $\tau_{j'}$ exhibits peculiar temperature and viscosity dependences.

In order to reassess the problem let us return to the total spin-rotational Hamiltonian for a molecule with a symmetric internal top

$$\mathcal{H}_{SR} = -h \sum_k \left\{ \vec{I}_k \cdot \mathcal{C}(k) \cdot \vec{J} + C_\alpha (1 - I_\alpha / I_{aa}) \vec{I}_k \cdot \vec{j} \right\} \qquad (27)$$

which may be abbreviated as

$$\mathcal{H}_{SR} = \mathcal{H}_J + \mathcal{H}_j \qquad (50)$$

where $\mathcal{H}_J$ is that part of the total Hamiltonian which is dependent upon the total angular momentum $\vec{J}$ and $\mathcal{H}_j$ is that part which is dependent upon the relative internal angular momentum $\vec{j}$. As was pointed out in the General Introduction, the rate of relaxation is proportional to the spectral energy density of the fluctuating Hamiltonian. Thus

$$R_C \propto \int_{-\infty}^{\infty} \overline{\langle m|\mathcal{H}_{SR}(t+\tau)|k\rangle \langle k|\mathcal{H}_{SR}(t)|m\rangle} e^{-i\omega_{mk}\tau} d\tau \qquad (51)$$

which, upon substitution of Eq. (50), becomes

$$\begin{aligned} R_C \propto & \int_{-\infty}^{\infty} \overline{\langle m|\mathcal{H}_J(t+\tau)|k\rangle \langle k|\mathcal{H}_J(t)|m\rangle} e^{-i\omega_{mk}\tau} d\tau \\ & + \int_{-\infty}^{\infty} \overline{\langle m|\mathcal{H}_J(t+\tau)|k\rangle \langle k|\mathcal{H}_j(t)|m\rangle} e^{-i\omega_{mk}\tau} d\tau \\ & + \int_{-\infty}^{\infty} \overline{\langle m|\mathcal{H}_j(t+\tau)|k\rangle \langle k|\mathcal{H}_J(t)|m\rangle} e^{-i\omega_{mk}\tau} d\tau \\ & + \int_{-\infty}^{\infty} \overline{\langle m|\mathcal{H}_j(t+\tau)|k\rangle \langle k|\mathcal{H}_j(t)|m\rangle} e^{-i\omega_{mk}\tau} d\tau \qquad (52) \end{aligned}$$

If the fluctuations of $\mathcal{H}_J$ and $\mathcal{H}_j$ were completely correlated, the relaxation could be characterized by a simple correlation time such as $\tau_{j'} = \tau_1$. However, if the fluctuations were completely uncorrelated, the cross-correlation terms--the second and third terms of Eq. (52)--would vanish and the rate of relaxation would be given by

$$R_C \propto \langle \mathcal{H}_J(0)^2 \rangle \tau_J + \langle \mathcal{H}_j(0)^2 \rangle \tau_j \tag{53}$$

with the customary assumptions of extreme narrowing and exponential time dependence of the auto-correlation functions. Since the first term is just the spin-rotation interaction in a rigid molecule and the second term is of the order of $(1 - I_\alpha/I_{aa})^2$ times Dubin and Chan's result, we may write

$$R_C \approx \frac{8\pi^2 kT(I_a + I_b + I_c)\,(C_{aa}^2 + C_{bb}^2 + C_{cc}^2)\,\tau_J}{9\hbar^2} + (1 - I_\alpha/I_{aa})^2 \times \frac{8\pi^2 kTI_\alpha C_\alpha^2 \tau_j}{3\hbar^2} \tag{54}$$

which, evaluated at 298°K, is

$$(1/T_1)_{intra} \approx R_C \approx \left\{ \begin{matrix} 8.36 \times 10^{11} \\ 10.82 \times 10^{11} \end{matrix} \right\} \tau_J + 1.43 \times 10^{11} \tau_j \tag{55}$$

The upper coefficient of τ_J pertains to φCF_3; the lower, to hexafluorobutyne-2.

The correlation time τ_J is equivalent to τ_1 and will be given by

$$\tau_J = n_J \tau_1 = n_J \overline{I}/6kT\,\tau_2 \tag{56}$$

where n_J is an undetermined numerical factor. The nature of the correlation time τ_j is less clear. However, we shall assume that τ_j is given by an expression analogous to Eq. (56):

$$\tau_j = n_j I_\alpha / kT \; \tau_2^{int} = n_j [I_\alpha / kT]^{\frac{1}{2}} \qquad (57)$$

Since the assumed form of τ_j is dependent only upon the properties of the top, it has the same value for both φCF_3 and hexafluorobutyne-2. Thus, according to Eq. (55), a plot of $(1/T_1)_{intra}$ versus τ_1 should give two straight lines with a common intercept. However, Figure 6 shows that, within experimental error, the data lie on a single straight line. A comparison of the calculated intercept and slopes with the experimental values leads to $n_j = 3.0$ and $n_J = 0.69$ and 0.53 for, respectively, benzotrifluoride and hexafluorobutyne-2. The difference between the values of n_J may arise from the fact that hexafluorobutyne-2 is "less spherical" than φCF_3 and that consequently Hubbard's treatment may be somewhat less valid. In any case, the values of n_J and n_j are not at all unreasonable.

We have calculated the temperature dependence of $(1/T_1)_{intra}$ for φCF_3 using Equations (54), (56), and (57) with the parameters $n_J = 0.69$ and $n_j = 3.0$. The results of this calculation are compared with the experimental results in Figure 7; the contribution from each term is also shown. The agreement is very good and may be regarded as a stringent test of the concepts behind Eq. (54).

The second term in Eq. (54), arising from the fluctuations of the

FIGURE 6

$(1/T_1)_{intra}$ vs. τ_1 for hexafluorobutyne-2 and benzotrifluoride.

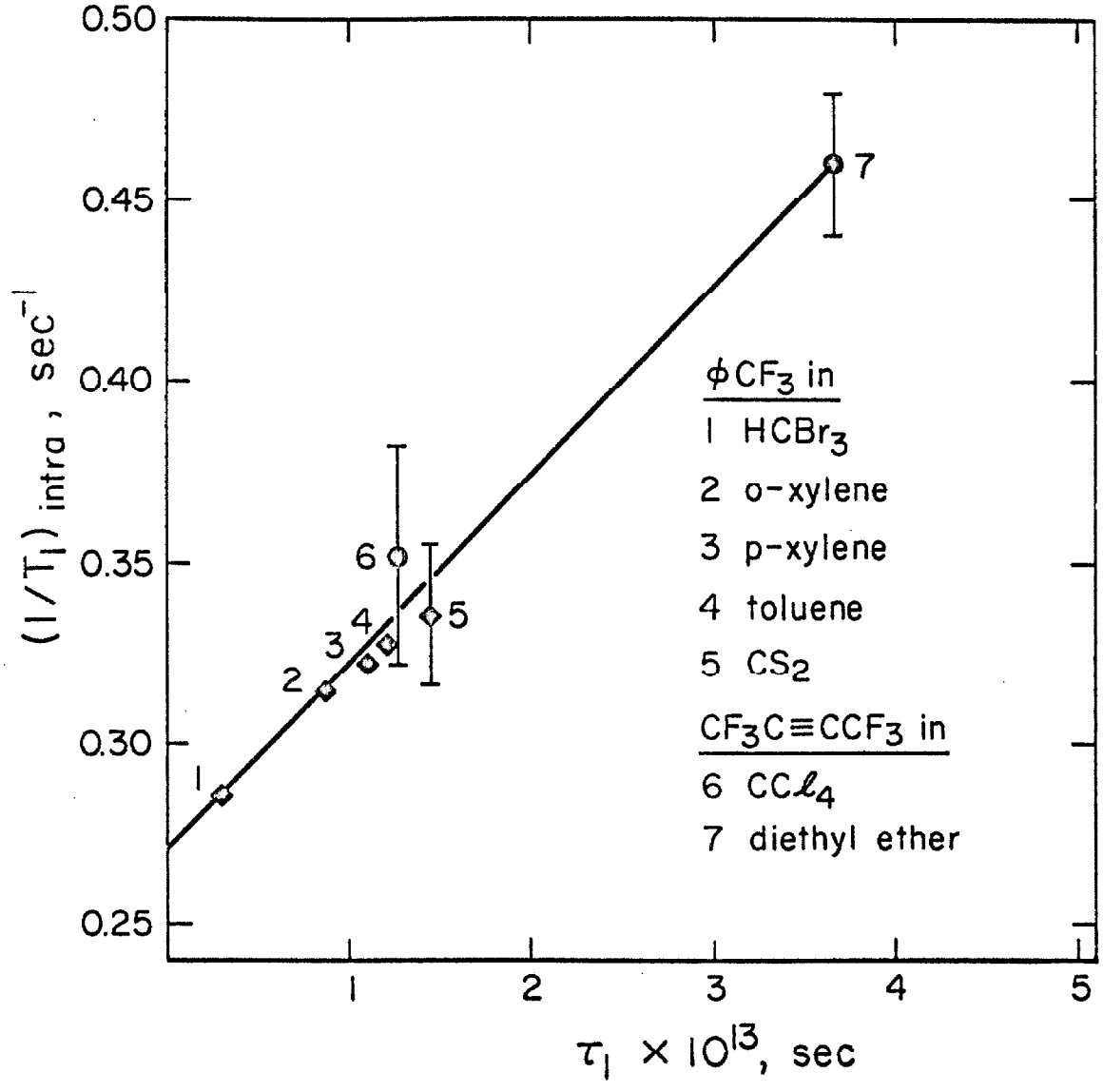
0.50
0.45
0.40
0.35
0.30
0.25
$(1/T_1)_{intra}$, sec^{-1}
1
2
3
4
5
6
7
ϕCF_3 in
1 $HCBr_3$
2 o-xylene
3 p-xylene
4 toluene
5 CS_2
$CF_3C\equiv CCF_3$ in
6 $CC\ell_4$
7 diethyl ether
1
2
3
4
5
$\tau_1 \times 10^{13}$, sec

FIGURE 7

A comparison of the experimental (o) and theoretical (—) temperature dependence of $(1/T_1)_{intra}$ for benzotrifluoride. The contributions to $(1/T_1)_{intra}$ arising from overall and internal rotation are also depicted.

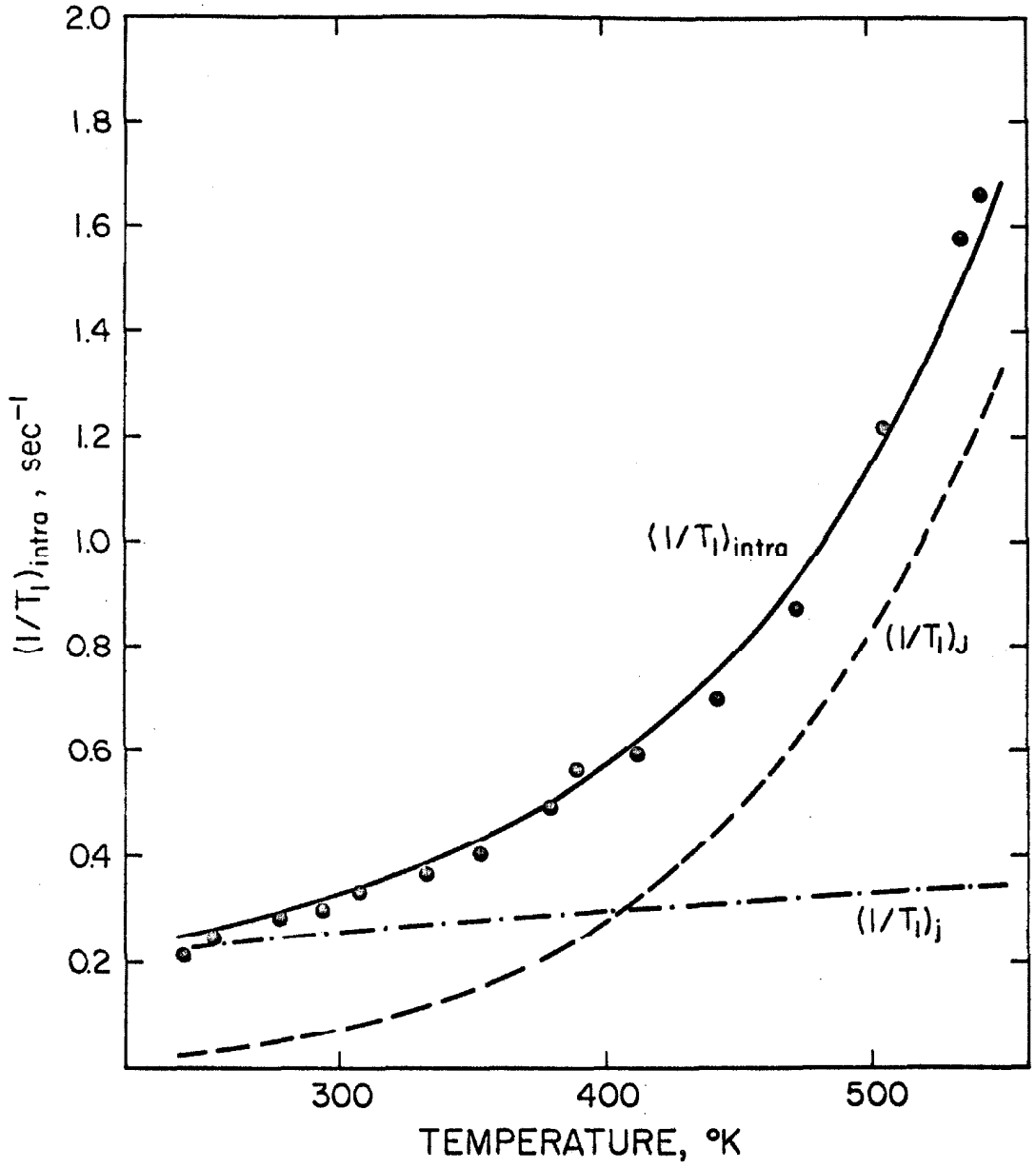
2.0
1.8
1.6
1.4
1.2
1.0
0.8
0.6
0.4
0.2
$(1/T_1)_{intra}$, sec^{-1}
$(1/T_1)_{intra}$
$(1/T_1)_J$
$(1/T_1)_j$
300
400
500
TEMPERATURE, °K

relative angular momentum $\vec{j}$, is dominant at room temperature; the first term contributes significantly only at higher temperatures. The observations of Dubin and Chan are consistent with this interpretation. Ortho substitution increases the barrier to internal rotation thereby quenching the fluctuations of $\vec{j}$. The "residual" relaxation of the ortho substituted benzotrifluorides is due to the slightly enhanced intramolecular dipolar interaction and to the small spin-rotational contribution arising from fluctuations of $\vec{J}$. Meta and para substitution have no effect on the barrier and, consequently, no effect on the fluctuations of $\vec{j}$; thus the rate of relaxation is unchanged.

When the correlation time for internal reorientation becomes very long in the high barrier limit the second term in Eq. (54) vanishes leaving the spin-rotational relaxation rate for a rigid molecule.

6. 2. Methyl Substituted Benzenes

Pritchard and Richards[17] have measured the rates of relaxation of the ring and methyl protons of toluene and para-xylene as a function of concentration in CS_2 and, assuming only dipolar interactions, have determined the correlation times from the rates extrapolated to infinite dilution. They note that for both molecules $(\tau_2^{\text{eff}})_{\text{methyl}} = 0.75\ (\tau_2)_{\text{ring}}$. Within the framework of their interpretation, Woessner's results for nuclei undergoing simultaneous overall and step-wise internal motion[37] lead to the conclusion that

$$\tau_2^{\text{int}} \approx 2(\tau_2)_{\text{ring}} = 2\tau_2 \qquad (58)$$

Therefore, according to the data and the interpretation of Pritchard and Richards, the correlation times for internal reorientation must be about 3.4×10^{-12} and 4.8×10^{-12} sec for toluene and para-xylene, respectively.

Their conclusions are highly suspect since the barriers to internal rotation are very low for toluene and para-xylene.[55, 56] The work of Stejskal and Gutowsky[57] indicates that, for a freely rotating CH_3 top, τ_2^{int} is about 6×10^{-14} sec which is identical to the value obtained from Steele's inertial model. We are led to the conclusion that $\tau_2^{int} \ll \tau_2$ and that, consequently, $\tau_2^{eff} \approx \frac{1}{4}\tau_2$. Thus the intramolecular dipolar interaction accounts for only one-third of the observed intramolecular relaxation.

We suggest that the spin-rotation interaction which has already been observed at high temperatures ($T > 500°K$)[11] accounts for the difference. Since $I_\alpha \ll I_{aa}$ and $C_\alpha^2 \gg C_{aa}^2 \sim C_{bb}^2 \sim C_{cc}^2$, at 298°K, Eq. (54) reduces to

$$R_C \approx \frac{8\pi^2 kT I_\alpha C_\alpha^2 \tau_j}{3\hbar^2} \approx 1.10 \times 10^{11} \tau_j \qquad (59)$$

Thus, Eq. (57) with $n_j = 3.0$ leads to

$$R_C \approx 0.04 \text{ sec}^{-1} \qquad (60)$$

Therefore the intramolecular contributions to relaxation, including intramolecular dipolar and spin–internal-rotation interactions, are 0.06 sec^{-1} for both toluene and para-xylene; the respective

experimental values are 0.06 and 0.08 sec^{-1}. This, we believe, is a more physically realistic interpretation than Pritchard and Richards'.

7. Conclusions

For molecules with internal rotors, the fluctuating rotational magnetic field at the site of nuclei on the top is composed of contributions from both the overall rotation and the internal rotation of the top. The problem of the interaction of the nuclei with the total fluctuating field may be approached by assuming that the two fields are completely coupled and that their time evolution is described by a single time constant. An alternative approach involves the assumption that the two fields are fluctuating independently and that each field is described by a distinct correlation time. We have shown that the latter approach provides a coherent explanation of the viscosity dependence of the fluorine relaxation of both benzotrifluoride and hexafluorobutyne-2, the temperature dependence of the fluorine relaxation in φCF_3, and the effect of ortho, meta, and para substituents on the fluorine relaxation in φCF_3. We have also shown that the spin-rotation coupling contributes to the room temperature relaxation of the methyl group protons in toluene and para-xylene.

REFERENCES

(1) See, for example, N. F. Ramsey, Molecular Beams (Oxford University Press, London, 1956), Chap. VIII.

(2) See, for example, C. H. Townes and A. L. Schalow, Microwave Spectroscopy (McGraw-Hill Book Company, Inc., New York, 1952).

(3) N. F. Ramsey, Am. Scientist 49, 509 (1961).

(4) C. H. Anderson and N. F. Ramsey, Phys. Rev. 149, 14 (1966).

(5) P. Yi, I. Ozier, A. Khosia, and N. F. Ramsey, Bull. Am. Soc. 12, 509 (1967).

(6) L. Crapo, Ph.D. Thesis, Harvard University, 1964, unpublished.

(7) S. I. Chan and A. S. Dubin, J. Chem. Phys. 46, 1745 (1967).

(8) A. Abragam, The Principles of Nuclear Magnetism (Oxford University Press, London, 1961), Chap. VIII.

(9) H. S. Gutowsky, I. J. Lawrenson, and K. Shimomura, Phys. Rev. Letters 6, 349 (1961).

(10) R. J. C. Brown, H. S. Gutowsky, and K. Shimomura, J. Chem. Phys. 38, 76 (1963).

(11) D. K. Green and J. G. Powles, Proc. Phys. Soc. (London) 85, 87 (1965).

(12) C. S. Johnson, Jr., J. S. Waugh, and J. N. Pinkerton, J. Chem. Phys. 35, 1128 (1961).

(13) C. S. Johnson, Jr., and J. S. Waugh, J. Chem. Phys. 35, 2020 (1961).

(14) P. S. Hubbard, Phys. Rev. 131, 1155 (1963).

(15) R. H. Faulk and M. Eisner, J. Chem. Phys. 44, 2926 (1966).

(16) A. S. Dubin and S. I. Chan, J. Chem. Phys. 46, 4534 (1967).

(17) A. M. Pritchard and R. E. Richards, Trans. Faraday Soc. 62, 1388 (1966).

(18) H. Y. Carr and E. M. Purcell, Phys. Rev. 94, 630 (1954).

(19) W. G. Clark, Rev. Sci. Instr. 35, 316 (1964).

(20) E. O. Stejskal, Rev. Sci. Instr. 34, 971 (1963).

(21) See, for example, R. R. Ernst, "Sensitivity Enhancement in Magnetic Resonance," in Advances in Magnetic Resonance, ed. by J. S. Waugh (Academic Press, New York, 1966), Vol. 2, p. 1.

(22) H. S. Gutowsky and D. E. Woessner, Phys. Rev. 104, 843 (1956).

(23) H. M. McConnell and C. H. Holm, J. Chem. Phys. 25, 1289 (1956).

(24) M. D. Zeidler, Ber. Bunsenges. physik. Chem. 69, 659 (1965).

(25) See, for example, J. R. Parington, An Advanced Treatise on Physical Chemistry (Longmans, Green, and Co., New York, 1950), Section VIII-C.

(26) G. P. Rutledge and W. T. Smith, Jr., J. Am. Chem. Soc. 75, 5762 (1953).

(27) S. Glasstone, K. J. Laidler, and H. Eyring, Theory of Rate Processes (McGraw-Hill Book Company, Inc., New York, 1941), Chap. VIII.

(28) R. B. Bird, W. E. Stewart, and E. N. Lightfoot, Transport Phenomena (John Wiley & Sons, Inc., New York, 1960), p. 26.

(29) P. S. Hubbard, Phys. Rev. 109, 1153 (1958); 128, 650 (1962).

(30) G. W. Kattawar and M. Eisner, Phys. Rev. 126, 1054 (1962).

(31) H. Schneider, Z. Naturforsch. 19a, 510 (1964).

(32) H. Schneider, Ann. Physik 7. Flg. 13, 313 (1964); 16, 135 (1965).

(33) L. K. Runnels, Phys. Rev. 134A, 28 (1964).

(34) H. G. Hertz, "Microdynamic Behaviour of Liquids as Studied by NMR Relaxation Times," in Progress in Nuclear Magnetic Resonance Spectroscopy, ed. by J. W. Emsley, J. Feeney, and L. H. Sutcliffe (Pergamon Press, Oxford, 1967), Vol. 3, p. 159.

(35) D. E. Woessner, J. Chem. Phys. 37, 647 (1962).

(36) H. Shimizu, J. Chem. Phys. 37, 765 (1962).

(37) D. E. Woessner, J. Chem. Phys. 36, 1 (1962); 42, 1855 (1965).

(38) W. F. Sheehan, Jr., and V. Schomaker, J. Am. Chem. Soc. 74, 4468 (1952).

(39) R. Schwartz, Ph. D. Thesis, Harvard University, 1953, unpublished.

(40) N. Muller and D. T. Carr, J. Phys. Chem. 67, 112 (1963).

(41) A. Carrington and A. D. McLachlan, Introduction to Magnetic Resonance (Harper & Row, New York, 1967), p. 62.

(42) A. B. Harris, E. Hunt, and H. Meyer, J. Chem. Phys. 42, 2851 (1965).

(43) J. W. Emsley, J. Feeney, and L. H. Sutcliffe, High Resolution Nuclear Magnetic Resonance Spectroscopy (Pergamon Press, Oxford, 1966), Vol. 2, p. 883.

(44) K. S. Pitzer, Disc. Faraday Soc. 10, 66 (1951).

(45) P. R. Bunker and H. C. Longuet-Higgins, Proc. Roy. Soc. (London) A280, 340 (1964).

(46) E. L. Pace, J. Chem. Phys. 16, 74 (1948).

(47) D. W. Scott, D. R. Douslin, J. F. Messerly, S. S. Todd, I. A. Hossenlopp, T. C. Kincheloe, and J. P. McCullough, J. Am. Chem. Soc. 81, 1015 (1959).

(48) W. A. Steele, J. Chem. Phys. 38, 2404 (1963); 38, 2411 (1963).

(49) W. B. Moniz, W. A. Steele, and J. A. Dixon, J. Chem. Phys. 38, 2418 (1963).

(50) P. Debye, Polar Molecules (Chemical Catalog Co., New York, 1929).

(51) N. Bloembergen, E. M. Purcell, and R. V. Pound, Phys. Rev. 73, 679 (1948).

(52) See, for example, W. P. Connor and C. P. Smyth, J. Am. Chem. Soc. 65, 382 (1943).

(53) A. Gierer and K. Wirtz, Z. Naturforsch. 8a, 532 (1953).

(54) A. A. Frost and R. G. Pearson, Kinetics and Mechanism (John Wiley & Sons, Inc., New York, 1961), 2nd ed., p. 129.

(55) K. S. Pitzer and D. W. Scott, J. Am. Chem. Soc. 65, 803 (1943).

(56) W. J. Taylor, D. D. Wagman, M. G. Williams, K. S. Pitzer, and F. D. Rossini, J. Research Natl. Bur. Standards 37, 95 (1946).

(57) E. O. Stejskal and H. S. Gutowsky, J. Chem. Phys. 28, 388 (1958).

III. THE EFFECT OF SOLVENTS ON NUCLEAR SPIN RELAXATION

1. Introduction[1]

According to the Debye theory of dielectric dispersion, the motion of a polar molecule is assumed to be the same as that of a sphere of radius a imbedded in a viscous medium. From the model, the dipolar relaxation time τ_μ is found to be

$$\tau_\mu = \frac{4\pi a^3 \eta}{kT} \tag{1}$$

Although qualitative agreement between experimental and calculated values is found for pure liquids, the results in solution are less satisfactory. Various models have been proposed to account for the observed discrepancies: some, such as Hase's,[2] are strictly empirical; others, most notably Hill's,[3] represent efforts to use a more realistic model than the Debye model. The validity of some models has been explored by dielectric relaxation techniques.

It is well known that the orientation fluctuations which lead to dielectric relaxation can also cause nuclear spin-lattice relaxation,[4] the rate of relaxation $(1/T_1)$ being related to the correlation time τ_2 where

$$\tau_2 \approx \tfrac{1}{3}\tau_\mu \tag{2}$$

Although the two methods overlap somewhat, each method is capable

of providing unique information. Dielectric relaxation measurements give information concerning the distribution of correlation times about a most probable value whereas nuclear spin relaxation provides only the most probable value. Dielectric relaxation measurements are generally restricted to polar molecules in the pure liquid or in non-polar solvents whereas nuclear spin relaxation techniques are applicable to polar and non-polar solutes in polar and non-polar solvents. Although nuclear resonance techniques have been extensively applied to studies of molecular motion, both internal and overall, there have been only a few rudimentary attempts to study the effects of solvents on such motions.[5]

We report the results of studies of the effects of solvents on the ^{19}F spin-lattice relaxation of a series of solute molecules; the effects of both polar and non-polar solvents are investigated. We discuss the results in terms of various models and establish several criteria which enable us to assess the validity of the models.

2. Experimental

2. 1. Relaxation Time Measurements

The spin-lattice relaxation times T_1 were determined according to the procedures outlined in Section II. 2. 1.

2. 2. Sample Preparation

The halogen substituted 1, 1, 1-trifluoroethanes (CF_3CH_2Cl,

CF_3CH_2Br, CF_3CH_2I, and CF_3CCl_3) were obtained from Pierce Chemical Company and from Peninsular Chemresearch, Inc. CF_3CH_2I and CF_3CCl_3 were distilled prior to use. CF_3CH_2Cl (bp 6.9°C), CF_3CH_2Br (bp 26°C), and the spectral grade solvents were used without further purification.

The CF_3CH_2Cl and CF_3CH_2Br samples were prepared by condensing the gas from a calibrated volume into a sample tube containing a known amount of solvent. The quantity of gas transferred was determined from the pressure change in the manifold; the quantity of solvent was determined volumetrically. The solute and solvent were then transferred to a second sample tube by means of a trap-to-trap distillation in order to rid the solution of any non-volatile materials. The solution was then carefully degassed by repeated freeze-pump-thaw cycles. Since CF_3CH_2I and CF_3CCl_3 are liquids, the quantities of both solute and solvent were determined volumetrically; otherwise, all samples were prepared in the same manner.

2.3. Viscosity and Density Measurements

The viscosities and densities were determined by standard techniques at 25.0°C. The viscometer (Ostwald-Cannon-Fenske) was calibrated with five liquids whose accurately known viscosities spanned the range of experimental interest (0.2 - 1.0 cP). The estimated error of the viscosity measurements is less than ± 2%.

2. 4. Determination of Molecular Dipole Moments

Molecular dipole moments were determined according to the method proposed by Guggenheim[6]:

$$\mu^2 = \frac{9kT}{4\pi N} \frac{3}{(\epsilon_0 + 2)(n_0^2 + 2)} \left(\frac{\Delta}{c}\right)_{c=0} \qquad (3)$$

in which $(\Delta/c)_{c=0}$ is the slope, evaluated at c = 0, of a plot of Δ versus c, where

$$\Delta = (\epsilon - n^2) - (\epsilon_0 - n_0^2) \qquad (4)$$

c is the concentration (moles per ml) of a dilute solution of the polar molecule in a non-polar solvent, ϵ and n are the dielectric constant and refractive index of the solution, and ϵ_0 and n_0 are the dielectric constant and refractive index of the pure solvent: sodium-dried benzene (ϵ = 2. 284 and n_D = 1. 501 at 20°C). Each dipole moment determination was based upon evaluation of the function Δ at four concentrations. The static dielectric constants were determined at 20°C with a heterodyne beat apparatus operating at 1 MHz. The refractive indices were determined at 20°C with an Abbe refractometer using the sodium-D line.

3. Experimental Results

3. 1. Spin-Lattice Relaxation Rates

The fluorine spin-lattice relaxation rates ($1/T_1$) have been determined as a function of concentration for solutions of CF_3CH_2Cl, CF_3CH_2Br, CF_3CH_2I, and CF_3CCl_3 in CS_2, CCl_4, a CS_2-CCl_4 mixture [20. 0% CS_2 + 80. 0% CCl_4 (v/v)], diethyl ether, CH_3CN, and $HCCl_3$ and also for solutions of CF_3CH_2I in benzene and acetone. In addition, the proton spin-lattice relaxation rates have been determined for several samples of CF_3CH_2Cl, CF_3CH_2Br, and CF_3CH_2I in aprotic solvents.

All experiments were performed at 25°C at a Larmor frequency of 12. 3 MHz; a number of experiments were repeated at 8. 8 MHz with no detectable difference.

Plots of the time dependence of the deviation of the magnetization from thermal equilibrium (relaxation curves) indicate that the data are in good agreement with the single exponential model and that the relaxation can be described by a single relaxation time. The relaxation curve for the least favorable experiment that we performed--a low ^{19}F concentration with a concomitantly low signal/noise ratio--is shown in Figure 1a. Relaxation curves for more typical experiments are shown in Figures 1b - 1d.

Figures 2 through 8 show the concentration dependence of the fluorine relaxation rates. The error bars correspond to ± 2%, a degree of precision indicated by repetitive experiments on approxi-

FIGURE 1

Relaxation curves for: (a) CF_3CH_2I in CS_2 [solute mole fraction $x_m = 0.080$, $T_1 = 4.91$ sec]; (b) CF_3CH_2I in CH_3CN [$x_m = 0.515$, $T_1 = 6.38$ sec]; (c) CF_3CCl_3 in CS_2 [$x_m = 0.336$, $T_1 = 7.49$ sec]; (d) CF_3CH_2Br in diethyl ether [$x_m = 0.395$, $T_1 = 5.39$ sec].

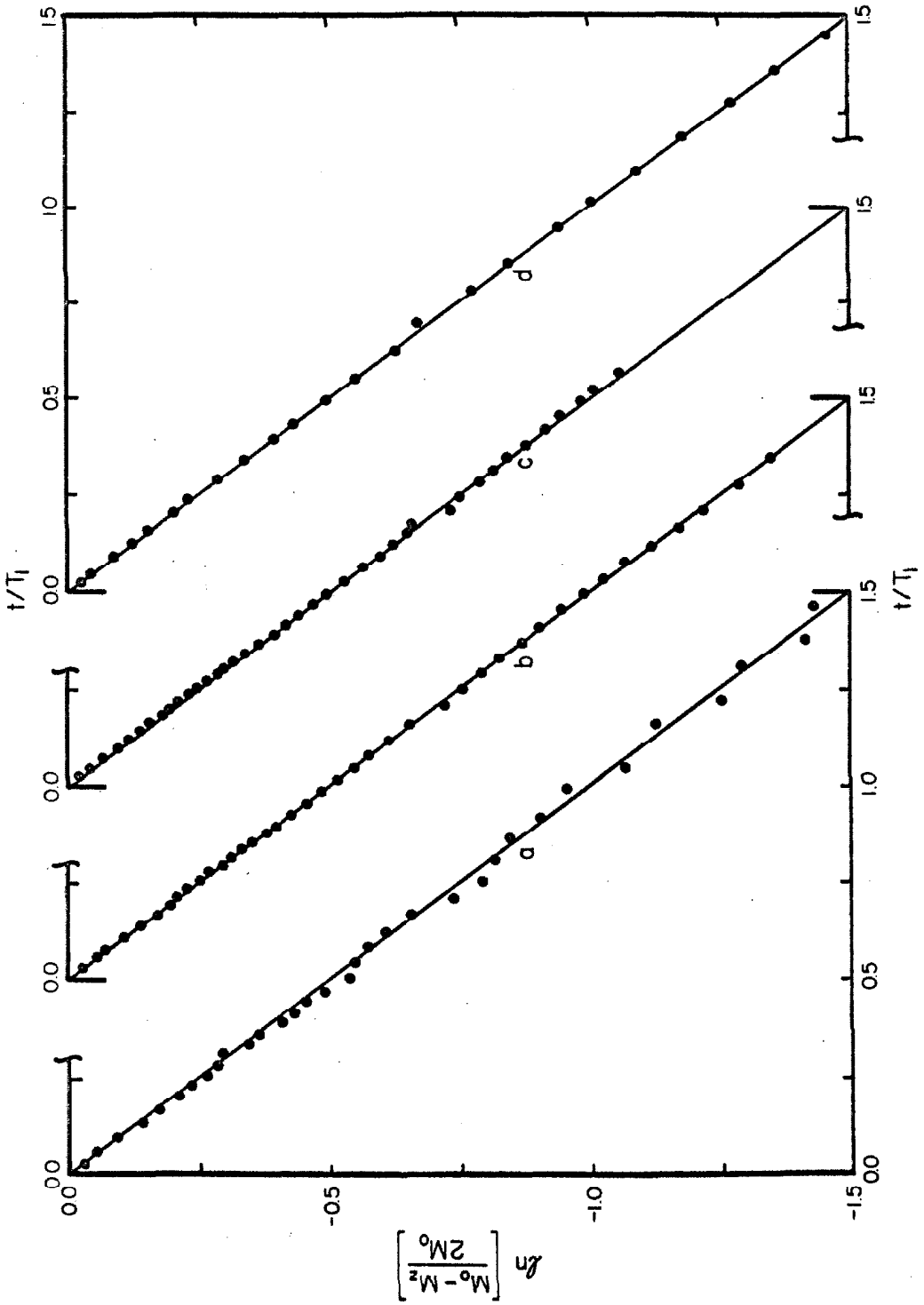
$\ln\left[\frac{M_o - M_z}{2M_o}\right]$
0.0
-0.5
-1.0
-1.5
t/T_1
0.0
0.5
1.0
1.5
a
b
c
d

FIGURE 2

Relaxation rates of CF_3CH_2Cl, CF_3CH_2Br, CF_3CH_2I, and CF_3CCl_3 as a function of concentration is CS_2. Several error bars are omitted for clarity.

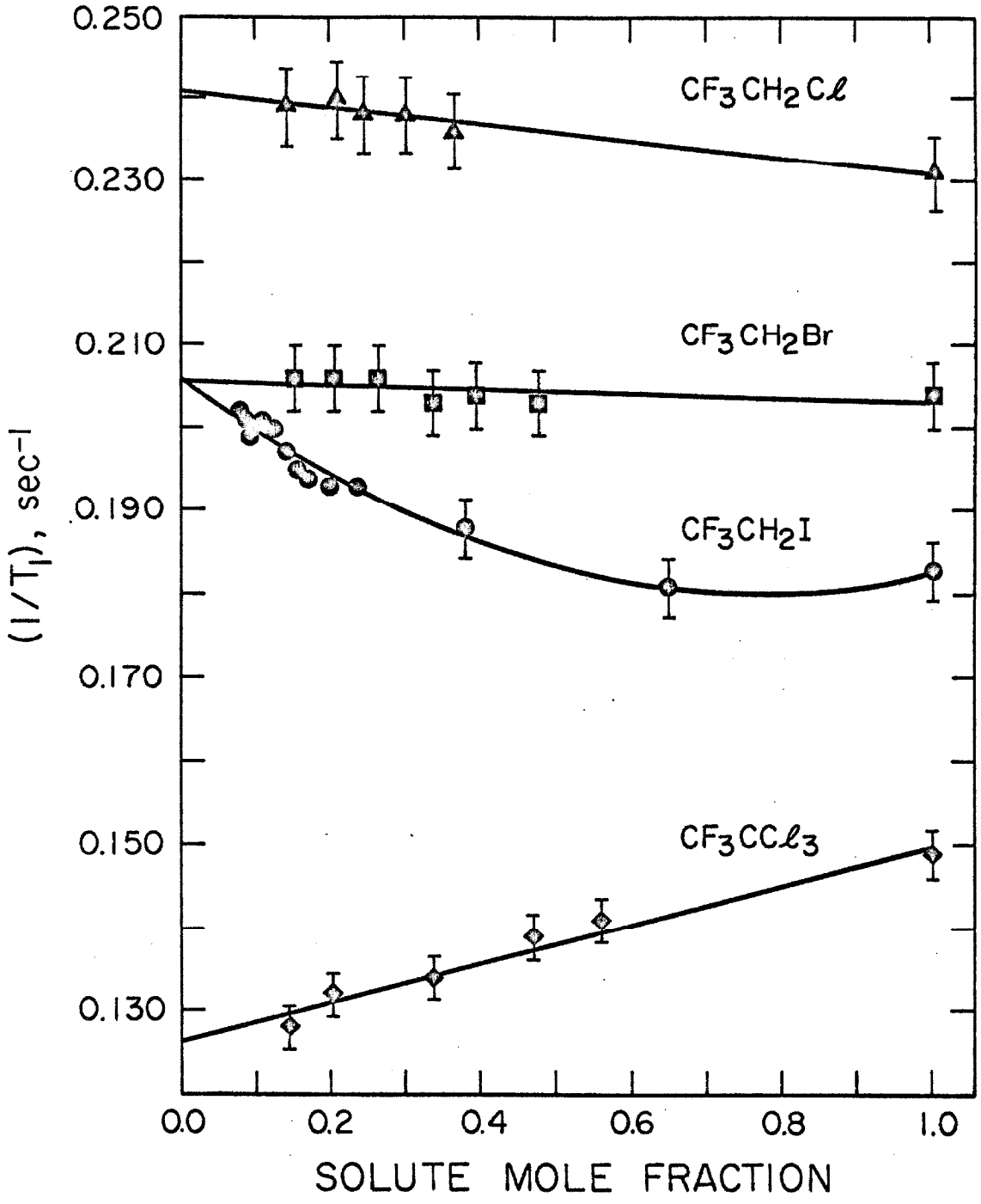
0.250
0.230
0.210
0.190
0.170
0.150
0.130
$(1/T_1)$, sec^{-1}
$CF_3CH_2C\ell$
CF_3CH_2Br
CF_3CH_2I
$CF_3CC\ell_3$
0.0
0.2
0.4
0.6
0.8
1.0
SOLUTE MOLE FRACTION

FIGURE 3

Relaxation rates of CF_3CH_2Cl, CF_3CH_2Br, CF_3CH_2I, and CF_3CCl_3 as a function of concentration in a mixture of CS_2 and CCl_4 [20.0% CS_2 + 80.0% CCl_4 (v/v)].

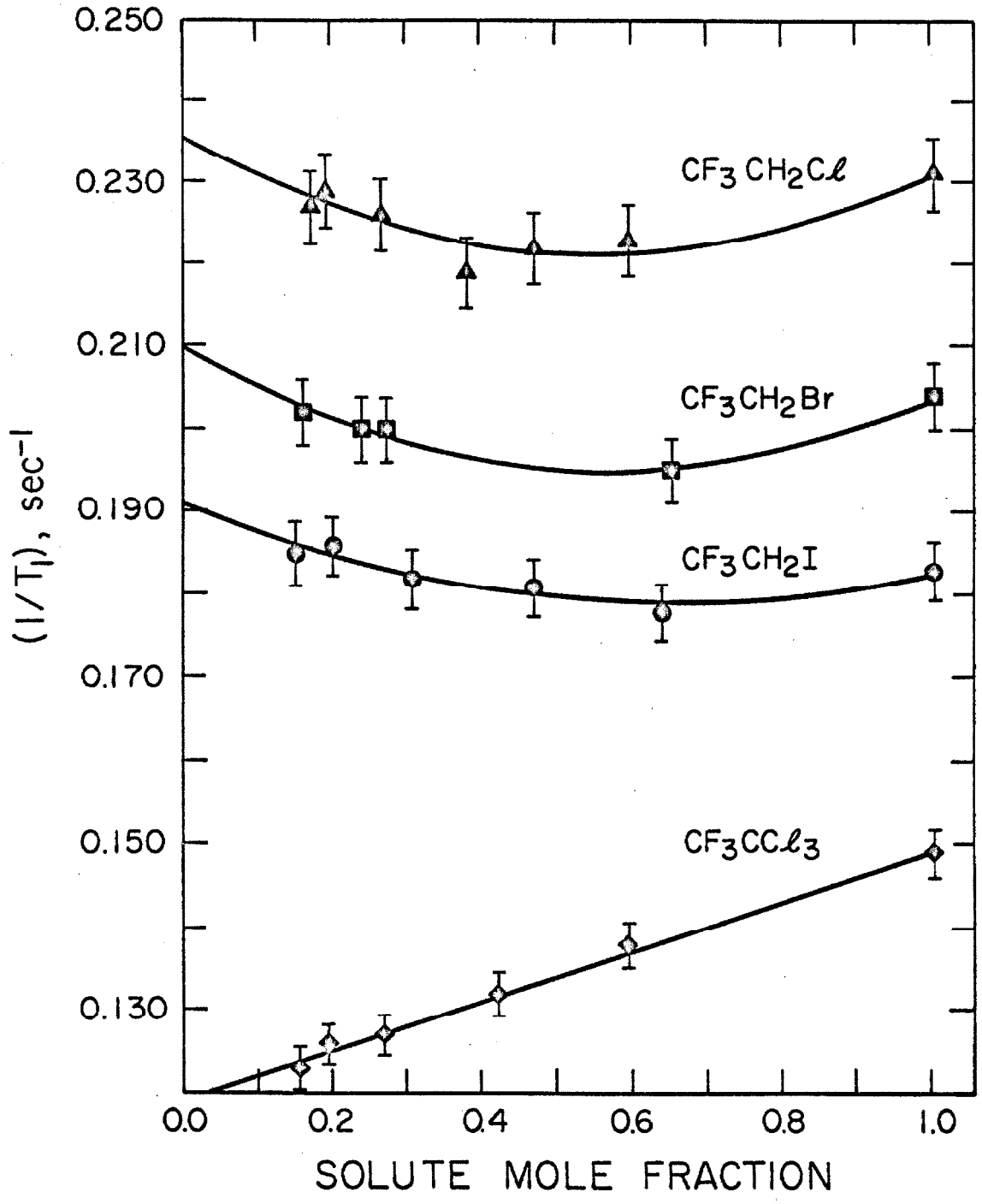
0.250
0.230
0.210
0.190
0.170
0.150
0.130
$(1/T_1)$, sec^{-1}
CF_3CH_2Cl
CF_3CH_2Br
CF_3CH_2I
CF_3CCl_3
0.0
0.2
0.4
0.6
0.8
1.0
SOLUTE MOLE FRACTION

FIGURE 4

Relaxation rates of CF_3CH_2Cl, CF_3CH_2Br, CF_3CH_2I, and CF_3CCl_3 as a function of concentration in CCl_4.

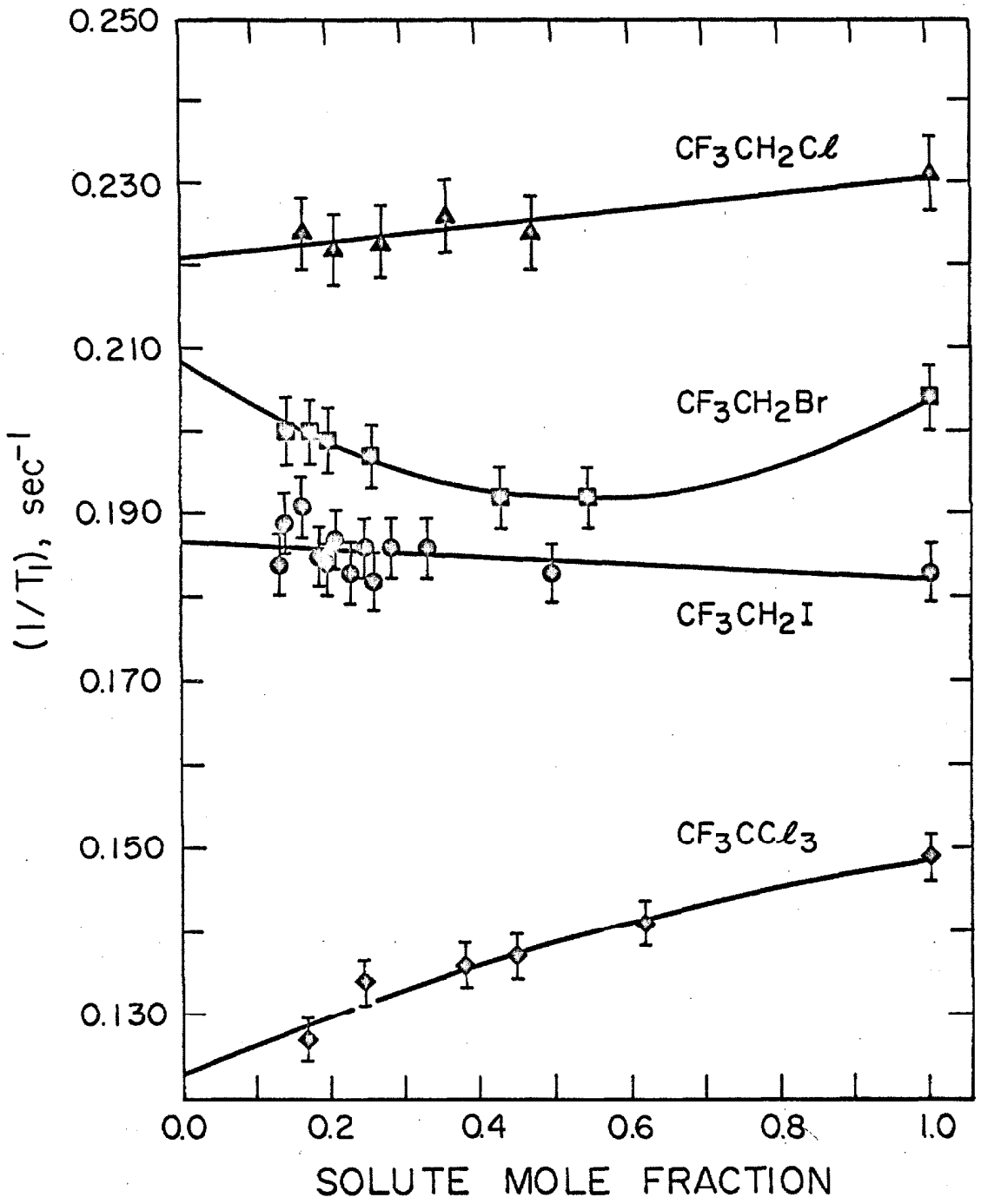
0.250
0.230
0.210
0.190
0.170
0.150
0.130
(1/T1), sec-1
CF3CH2Cl
CF3CH2Br
CF3CH2I
CF3CCl3
0.0
0.2
0.4
0.6
0.8
1.0
SOLUTE MOLE FRACTION

FIGURE 5

Relaxation rates of CF_3CH_2Cl, CF_3CH_2Br, CF_3CH_2I, and CF_3CCl_3 as a function of concentration in diethyl ether.

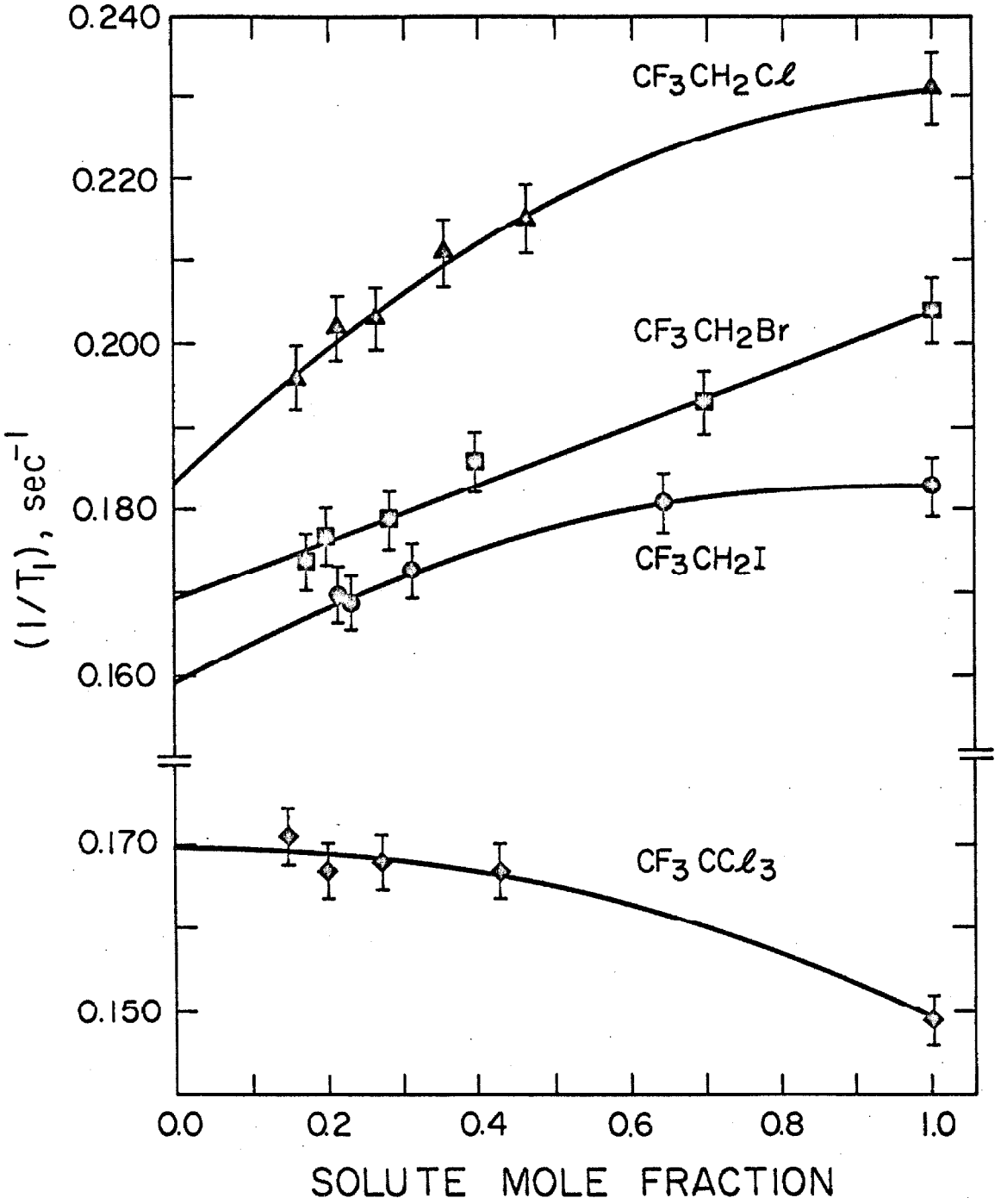
0.240
0.220
0.200
0.180
0.160
0.170
0.150
$(1/T_1)$, sec^{-1}
$CF_3CH_2C\ell$
CF_3CH_2Br
CF_3CH_2I
$CF_3CC\ell_3$
0.0
0.2
0.4
0.6
0.8
1.0
SOLUTE MOLE FRACTION

FIGURE 6

Relaxation rates of CF_3CH_2Cl, CF_3CH_2Br, CF_3CH_2I, and CF_3CCl_3 as a function of concentration in CH_3CN.

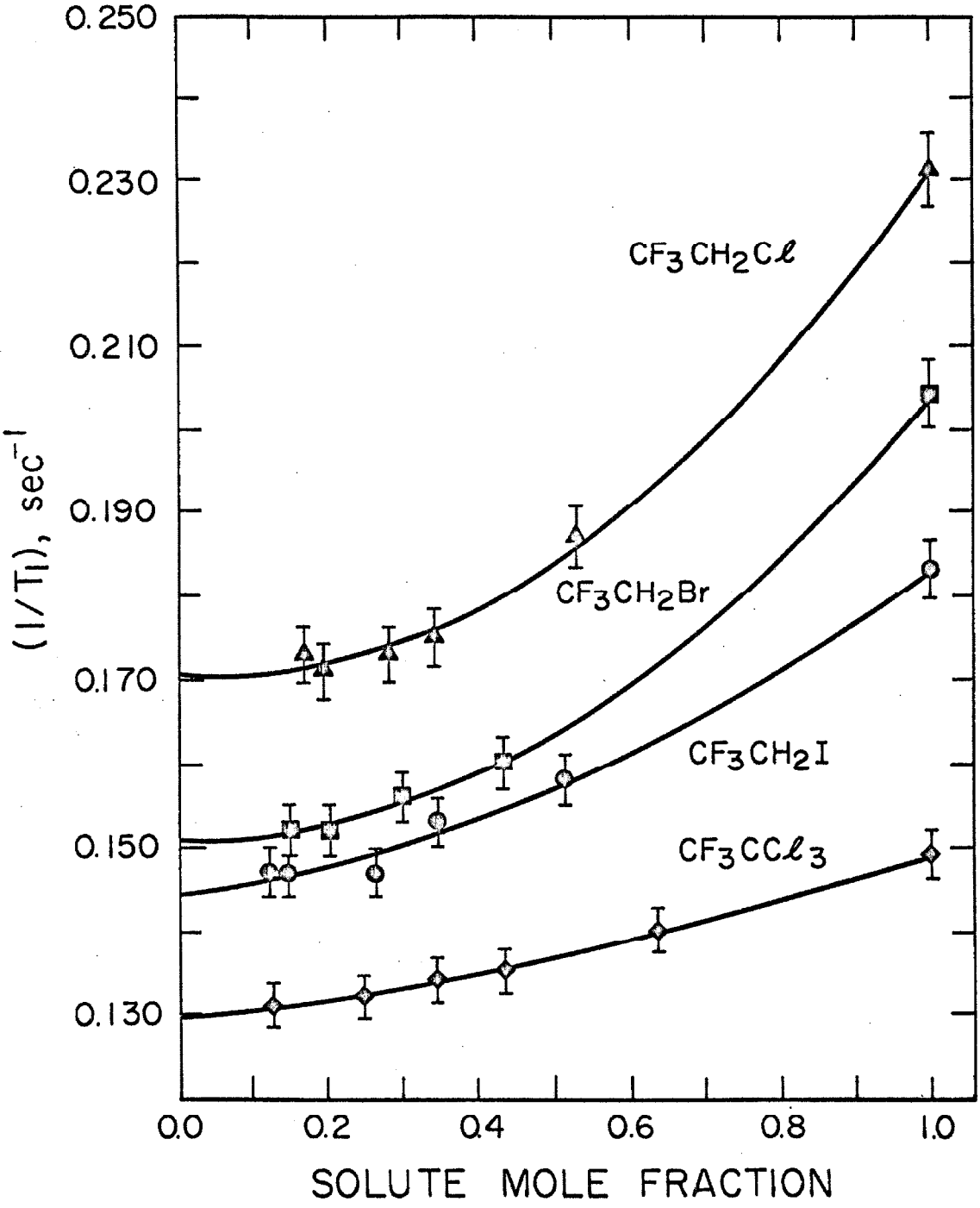
0.250
0.230
0.210
0.190
0.170
0.150
0.130
(1/T1), sec-1
CF3CH2Cℓ
CF3CH2Br
CF3CH2I
CF3CCℓ3
0.0
0.2
0.4
0.6
0.8
1.0
SOLUTE MOLE FRACTION

FIGURE 7

Relaxation rates of CF_3CH_2Cl, CF_3CH_2Br, CF_3CH_2I, and CF_3CCl_3 as a function of concentration in $HCCl_3$. Several error bars are omitted for clarity.

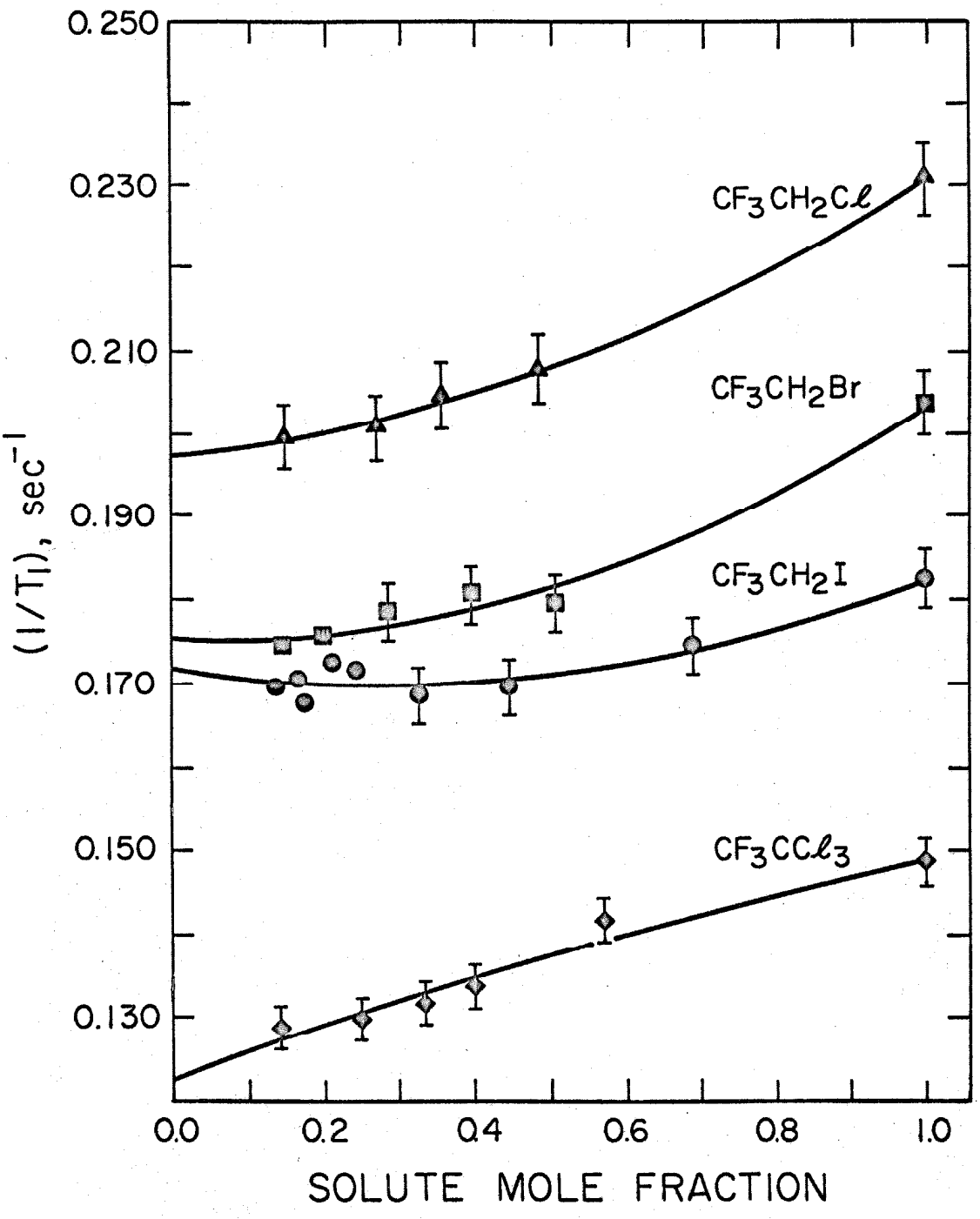
0.250
0.230
0.210
0.190
0.170
0.150
0.130
(1/T1), sec-1
CF3CH2Cℓ
CF3CH2Br
CF3CH2I
CF3CCℓ3
0.0
0.2
0.4
0.6
0.8
1.0
SOLUTE MOLE FRACTION

FIGURE 8

Relaxation rates of CF_3CH_2I as a function of concentration in benzene and acetone.

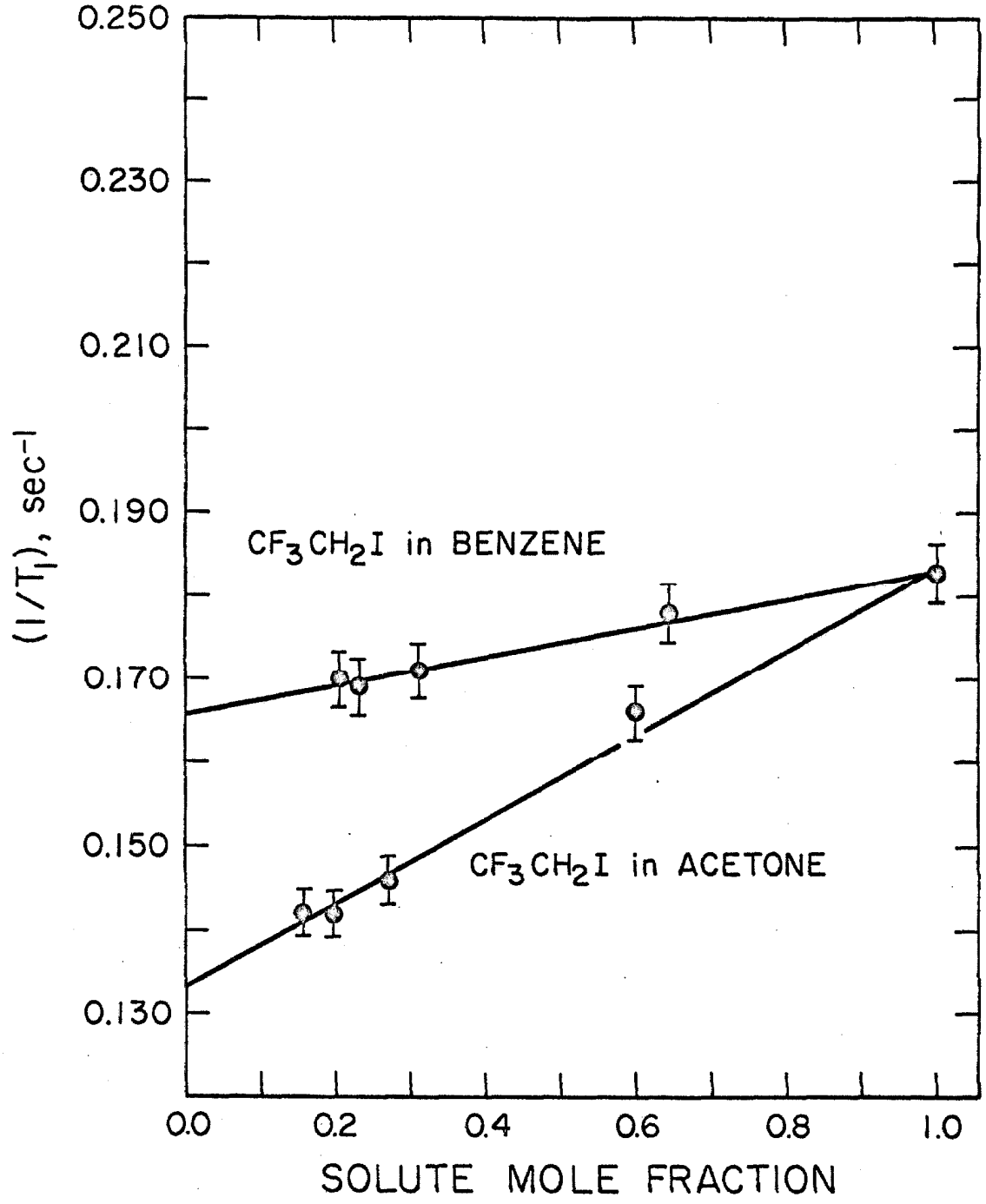
0.250
0.230
0.210
0.190
0.170
0.150
0.130
(1/T1), sec-1
CF3CH2I in BENZENE
CF3CH2I in ACETONE
0.0
0.2
0.4
0.6
0.8
1.0
SOLUTE MOLE FRACTION

mately three-fourths of the samples. The solid lines, used to extrapolate the relaxation rates to infinite dilution, represent polynomial expansions of the rates in terms of the solute mole fractions: the expansion coefficients were obtained by least-square analyses. The infinite dilution values of $(1/T_1)$ are presented in Table I.

The infinite values of the proton relaxation rates are presented in Table II. Each value is based on a linear extrapolation of only two data points since their sole purpose is to provide a crude estimate of the correlation time τ_2.

3. 2. Viscosity and Density Data

We have measured the viscosities and densities of CF_3CH_2I and CF_3CCl_3 neat and as a function of concentration in various solvents. Since the data are relevant to the interpretation of the relaxation measurements, they are presented in full in Table III. Unfortunately, it was not possible to perform comparable measurements for CF_3CH_2Cl and CF_3CH_2Br because of their low boiling points.

4. Relaxation Mechanisms

4. 1. Correction for Intermolecular Contributions to Relaxation

Since the intramolecular contributions to relaxation are of primary interest, it is necessary to separate the intra- and intermolecular contributions to relaxation. A common procedure is to measure

TABLE I

^{19}F Relaxation Rates (sec^{-1}) at Infinite Dilution

solvent	CF_3CH_2Cl	CF_3CH_2Br	CF_3CH_2I	CF_3CCl_3
CS_2	0. 241	0. 206	0. 206	0. 126
CS_2-CCl_4[a]	0. 236	0. 210	0. 191	0. 119
CCl_4	0. 221	0. 209	0. 187	0. 123
diethyl ether	0. 184	0. 170	0. 160	0. 169
CH_3CN	0. 171	0. 151	0. 144	0. 129
$HCCl_3$	0. 198	0. 176	0. 172	0. 123
acetone	---	---	0. 133	---
benzene	---	---	0. 166	---

[a] 20. 0% CS_2 + 80. 0% CCl_4 (v/v).

TABLE II

^1H Relaxation Rates (sec^{-1}) at Infinite Dilution[a]

solvent	CF_3CH_2Cl	CF_3CH_2Br	CF_3CH_2I
CS_2-CCl_4[b]	0. 06	0. 03	---
CCl_4	0. 07	0. 05	0. 05

[a]Estimated uncertainty ± 50%.

[b]20. 0% CS_2 + 80. 0% CCl_4 (v/v).

TABLE III

Density and Viscosity Data for Solutions of CF_3CH_2I and CF_3CCl_3

Solvent	CF_3CH_2I			CF_3CCl_3		
	x[a]	$\eta_{25.0°C}$ (cP)	$\rho_{25.0°C}$ (g cm^{-3})	x[a]	$\eta_{25.0°C}$ (cP)	$\rho_{25.0°C}$ (g cm^{-3})
CS_2	1.000	0.650	0.107	1.000	0.720	1.559
	0.752	0.542	1.956	0.751	0.570	1.505
	0.477	0.442	1.716	0.577	0.452	1.423
	0.278	0.391	1.510	0.272	0.392	1.343
	0.144	0.373	1.398	0.154	0.372	1.301
	0.000	0.356	1.261	0.000	0.356	1.261
CCl_4	1.000	0.650	2.107	1.000	0.720	1.559
	0.709	0.646	1.939	0.829	0.731	1.563
	0.480	0.692	1.779	0.527	0.777	1.567
	0.319	0.765	1.677	0.254	0.834	1.576
	0.157	0.834	1.615	0.110	0.870	1.580
	0.000	0.888	1.584	0.000	0.888	1.584
diethyl ether	1.000	0.650	2.107	1.000	0.720	1.559
	0.759	0.539	1.765	0.839	0.593	1.441
	0.515	0.411	1.333	0.549	0.373	1.113
	0.245	0.289	0.952	0.277	0.281	0.890
	0.000	0.222	0.708	0.162	0.248	0.788
				0.000	0.222	0.708
CH_3CN	1.000	0.650	2.107	1.000	0.720	1.559
	0.761	0.622	1.923	0.725	0.647	1.450
	0.502	0.531	1.593	0.443	0.491	1.248
	0.262	0.435	1.242	0.245	0.405	1.058
	0.154	0.387	1.035	0.148	0.366	0.925
	0.000	0.346	0.777	0.000	0.346	0.777

the rate of relaxation as a function of solute concentration in a "magnetically inert" solvent: the rate at infinite dilution of the solute is purely intramolecular. CS_2 is often used as a solvent because I = 0 for both ^{12}C and ^{32}S; the stable isotopes with non-zero spin (^{13}C and ^{33}S) have low natural abundances. For proton relaxation studies, the perdeuterated analogue of the subject molecule may be used as the solvent because, although the deuteron possess a nuclear moment (I = 1), the dipolar interaction between protons and deuterons is negligible; a further advantage is that complication due to changes of the molecular environment are avoided. Calculation of the intermolecular contribution is another possible approach since the appropriate equations are straightforward and reasonably reliable.[7]

We have determined the intramolecular contributions to relaxation $(1/T_1)_{intra}$ by correcting the relaxation rates at infinite dilution $(1/T_1)_0$ for the effects, if any, of the solvent molecules

$$(1/T_1)_{intra} = (1/T)_0 - R_B = R_A + R_C \qquad (5)$$

where R_A, R_B, and R_C are, respectively, the intramolecular dipolar, the intermolecular dipolar, and the spin-rotational contributions to relaxation.

The intermolecular contribution of the protic solvents to fluorine relaxation, evaluated at infinite dilution of solute, is approximately[8]

$$R_B \approx \frac{4\pi^2\hbar^2\gamma_F^2\gamma_H^2\eta}{5kT}\left[\frac{n_H\rho N_0}{M}\right] \tag{6}$$

where η, ρ, and M are, respectively, the viscosity, density, and molecular weight of the solvent; the term in brackets is the proton spin density (spins per cm^3) expressed in terms of n_H, the number of protons per solvent molecule. The effect of nuclei other than protons can be ignored. The calculated values of R_B for the various solvents are presented in Table IV. The intramolecular contributions to fluorine relaxation are presented in Table V.

4. 2. Intramolecular Dipolar Relaxation

The intramolecular contribution to the relaxation of a fluorine nucleus is given by[8]

$$R_A = \hbar^2\gamma_F^2\left[\tfrac{3}{2}\gamma_F^2\sum_{F'} r_{FF'}^{-6} + \sum_H \gamma_H^2 r_{FH}^{-6}\right]\tau_2 \tag{7}$$

where the first summation is over the remaining fluorine nuclei and the second summation is over the protons--the effect of the other nuclei may be ignored. With the internuclear distances of Ward and Ward,[9] Eq. (7) gives

$$R_A = A\tau_2 \tag{8}$$

where $A \approx 1.33 \times 10^{10}$ sec^{-2} for CF_3CCl_3 and $A \approx 1.75 \times 10^{10}$ sec^{-2}

TABLE IV

Intermolecular Dipolar Contributions to Fluorine Relaxation

Solvent	R_B (sec^{-1})
CS_2	0. 0
CS_2-CCl_4[a]	0. 0
CCl_4	0. 0
diethyl ether	0. 0124
CH_3CN	0. 0115
$HCCl_3$	0. 0039
acetone	0. 0149
benzene	0. 0232

[a]20. 0% CS_2 + 80. 0% CCl_4 (v/v).

TABLE V

^{19}F Intramolecular Relaxation Rates (sec^{-1})

Solvent	CF_3CH_2Cl	CF_3CH_2Br	CF_3CH_2I	CF_3CCl_3
CS_2	0. 241	0. 206	0. 206	0. 126
CS_2-CCl_4[a]	0. 236	0. 210	0. 191	0. 119
CCl_4	0. 221	0. 209	0. 187	0. 123
diethyl ether	0. 172	0. 158	0. 148	0. 157
CH_3CN	0. 160	0. 140	0. 133	0. 118
$HCCl_3$	0. 194	0. 172	0. 168	0. 119
acetone	---	---	0. 118	---
benzene	---	---	0. 143	---

[a] 20. 0% CS_2 + 80. 0% CCl_4 (v/v).

for CF_3CH_2Cl, CF_3CH_2Br, and CF_3CH_2I.

The intramolecular dipolar contribution to proton relaxation, described by a similar expression, is

$$R_{A,H} \approx 2.7 \times 10^{10} \tau_2 \tag{9}$$

Despite the fact that CF_3CH_2Cl, CF_3CH_2Br, CF_3CH_2I, and CF_3CCl_3 are non-spherical, the works of both Woessner[10] and Shimizu[11] suggest that the effects of anisotropic reorientation will be negligible. The effects of internal rotation can also be ignored because the barriers to internal rotation are sufficiently high that the molecules are essentially rigid.[9, 12]

4. 3. Spin-Rotational Relaxation

The spin-rotational contribution to relaxation for a rigid molecule undergoing isotropic Brownian motion may be written[13]

$$R_C = C' \tau_2^{-1} \tag{10}$$

where

$$C' \approx \frac{4\pi \bar{I}^2 (C_{aa}^2 + C_{bb}^2 + C_{cc}^2)}{9\hbar^2} \tag{11}$$

The components for the spin-rotational coupling tensors, calculated according to the procedure outlines in Section II. 5, are presented in Table VI together with the principal components of the inertial tensors,

TABLE VI

The Spin-Rotational and Inertial Constants of the Halogen-Substituted 1, 1, 1-Trifluoroethanes

	CF_3CH_2Cl	CF_3CH_2Br	CF_3CH_2I	CF_3CCl_3
δ_{FCCl_3} ppm	+ 74[a]	+ 71[a]	+ 66[b]	+ 82[c]
δ_{F_2} ppm	+500	+497	+492	+508
C_{aa} kHz	- 3.8	- 3.7	- 3.7	- 1.7
C_{bb} kHz	- 2.1	- 1.4	- 1.1	- 1.7
C_{cc} kHz	- 2.1	- 1.4	- 1.1	- 1.4
I_{aa} 10^{-40} g cm^2	164[b]	164[b]	164[b]	448
I_{bb} 10^{-40} g cm^2	469[b]	723[b]	941[b]	448
I_{bb} 10^{-40} g cm^2	470[b]	725[b]	942[b]	655
$C' \times 10^{13}$	1.25	2.04	2.91	0.84

[a]N. Muller and D. T. Carr, J. Phys. Chem. 67, 112 (1963). [b]Measured at 56.4 MHz relative to internal $FCCl_3$; T = 41°C. [c]G. Filipovich and G. V. D. Tiers, J. Phys. Chem. 63, 761 (1959).

the fluorine chemical shifts, and the coefficients C′. The coordinate systems are depicted in Figures 9a and 9b.

5. Discussion of Results

It is immediately apparent from a perusal of the relaxation data in Table V that $(1/T_1)_{intra}$ depends, in some way, upon the nature of the solute-solvent system. Since Steele's[14, 15] inertial model of molecular reorientation is obviously not applicable, we may conclude, as a first approximation, that molecular motion is dominated by viscous damping. It is also apparent that $(1/T_1)_{intra}$ is not proportional to either η or η^{-1} since the relaxation rates of, for example, CF_3CH_2I are quite different in CS_2, CH_3CN, and acetone even though these solvents have nearly identical viscosities.

The intramolecular contribution to fluorine relaxation, obtained by combining Equations (8) and (10), is given by

$$(1/T_1)_{intra} = A\tau_2 + C'\tau_2^{-1} \qquad (12)$$

If we make the customary assumption that τ_2 is proportional to η, Eq. (10) may be written

$$(1/T_1)_{intra} = A\kappa\eta + C'(\kappa\eta)^{-1} \qquad (13)$$

where κ is the proportionality constant. Thus, for each of the solute

FIGURE 9a

Principal inertial coordinate systems for CF_3CH_2Cl ($\theta = 37^\circ\ 38'$), CF_3CH_2Br ($\theta = 39^\circ\ 31'$), and CF_3CH_2I ($\theta = 41^\circ\ 28'$). [9]

FIGURE 9b

Principal inertial coordinate system for CF_3CCl_3.

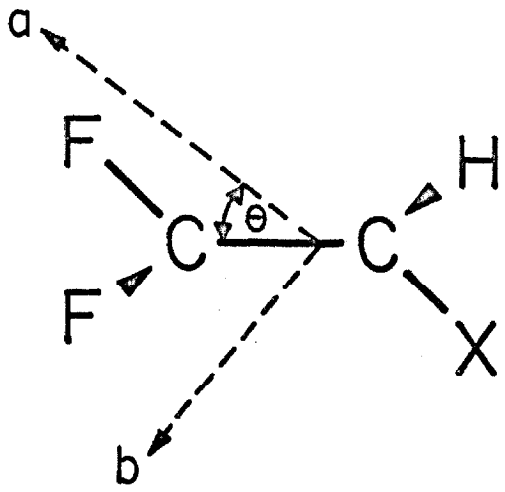
a
F
F
C
θ
C
H
X
b

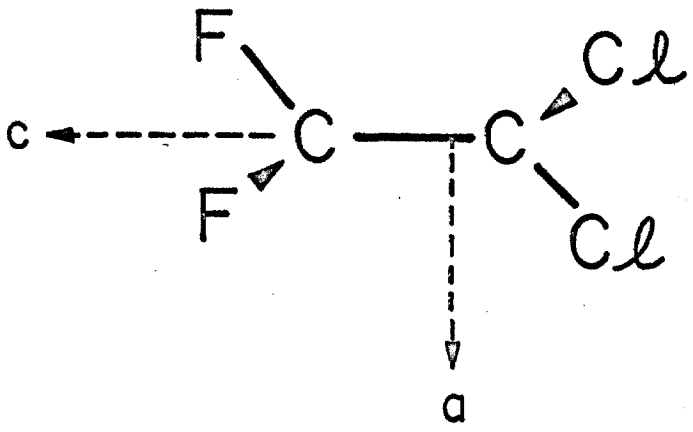
F
F
C
c
C
Cl
Cl
a

molecules, a plot of $\eta(1/T_1)_{intra}$ versus η^2 should be a straight line with slope $A\kappa$ and intercept $C'\kappa^{-1}$. Such plots are presented as Figures 10 through 13. The vertical bars represent what we consider to be conservative estimates of the errors in $(1/T_1)_{intra}$. With the sole exception of CF_3CCl_3, the "expected" linear relationships are not observed.

There are three possible reasons why the plots are non-linear for CF_3CH_2Cl, CF_3CH_2Br, and CF_3CH_2I: (a) the "constant" κ ($\equiv \tau_2 \eta^{-1}$) is not independent of the nature of the solvent--in other words, the Debye relation for τ_2 is not valid; (b) the solute molecules are interacting with some of the solvents; (c) the macroscopic viscosity η does not adequately describe the frictional forces acting on a solute molecule. However, before considering these possibilities we shall indicate the criteria which may be used to assess the goodness of any particular model.

5.1. Criteria for Analysis of Results

We have two independent criteria for assessing the validity of any assumed model for τ_2: (a) a plot of $\tau_2(1/T_1)_{intra}$ versus τ_2^2 should be a straight line with slope A and intercept C'; (b) the calculated correlation times must be in agreement with the experimental values, presented in Table VII, that were obtained from the proton relaxation rates at infinite dilution $(1/T_{1,H})_0$

$$\tau_2 = 0.37 \times 10^{10} (1/T_{1,H})_0 \qquad (14)$$

FIGURE 10

$\eta(1/T_1)_{intra}$ vs. η^2 for CF_3CH_2Cl in different solvents (1 = CS_2; 2 = CS_2-CCl_4; 3 = CCl_4; 4 = diethyl ether; 5 = CH_3CN; 6 = $HCCl_3$).

FIGURE 11

$\eta(1/T_1)_{intra}$ vs. η^2 for CF_3CH_2Br in different solvents (the legend is the same as in Fig. 10).

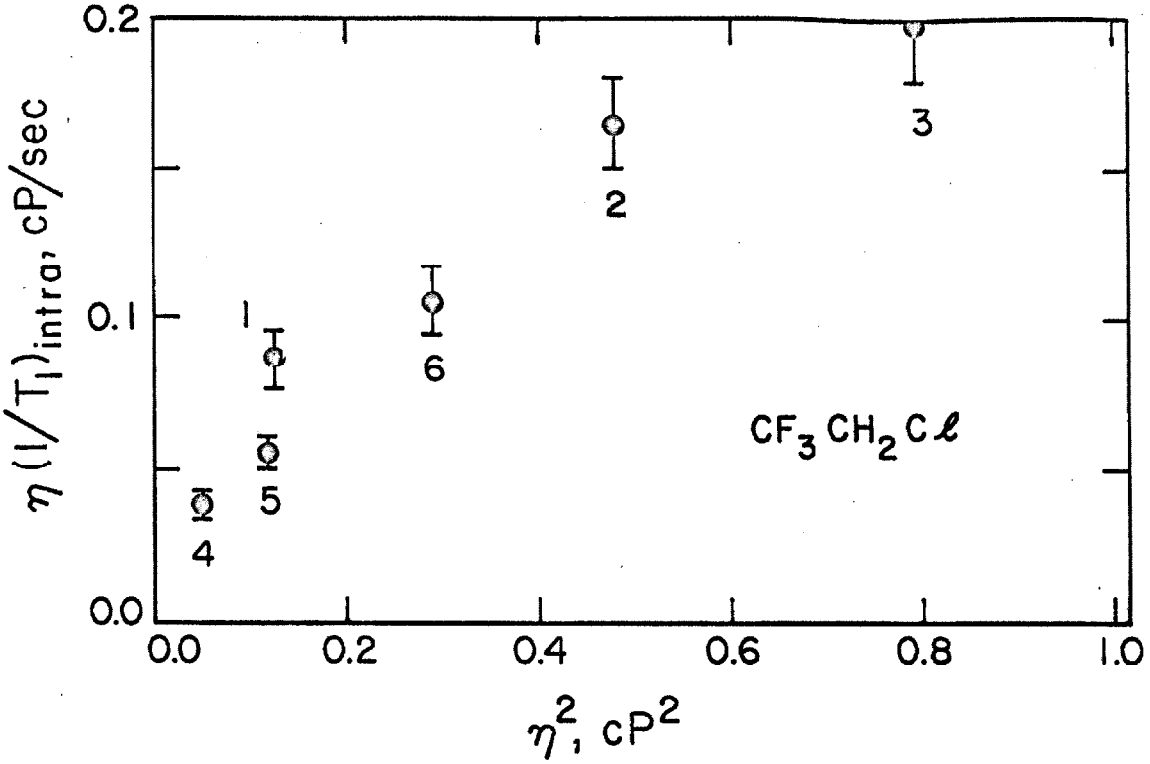
0.2
0.1
0.0
0.0
0.2
0.4
0.6
0.8
1.0
$\eta\,(1/T_1)_{intra}$, cP/sec
η^2, cP^2
1
2
3
4
5
6
$CF_3CH_2C\ell$

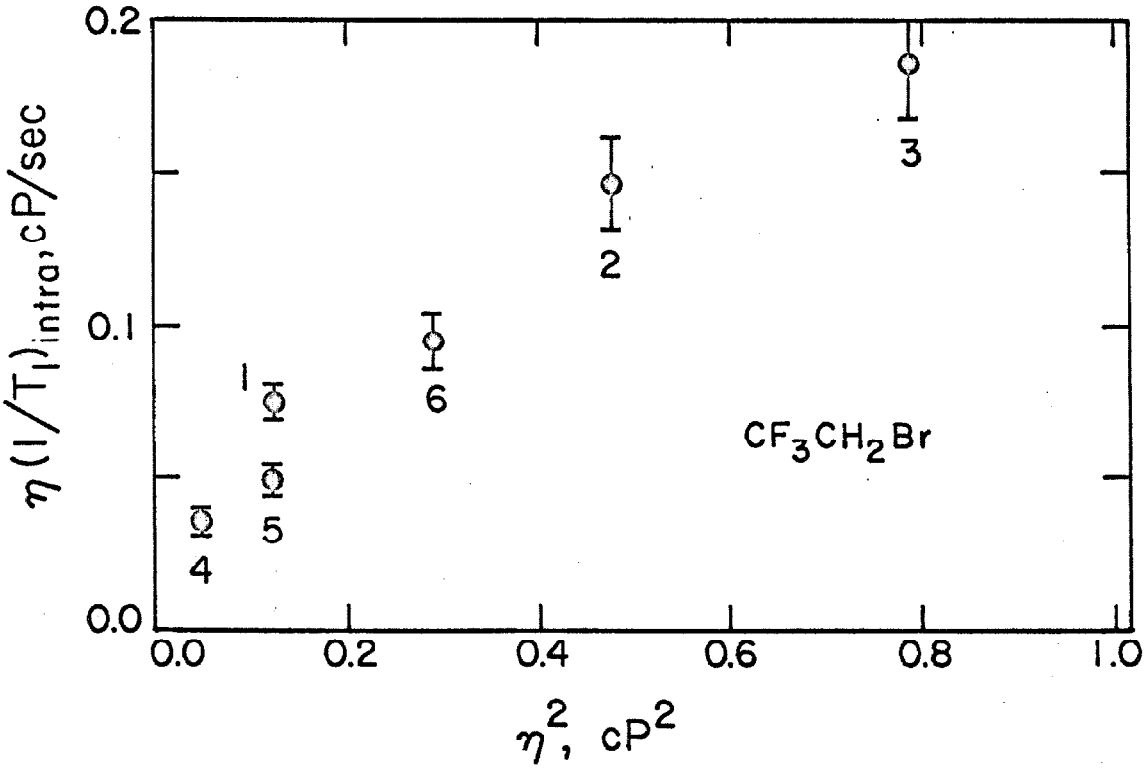
0.2
0.1
0.0
0.0
0.2
0.4
0.6
0.8
1.0
$\eta\,(1/T_1)_{intra}$, cP/sec
η^2, cP^2
1
2
3
4
5
6
CF_3CH_2Br

FIGURE 12

$\eta(1/T_1)_{intra}$ vs. η^2 for CF_3CH_2I in different solvents (1 = CS_2; 2 = CS_2-CCl_4; 3 = CCl_4; 4 = diethyl ether; 5 = CH_3CN; 6 = $HCCl_3$; 7 = acetone; 8 = benzene).

FIGURE 13

$\eta(1/T_1)_{intra}$ vs. η^2 for CF_3CCl_3 in different solvents (the legend is the same as in Fig. 12).

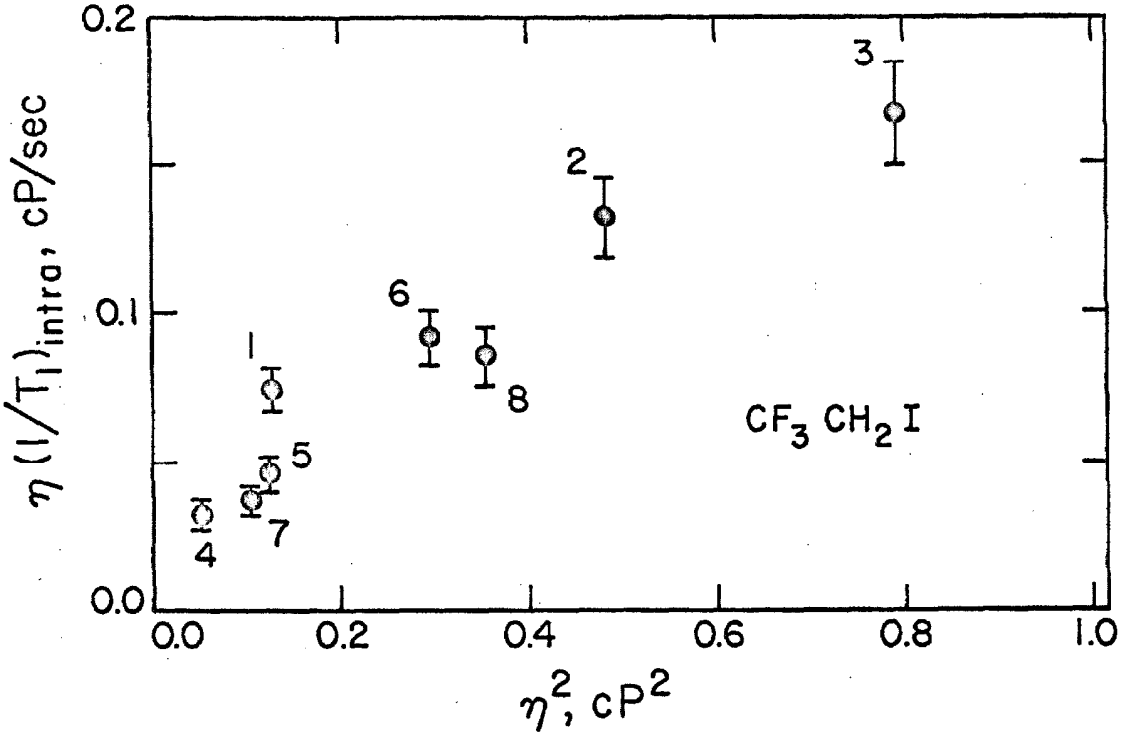
0.2
0.1
0.0
0.0
0.2
0.4
0.6
0.8
1.0
$\eta\,(1/T_1)_{intra}$, cP/sec
η^2, cP^2
$CF_3\,CH_2\,I$
1
2
3
4
5
6
7
8

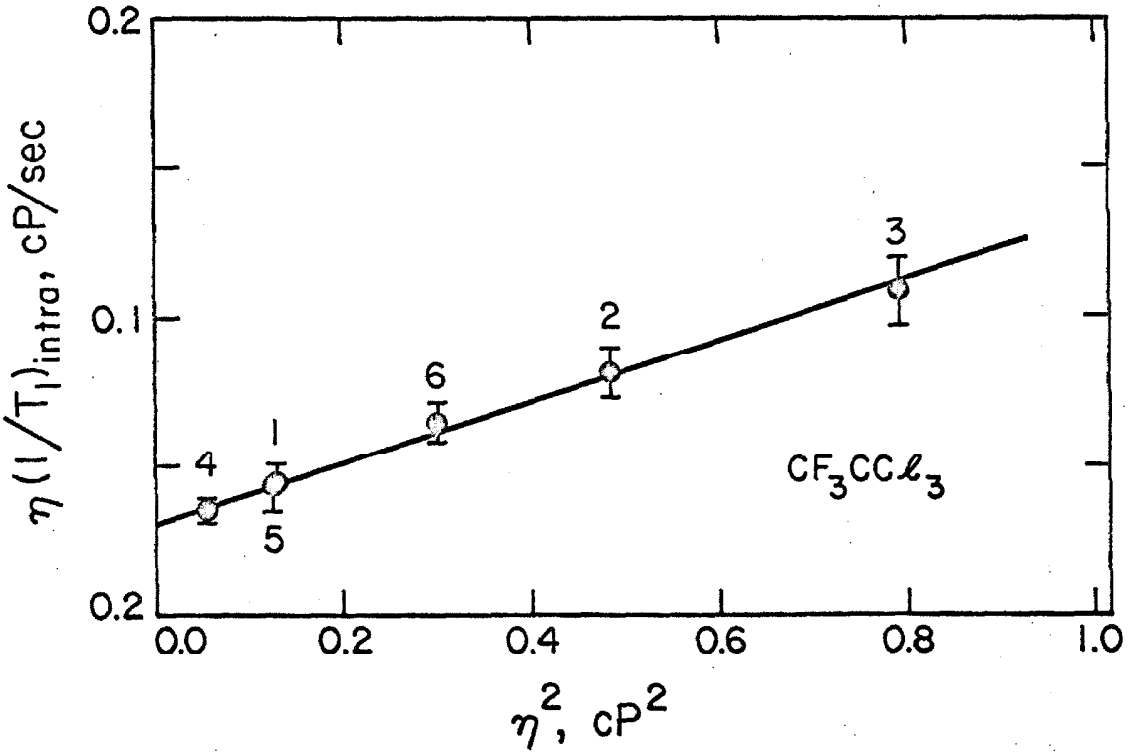
0.2
0.1
0.2
0.0
0.2
0.4
0.6
0.8
1.0
$\eta\,(1/T_1)_{intra}$, cP/sec
η^2, cP^2
$CF_3CC\ell_3$
1
2
3
4
5
6

TABLE VII

Experimental Correlation Times (10^{-12} sec)[a]

	CF_3CH_2Cl	CF_3CH_2Br	CF_3CH_2I
CS_2-CCl_4[b]	2.2	1.1	---
CCl_4	2.6	1.9	1.9

[a]Estimated uncertainty ± 50%.

[b]20.0% CS_2 + 80.0% CCl_4 (v/v).

Since the proton relaxation at infinite dilution in "magnetically inert" solvents is due entirely to the intramolecular dipolar interaction, Eq. (14) follows immediately from Eq. (9).

5. 2. The Validity of the Debye Equation for τ_2

As was pointed out in Section I. 3, Gierer and Wirtz[16] have proposed a correlation time, based on Debye's model, that incorporates a microviscosity correction factor:

$$\tau_2 = \frac{4\pi a_2^3 \eta_1}{3kT} \left[(6a_1/a_2) + (1 + a_1/a_2)^{-3} \right]^{-1} \qquad (15)$$

where a_1 and a_2 are, respectively, the radii of the solvent and solute molecules.

We have calculated, using Eq. (15), a value of τ_2 for each solute-solvent pair. The results for CF_3CH_2Cl and CF_3CCl_3 are presented as plots of $\tau_2(1/T_1)_{intra}$ versus τ_2^2 in Figures 14 and 15. The data for CF_3CCl_3 lie on a straight line with slope $A = 1.05 \times 10^{10}$ sec^{-2} and intercept $C' = 3.32 \times 10^{-13}$; these values are in good agreement with the corresponding predicted values 1.33×10^{10} sec^{-2} and 0.84×10^{-13}. The data for CF_3CH_2Cl, as is also the case for CF_3CH_2Br and CF_3CH_2I, do not lie on a straight line; consequently, Gierer and Wirtz's model appears to be invalid--at least for CF_3CH_2Cl, CF_3CH_2Br, and CF_3CH_2I.

We have gone through the same procedure with Mitchell and Eisner's[5] approximation to the Hill equation

FIGURE 14

$\tau_2(1/T_1)_{intra}$ vs. τ_2^2 for CF_3CH_2Cl in different solvents (1 = CS_2; 2 = CS_2-CCl_4; 3 = CCl_4; 4 = diethyl ether; 5 = CH_3CN; 6 = $HCCl_3$). The correlation times τ_2 were calculated using Eq. (15).

FIGURE 15

$\tau_2(1/T_1)_{intra}$ vs. τ_2^2 for CF_3CCl_3 in different solvents (the legend is the same as in Fig. 14). The correlation times τ_2 were calculated using Eq. (15).

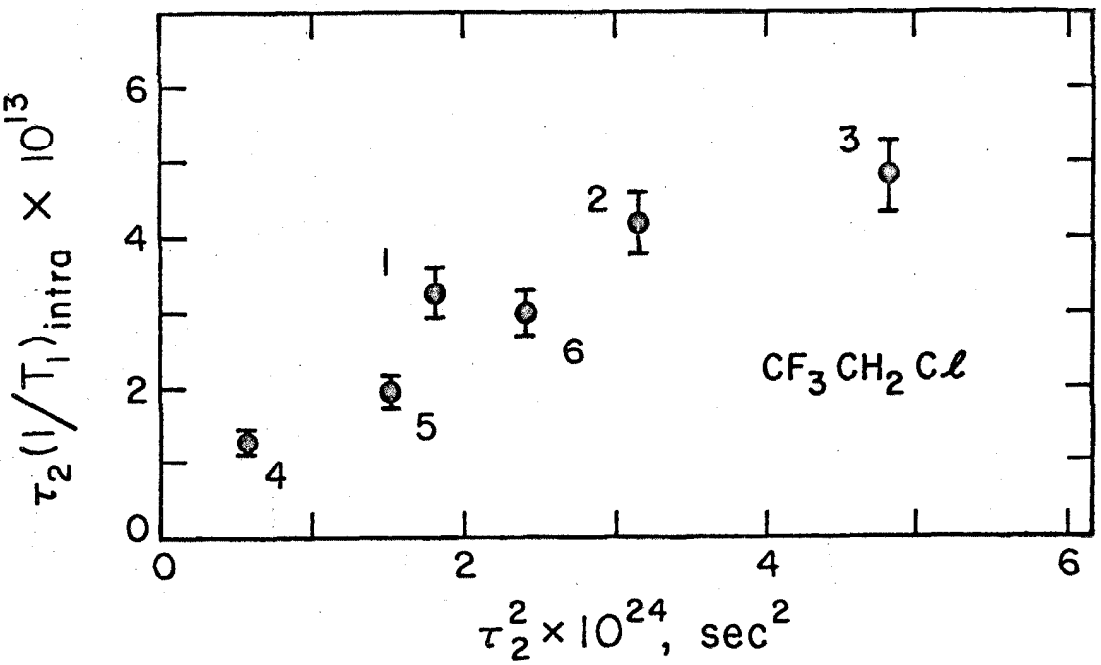
$\tau_2(1/T_1)_{intra} \times 10^{13}$
$\tau_2^2 \times 10^{24}$, sec^2
CF_3CH_2Cl
1
2
3
4
5
6

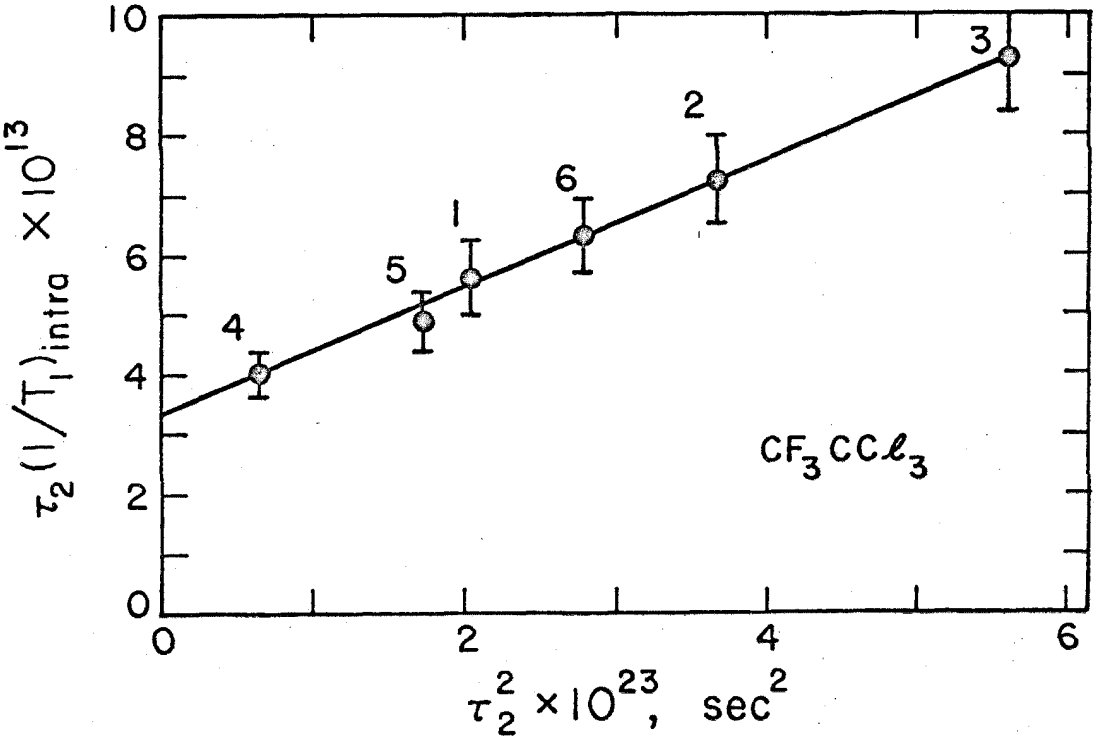
$\tau_2(1/T_1)_{intra} \times 10^{13}$
$\tau_2^2 \times 10^{23}$, sec^2
CF_3CCl_3
1
2
3
4
5
6

$$\tau_2 = \frac{2 I_2 a_2 \eta_1}{\mu k T} \qquad (16)$$

where the subscripts 1 and 2 denote, respectively, the solvent and solute; I_2 is the moment of inertia of the solute molecule; μ is the reduced mass of the solute-solvent pair. Equation (16) gives results that are quite similar to those described previously: a good fit for CF_3CCl_3 and no fit for the CF_3CH_2X molecules.

In view of the fact that all models gave satisfactory results for CF_3CCl_3, it appeared to be important to consider the possibility that the poor results for CF_3CH_2Cl, CF_3CH_2Br, and CF_3CH_2I were due to interactions between the solute molecules and some, if not all, of the solvents. This possibility is considered next.

5. 3. Solute-Solvent Interactions

Since one possible, though not too probable, mode of interaction involves the formation of hydrogen bonds between the CF_3CH_2X protons and basic solvents such as CH_3CN and acetone, we have measured the proton chemical shifts and the proton-fluorine coupling constants for CF_3CH_2I at low concentrations in the various solvents. The results are presented in Table VIII. The proton chemical shift of neat CF_3CH_2I, comparable to the chemical shift of the α-protons of $CH_3\underline{CH_2}OH$, leads to the conclusion that the protons are not sufficiently acidic to form hydrogen bonds. The small, solvent induced shifts of δ and the constancy of J_{HF} support this conclusion.[17] Since CF_3CH_2I

TABLE VIII

The Solvent Dependence of the Proton Chemical Shift and J_{HF} for CF_3CH_2I

Solvent	ϵ of Solvent	δ_{TMS}[a] (ppm)	J_{HF}[a] (Hz)
C_6H_6	2.26	-2.627	9.8
C_6H_{12}	2.02	-3.400	9.5
CS_2	2.64	-3.504	9.6
neat	--	-3.523	9.7
CCl_4	2.24	-3.528	9.6
CH_3CN	35.1	-3.546	9.7
diethyl ether	4.34	-3.701	9.9
$HCCl_3$	4.81	-3.733	10.3
acetone	20.7	-3.907	10.3

[a]Measured at 100 MHz with TMS as internal standard; solute concentration 5% (v/v); T = 32°C.

does not form hydrogen bonds, it is expected that CF_3CH_2Cl and CF_3CH_2Br will also not form hydrogen bonds.

A re-examination of the plots of $\tau_2(1/T_1)_{intra}$ versus τ_2^2 [for example, Fig. 14] suggests an intriguing interpretation: the solute molecules experience a torque produced by a dipolar interaction with the polar solvent molecules. Such an interaction would be expected to increase the correlation time

$$\tau_2' = \tau_2 \exp(-\epsilon/kT) \tag{17}$$

where ϵ is the first approximation to the weighted mean of the dipole-dipole interaction energy V:[18]

$$\langle V e^{-V/kT} \rangle \approx \frac{-2\mu_1^2\mu_2^2}{3kT r^6} \equiv \epsilon \tag{18}$$

The dipole moments of the solute and solvent molecules are presented in Table IX.

The data for CF_3CH_2Cl are presented in Figure 16 as a plot of $\tau_2(1/T_1)_{intra}$ versus τ_2^2: the correlation times were calculated using Gierer and Wirtz's microviscosity model [Eq. (15)] with molecular dimensions determined from molecular models. One straight line is drawn through the data for non-polar solvents, and another, through the data for polar solvents. We find that, while the correlation times compare favorably with the experimental values, the slope of the non-polar data is approximately four times too large. This discrepancy

TABLE IX

Molecular Dipole Moments

molecule	μ (10^{-18} esu cm^2)
CF_3CH_2Cl	1.65[a]
CF_3CH_2Br	1.7 [b]
CF_3CH_2I	1.86
CF_3CCl_3	0.75
CS_2	0.0 [c]
CCl_4	0.0 [c]
benzene	0.0 [c]
$HCCl_3$	1.1 [c]
diethyl ether	1.25[c]
acetone	3.0 [c]
CH_3CN	3.5 [c]

[a]R. M. Fuoss, J. Am. Chem. Soc. 60, 1633 (1938).

[b]Calculated from bond moments. [c]A. L. McClellan, Tables of Experimental Dipole Moments (W. H. Freeman and Company, San Francisco, 1963).

FIGURE 16

The apparent effect of solvent polarity upon spin-lattice relaxation. The data are the same as in Fig. 14.

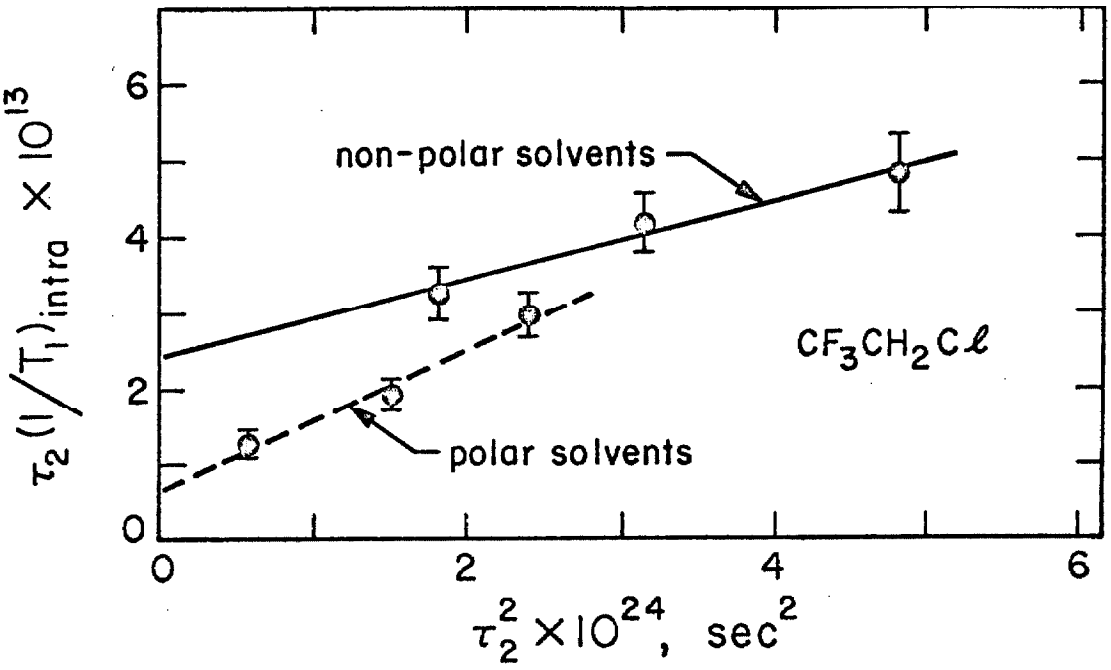
$\tau_2(1/T_1)_{intra} \times 10^{13}$
6
4
2
0
0
2
4
6
$\tau_2^2 \times 10^{24}$, sec^2
non-polar solvents
polar solvents
$CF_3CH_2C\ell$

between the "experimental" and predicted slopes can be reduced somewhat by using molecular dimensions calculated from density data, but then the calculated correlation times are far too large. Furthermore, the product of the slope and intercept of the line for the polar solvents, given by

$$(A\, e^{-\epsilon/kT})\,(C'\, e^{+\epsilon/kT}) = AC' \qquad (19)$$

should be identical to the product of the slope and intercept of the line for the non-polar solvents AC'; such is not the case. The discrepancies also occur for the CF_3CH_2Br and CF_3CH_2I data. A similar analysis using Eq. (16) gives equally unsatisfactory results. Thus we conclude that neither general nor specific solute-solvent interactions can explain the relaxation data.

5.4. Mutual Viscosity

The use of viscosity to describe the frictional forces acting on a molecule has long been a source of contention. Hill[3] has suggested that the mutual viscosity is a better measure of the interaction between the solute and solvent. The mutual viscosity η_{12} can be calculated from Hill's expression for the viscosity η_m of a mixture

$$\eta_m = x_1^2 \eta_1 \frac{\sigma_1}{\sigma_m} + x_2^2 \eta_2 \frac{\sigma_2}{\sigma_m} + 2x_1x_2 \eta_{12} \frac{\sigma_{12}}{\sigma_m} \qquad (20)$$

where the x's are the mole fractions. The σ's, intermolecular

distances, are given by

$$\sigma_m = \left[\frac{x_1 M_1 + x_2 M_2}{\rho_m N_0} \right]^{\frac{1}{3}}$$

$$\sigma_i = \left[\frac{M_i}{\rho_i N_0} \right]^{\frac{1}{3}} \qquad i = 1, 2$$

$$\sigma_{12} = \tfrac{1}{2} (\sigma_1 + \sigma_2)$$

Following Smyth,[19] we rewrite Eq. (20)

$$\frac{\eta_m \sigma_m - x_2^2 \eta_2 \sigma_2}{x_1^2 \sigma_1} = \eta_1 + \left[\frac{2 x_2 \sigma_{12}}{x_1 \sigma_1} \right] \eta_{12} \qquad (21)$$

A plot of $[(\eta_m \sigma_m - x_2^2 \eta_2 \sigma_2)/x_1^2 \sigma_1]$ versus $[2x_2 \sigma_{12}/x_1 \sigma_1]$ should be a straight line with slope η_{12} and intercept η_1. We have performed such an analysis using the viscosity and density data which are tabulated in Section 3. 2; the graphs are presented as Figures 17 - 19. The calculated values of η_{12} and η_1 are presented in Table X together with the actual values of η_1. Since the viscosity of the CS_2-CCl_4 mixture is given by the empirical expression

$$\log (\eta_{CS_2\text{-}CCl_4}) = (x_{CS_2}) \log (\eta_{CS_2}) + (x_{CCl_4}) \log (\eta_{CCl_4}) \qquad (22)$$

FIGURE 17

Graphical determination of the mutual viscosity η_{12} for CF_3CH_2I in solutions of CS_2, CCl_4, diethyl ether, and $HCCl_3$.

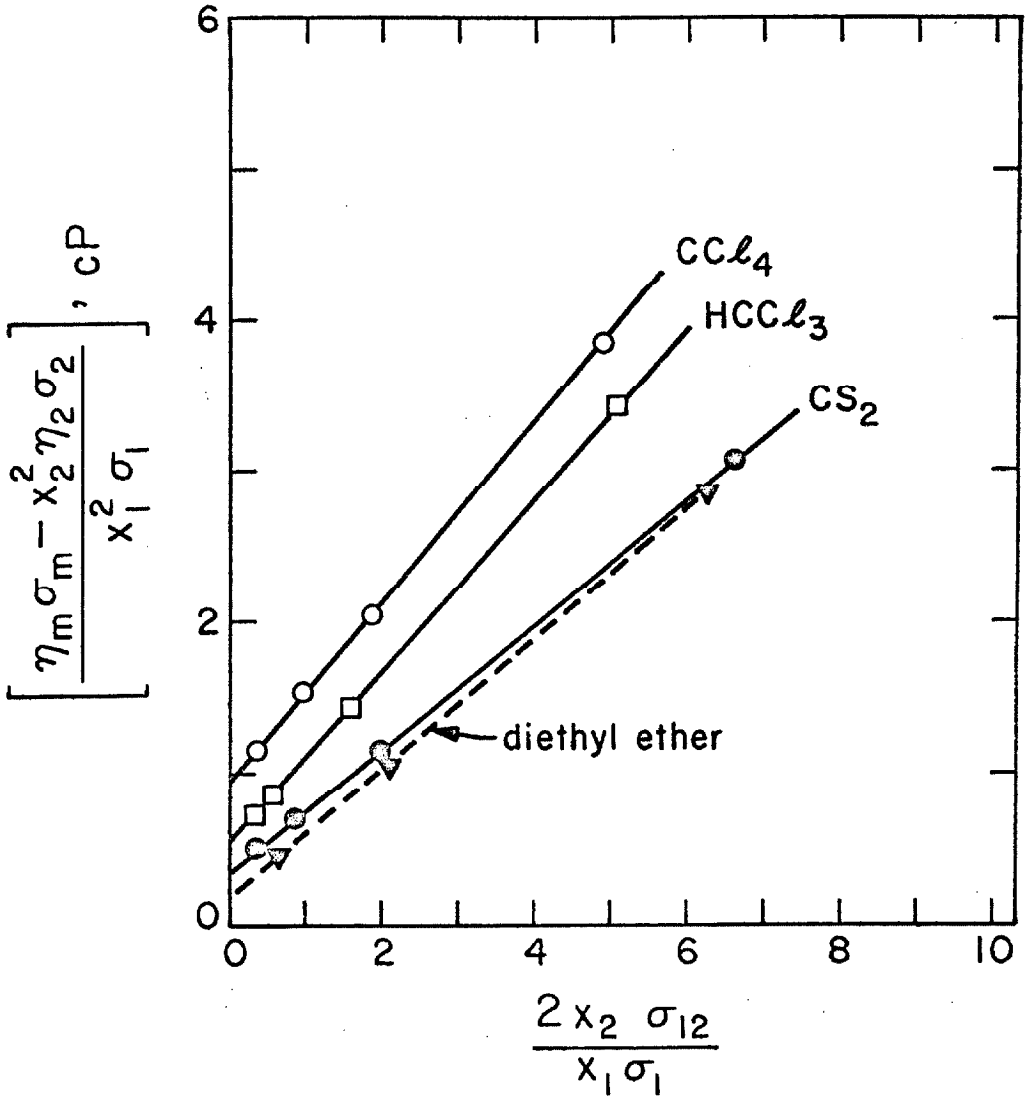
6
4
2
0
0
2
4
6
8
10
$CC\ell_4$
$HCC\ell_3$
CS_2
diethyl ether
$\left[\frac{\eta_m\sigma_m - x_2^2\eta_2\sigma_2}{x_1^2\sigma_1}\right]$, cP
$\frac{2x_2\sigma_{12}}{x_1\sigma_1}$

FIGURE 18

Graphical determination of the mutual viscosity η_{12} for CF_3CH_2I in solutions of CH_3CN, acetone, and benzene.

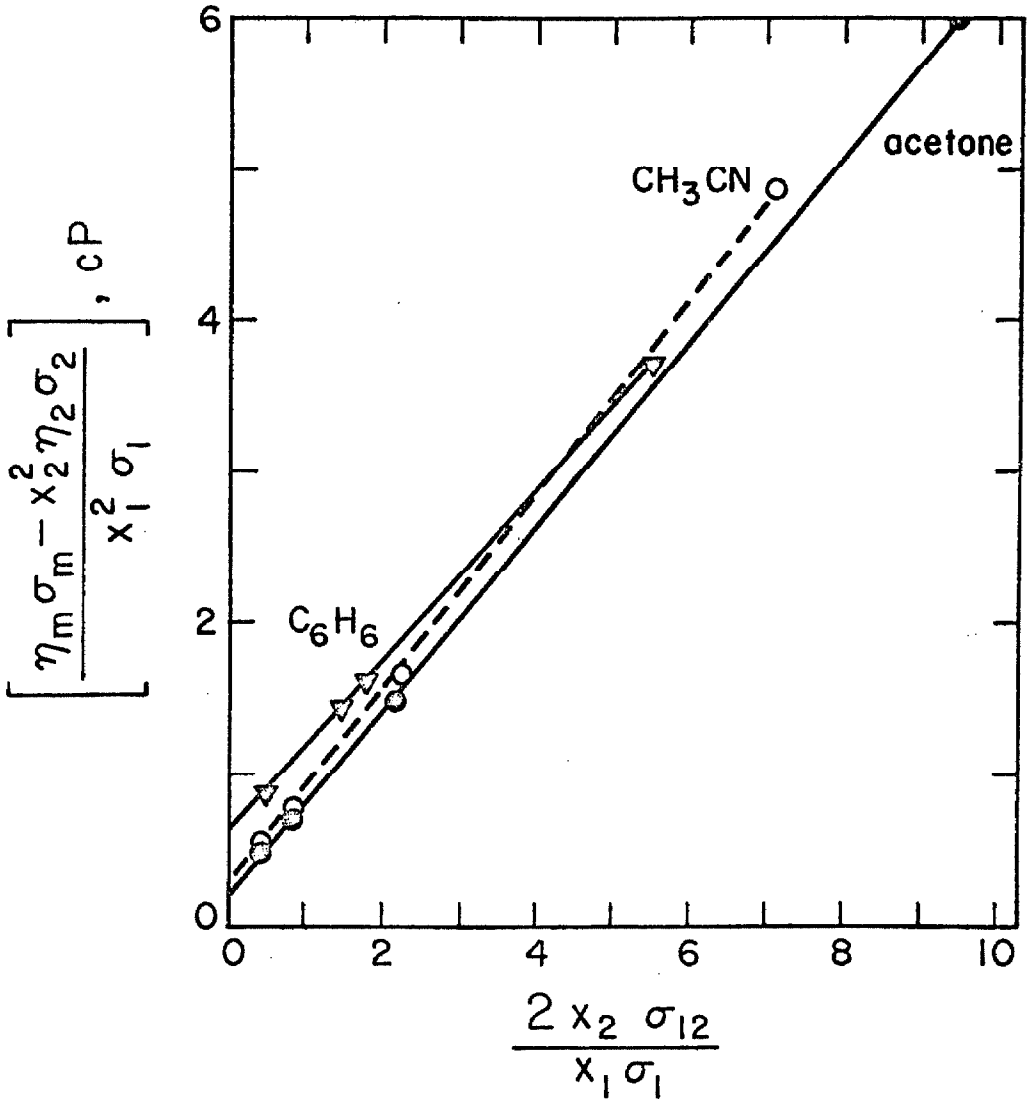
6
4
2
0
0
2
4
6
8
10
acetone
CH3CN
C6H6
$\left[\frac{\eta_m \sigma_m - x_2^2 \eta_2 \sigma_2}{x_1^2 \sigma_1}\right]$, cP
$\frac{2 x_2 \sigma_{12}}{x_1 \sigma_1}$

FIGURE 19

Graphical determination of the mutual viscosity η_{12} for CF_3CCl_3 in solutions of CS_2, CCl_4, diethyl ether, and $HCCl_3$.

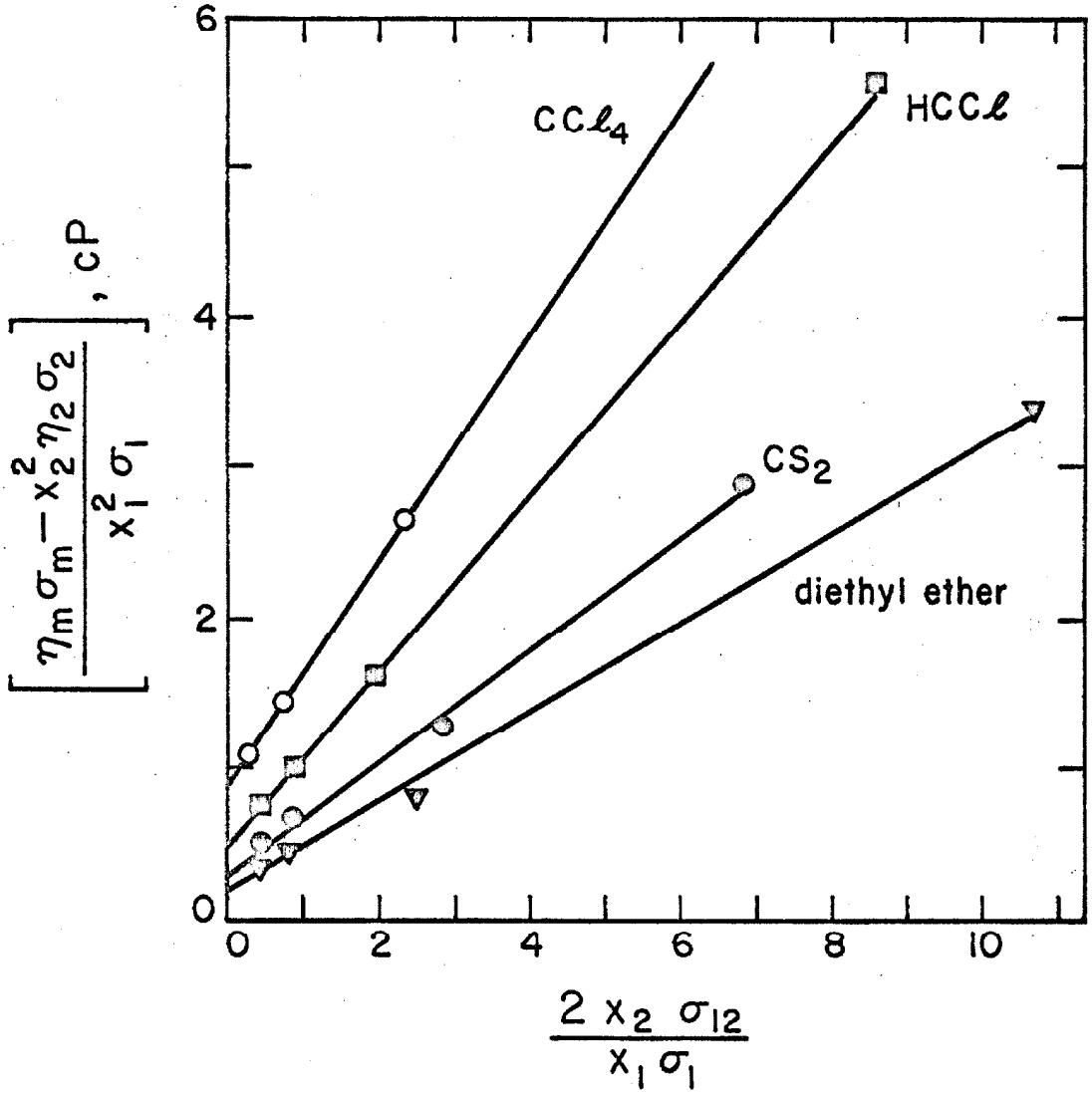
6
4
2
0
0
2
4
6
8
10
CCl_4
HCCl
CS_2
diethyl ether
$\left[\frac{\eta_m \sigma_m - x_2^2 \eta_2 \sigma_2}{x_1^2 \sigma_1}\right]$, cP
$\frac{2 x_2 \sigma_{12}}{x_1 \sigma_1}$

TABLE X

Mutual Viscosities for CF_3CH_2I and CF_3CCl_3 Solutions

solvent	η_1 (25.0°C)	CF_3CH_2I		CF_3CCl_3	
		η_1 [a]	η_{12} [a]	η_1 [a]	η_{12} [a]
	cP	cP	cP	cP	cP
CS_2	0.356	0.36	0.40	0.40	0.31
CS_2-CCl_4	0.693	--	0.55[b]	--	0.66
CCl_4	0.888	0.93	0.60	0.88	0.76
diethyl ether	0.222	0.19	0.41	0.24	0.23
CH_3CN	0.346	0.31	0.59	0.33	0.514
$HCCl_3$	0.542	0.55	0.56	0.53	0.576
acetone	0.316	0.27	0.58	--	--
benzene	0.593	0.62	0.55	--	--

[a]Graphically evaluated from experimental data.

[b]Calculated from Eq. (23).

and since we have not evaluated η_{12} for any solutions with the CS_2-CCl_4, we shall assume that the mutual viscosity of a particular solute in CS_2-CCl_4 is related to its mutual viscosities in CS_2 and CCl_4 separately:

$$\log (\eta_{12}{}^{CS_2\text{-}CCl_4}) = (x_{CS_2}) \log (\eta_{12}{}^{CS_2}) + (x_{CCl_4}) \log (\eta_{12}{}^{CCl_4}) \qquad (23)$$

The calculated values of η_{12} for CF_3CH_2I and CF_3CCl_3 are also presented in Table X.

The agreement between the actual and graphical values of η_1 is quite good. However, the most interesting and, by far, the most important point is that in some cases the solvent viscosity and the mutual viscosity are clearly different!

We are now in a position to evaluate our data for CF_3CH_2I and CF_3CCl_3 with Hill's model for the correlation time:

$$\tau_2 = \left[\frac{I_2 I_{12}}{I_2 + I_{12}}\right]\left[\frac{m_1 + m_2}{m_1 m_2}\right] \frac{\eta_{12}\sigma_{12}}{kT} \qquad (24)$$

The solute moment of inertia I_2 was taken to be the harmonic average of the principal moments of inertia. The data are presented in Figures 20 and 21 as plots of $\tau_2(1/T_1)_{intra}$ versus τ_2^2. The straight line through the CF_3CH_2I data has a slope 1.50×10^{10} sec^{-2} and an intercept 2.80×10^{-13}; these compare very well with the predicted values 1.75×10^{10} sec^{-2} and 2.91×10^{-13}. The straight line through the CF_3CCl_3 data has a slope 1.65×10^{10} sec^{-2} and an intercept

FIGURE 20

$\tau_2(1/T_1)_{intra}$ vs. τ^2 for CF_3CH_2I in different solvents (1 = CS_2; 2 = CS_2-CCl_4; 3 = CCl_4; 4 = diethyl ether; 5 = CH_3CN; 6 = $HCCl_3$; 7 = acetone; 8 = benzene). The correlation times τ_2 were calculated using Eq. (24).

FIGURE 21

$\tau_2(1/T_1)_{intra}$ vs. τ_2^2 for CF_3CCl_3 in different solvents (the legend is the same as in Fig. 20). The correlation times τ_2 were calculated using Eq. (24).

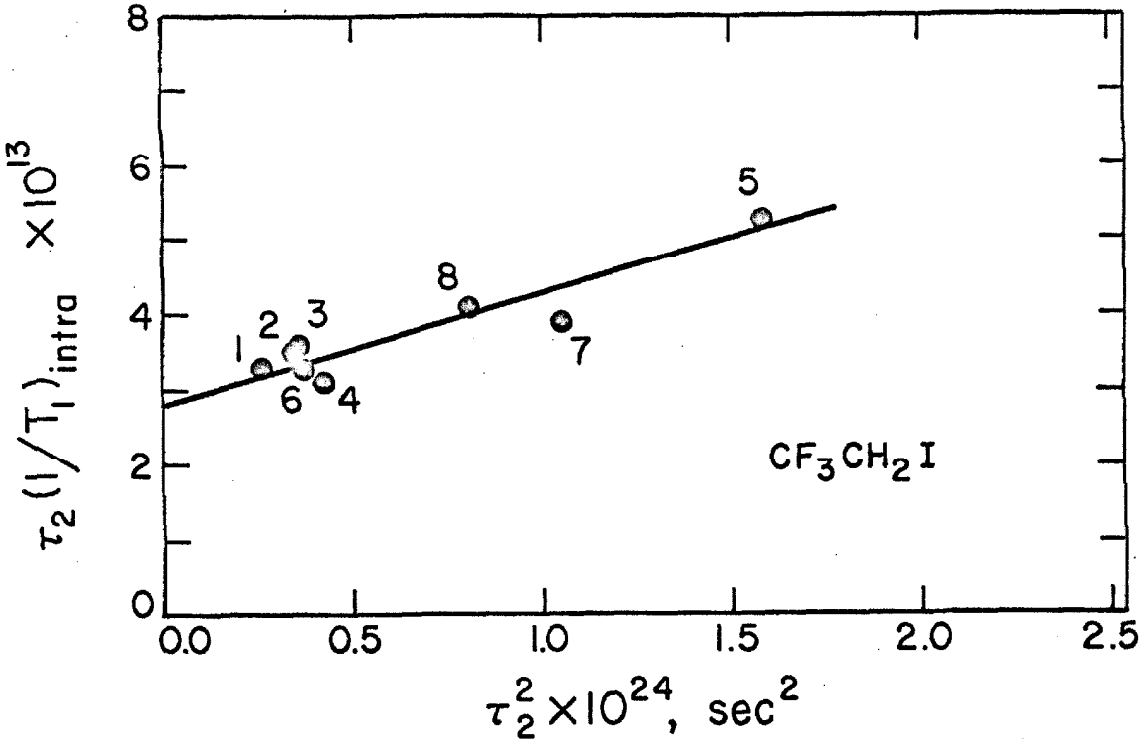
8
6
4
2
0
0.0
0.5
1.0
1.5
2.0
2.5
$\tau_2(1/T_1)_{intra} \times 10^{13}$
$\tau_2^2 \times 10^{24}$, sec^2
1
2
3
4
5
6
7
8
CF_3CH_2I

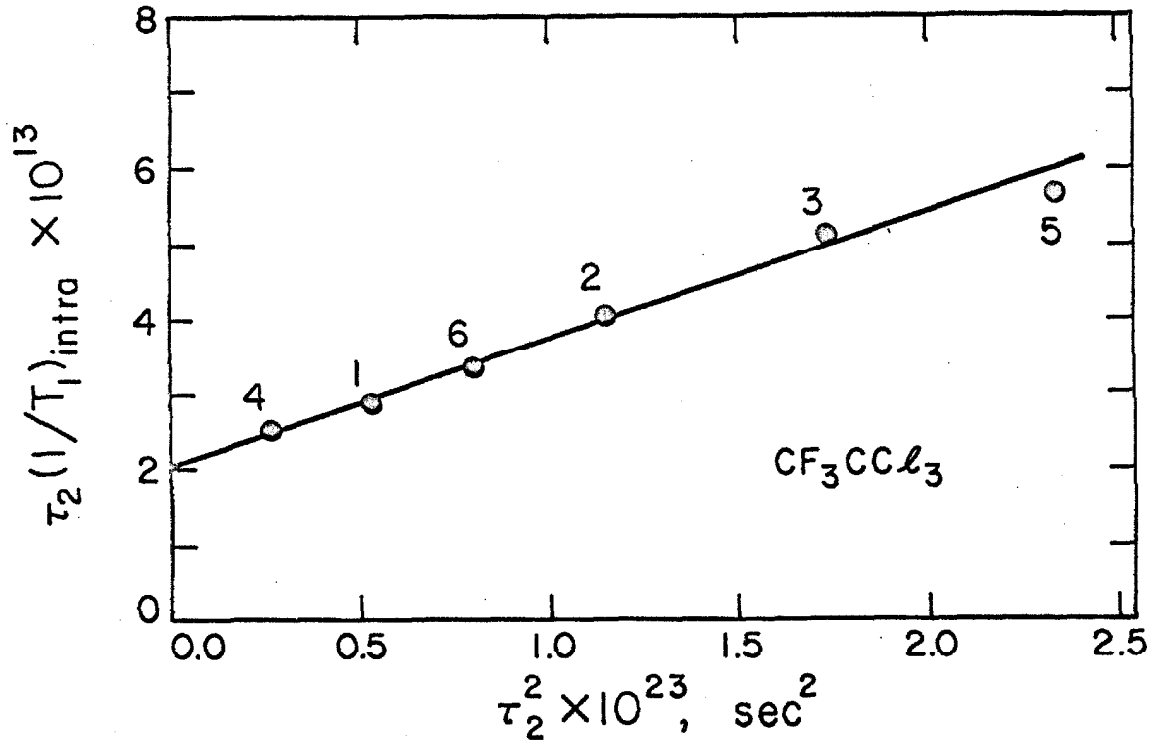
8
6
4
2
0
0.0
0.5
1.0
1.5
2.0
2.5
$\tau_2(1/T_1)_{intra} \times 10^{13}$
$\tau_2^2 \times 10^{23}$, sec^2
1
2
3
4
5
6
CF_3CCl_3

2.05×10^{-13}; these are also in good agreement with the predicted values 1.33×10^{10} sec^{-2} and 0.84×10^{-13}.

Because of the lack of viscosity and density data we are compelled to assume that the mutual viscosities of CF_3CH_2Cl and CF_3CH_2Br in a particular solvent are the same as the mutual viscosity of CF_3CH_2I in the same solvent. The data are plotted in Figures 22 and 23. The line through the CF_3CH_2Cl data has a slope 1.95×10^{10} sec^{-2} and an intercept 3.25×10^{-13}; the predicted values are 1.75×10^{10} sec^{-2} and 1.25×10^{-13}. The line through the CF_3CH_2Br data has a slope 1.70×10^{10} sec^{-2} and an intercept 2.85×10^{-13}; the predicted values are 1.75×10^{10} sec^{-2} and 2.04×10^{-13}.

The correlation times calculate from Hill's equation with experimentally determined values of η_{12} are presented in Table XI.

6. Conclusions

It is evident that the Hill model for molecular reorientation provides the only satisfactory explanation for all of our results; it is also evident, contrary to the suggestion of Mitchell and Eisner, that the efficacy of the Hill model is dependent upon the mutual viscosity. Therefore we conclude that the frictional forces which damp the rotational motion of a molecule in the liquid state cannot, in general, be related to the macroscopic viscosity.

The results for CF_3CCl_3 are somewhat surprising in light of the various criteria which supposedly delimit the applicability of

FIGURE 22

$\tau_2(1/T_1)_{intra}$ vs. τ_2^2 for CF_3CH_2Cl in different solvents (1 = CS_2; 2 = CS_2-CCl_4; 3 = CCl_4; 4 = diethyl ether; 5 = CH_3CN; 6 = $HCCl_3$). The correlation times τ_2 were calculated using Eq. (24).

FIGURE 23

$\tau_2(1/T_1)_{intra}$ vs. τ_2^2 for CF_3CH_2Br in different solvents (the legend is the same as in Fig. 22). The correlation times τ_2 were calculated using Eq. (24).

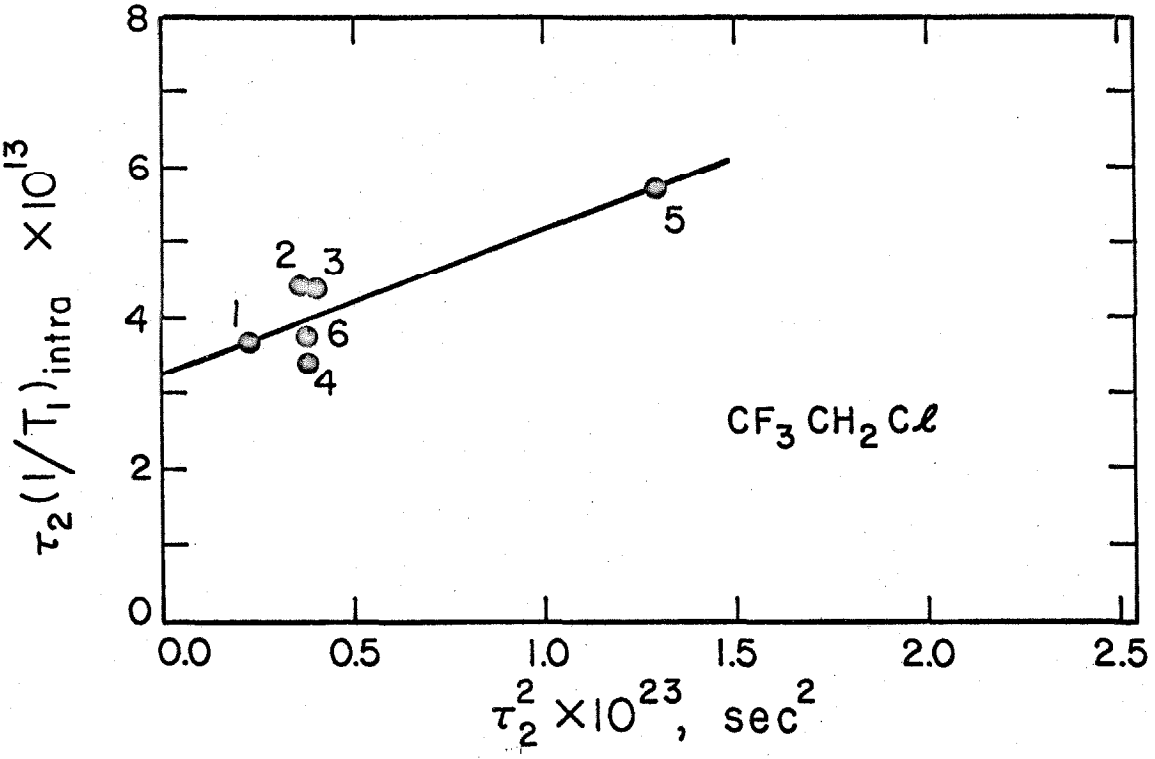
8
6
4
2
0
0.0
0.5
1.0
1.5
2.0
2.5
$\tau_2(1/T_1)_{intra} \times 10^{13}$
$\tau_2^2 \times 10^{23}$, sec^2
1
2
3
4
5
6
$CF_3CH_2C\ell$

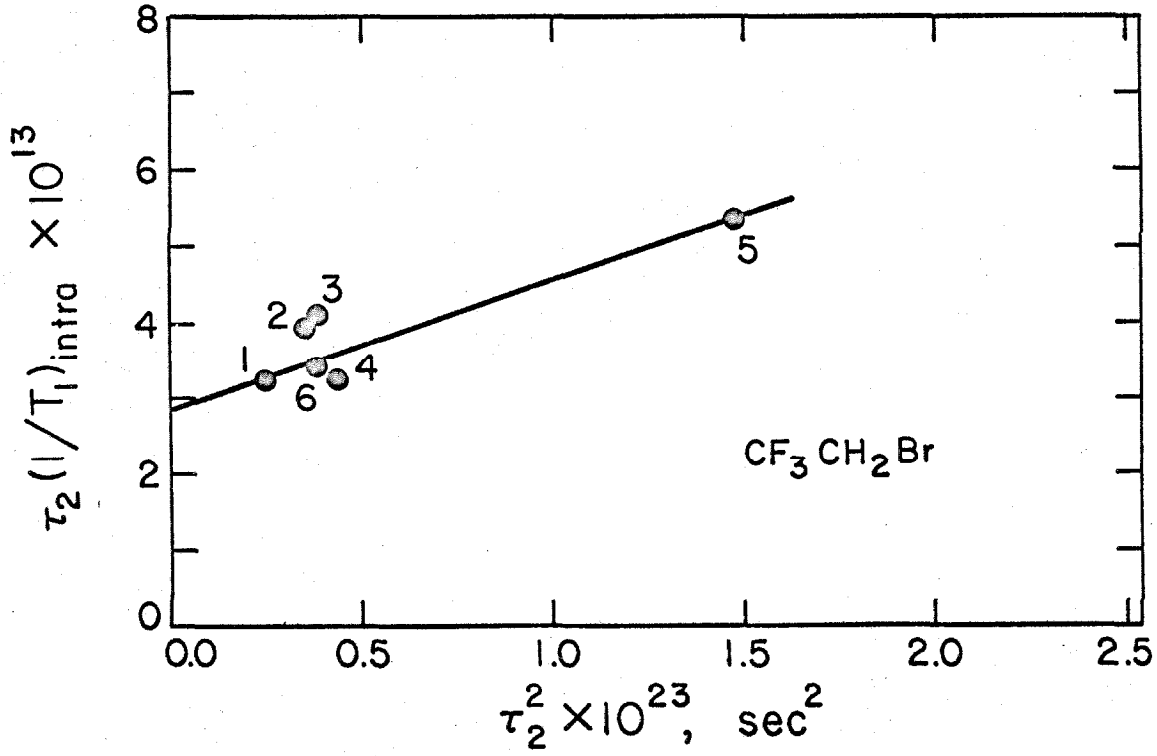
8
6
4
2
0
0.0
0.5
1.0
1.5
2.0
2.5
$\tau_2(1/T_1)_{intra} \times 10^{13}$
$\tau_2^2 \times 10^{23}$, sec^2
1
2
3
4
5
6
CF_3CH_2Br

TABLE XI

Calculated Correlation Times (10^{-12} sec)[a]

solvent	CF_3CH_2I	CF_3CCl_3
CS_2	1.60	2.30
CCl_4	1.91	4.16
diethyl ether	2.07	1.61
CH_3CN	3.97	4.84
$HCCl_3$	1.93	2.82
acetone	3.25	--
benzene	2.81	--

viscosity dependent models for molecular reorientation: even though CF_3CCl_3 is nearly spherical and is comparable in size to the various solvent molecules, the solvent viscosity appears to adequately represent the frictional forces. Unfortunately, our results do not suggest alternative criteria.

The rotational friction coefficient, ξ, a manifestation of the intermolecular potential function $V(r, \theta, \varphi)$, is obviously dependent in a very subtle way upon the structural and electrostatic properties of both the solute and solvent. For example, the extrapolation of CF_3CH_2I mutual viscosities to CF_3CH_2Cl and CF_3CH_2Br, molecules only slightly different from CF_3CH_2I, is not completely satisfactory. The interaction of diethyl ether with CF_3CH_2I, as indicated by the mutual viscosity, is much stronger than its interaction with CF_3CCl_3; for CCl_4, the opposite is true: CCl_4 interacts more strongly with CF_3CCl_3 than with CF_3CH_2I. Thus, although the mutual viscosity provides a good explanation of the experimental results, it is readily apparent that we are far removed from a fundamental interpretation of the problem of molecular reorientation in liquids.

REFERENCES

(1) K. H. Illinger, "Absorption and Dispersion of Microwaves in Gases and Liquids," in Progress in Dielectrics, ed. by J. B. Birks (Academic Press, New York, 1962), Vol. 4.

(2) H. Hase, Z. Naturforsch. 8a, 695 (1953).

(3) N. E. Hill, Proc. Phys. Soc. (London) B67, 149 (1954).

(4) N. Bloembergen, E. M. Purcell, and R. V. Pound, Phys. Rev. 73, 679 (1948).

(5) R. W. Mitchell and M. Eisner, J. Chem. Phys. 33, 86 (1960).

(6) E. A. Guggenheim, Trans. Faraday Soc. 45, 714 (1949).

(7) M. Bloom, Proc. Colloque Ampère XIV (Ljubljana), 65 (1966).

(8) H. S. Gutowsky and D. E. Woessner, Phys. Rev. 104, 843 (1956).

(9) C. R. Ward and C. H. Ward, J. Mol. Spectry. 12, 289 (1964).

(10) D. E. Woessner, J. Chem. Phys. 37, 647 (1962).

(11) H. Shimizu, J. Chem. Phys. 37, 765 (1962).

(12) N. W. Luft, J. Phys. Chem. 59, 92 (1955).

(13) P. S. Hubbard, Phys. Rev. 131, 1155 (1963).

(14) W. A. Steele, J. Chem. Phys. 38, 2404 (1963); 38, 2411 (1963).

(15) W. B. Moniz, W. A. Steele, and J. A. Dixon, J. Chem. Phys. 38, 2418 (1963).

(16) A. Gierer and K. Wirtz, Z. Naturforsch. 8a, 532 (1953).

(17) T. D. Alger and H. S. Gutowsky, J. Chem. Phys. 48, 4625 (1968).

(18) H. Margenau, Rev. Mod. Phys. 11, 1 (1939).

(19) D. A. Pitt and C. P. Smyth, J. Am. Chem. Soc. 81, 783 (1959).

IV. PULSED NMR SPECTROMETER

1. Introduction

The necessary condition for a pulsed nuclear magnetic resonance experiment is that the amplitude of the circularly polarized radio-frequency magnetic field H_1 is sufficiently large to invert the resultant magnetization vector in a time t_π that is short compared with the characteristic times of the system

$$t_\pi = \frac{\pi}{\gamma H_1} < T_2^* < T_1, T_2 \qquad (1)$$

where T_2^* is the characteristic time of the free induction decay, and T_1 and T_2 are, respectively, the longitudinal and transverse relaxation times. In order to investigate relaxation phenomena in solids, where T_2 is usually short, H_1 must be of the order of 50 gauss. Since liquids and gases generally have much longer relaxation times than solids, a spectrometer that is suitable for investigations of solids may also be used for liquids and gases. Since the magnitude of H_1 is proportional to the square root of the radio-frequency power applied to the transmitter coil, one generally seeks as much power as possible, 5000 watts not being uncommon.

A pulsed NMR spectrometer is described in the following Section. A block diagram of the spectrometer is given in Figure 1. Among the principal features of the spectrometer are a designed

FIGURE 1

Block Diagram of the Pulsed Nuclear Magnetic Resonance Spectrometer.

LAYOUT OF PULSED NMR SPECTROMETER

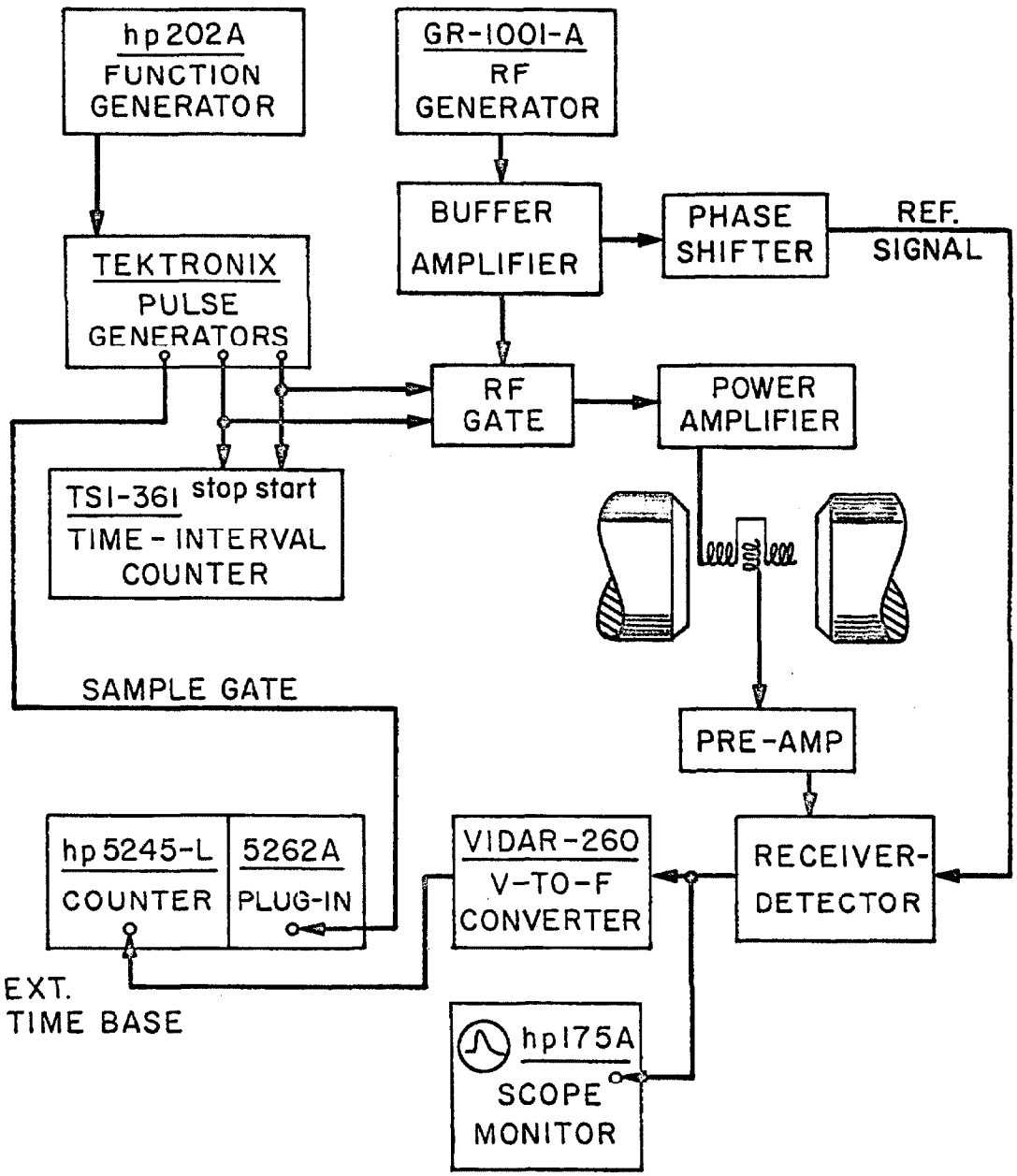

output of 5 kW, a useful frequency range of 2 - 30 MHz, phase-coherent operation with phase-sensitive detection, and rapid recovery of the preamplifier-receiver from saturation due to coupling with the transmitter pulses.

2. Description of the Spectrometer Components

2. 1. *Radio-Frequency Source*

The phase-coherent radio-frequency signal is supplied by a General Radio 1001-A Standard Signal Generator. It is tunable over the entire useful range of the spectrometer and is capable of supplying 400 mW. After a warm-up of from 2 to 3 hours, the long term frequency stability is of the order of 1 part in 10^5.

2. 2. *Buffer Amplifiers, Phase Shifter, and Attenuator*

In order to use phase-sensitive detection, it is necessary to separate the output of the signal generator into two channels: one, with an output of 2. 5 volts, to drive the transmitter, and the second, with a variable output of 0. 0 - 0. 3 volts, to provide the reference signal for the phase-sensitive detector. The two channels must be buffered in order to prevent disturbances from being propagated from one channel to the other. A method for controlling the relative phase between two channels must be included.

The circuit diagram of an instrument incorporating the above features is given in Figure 2. The continuously variable delay line,

FIGURE 2

Circuit Diagram of the Buffer Amplifier and Phase Shifter

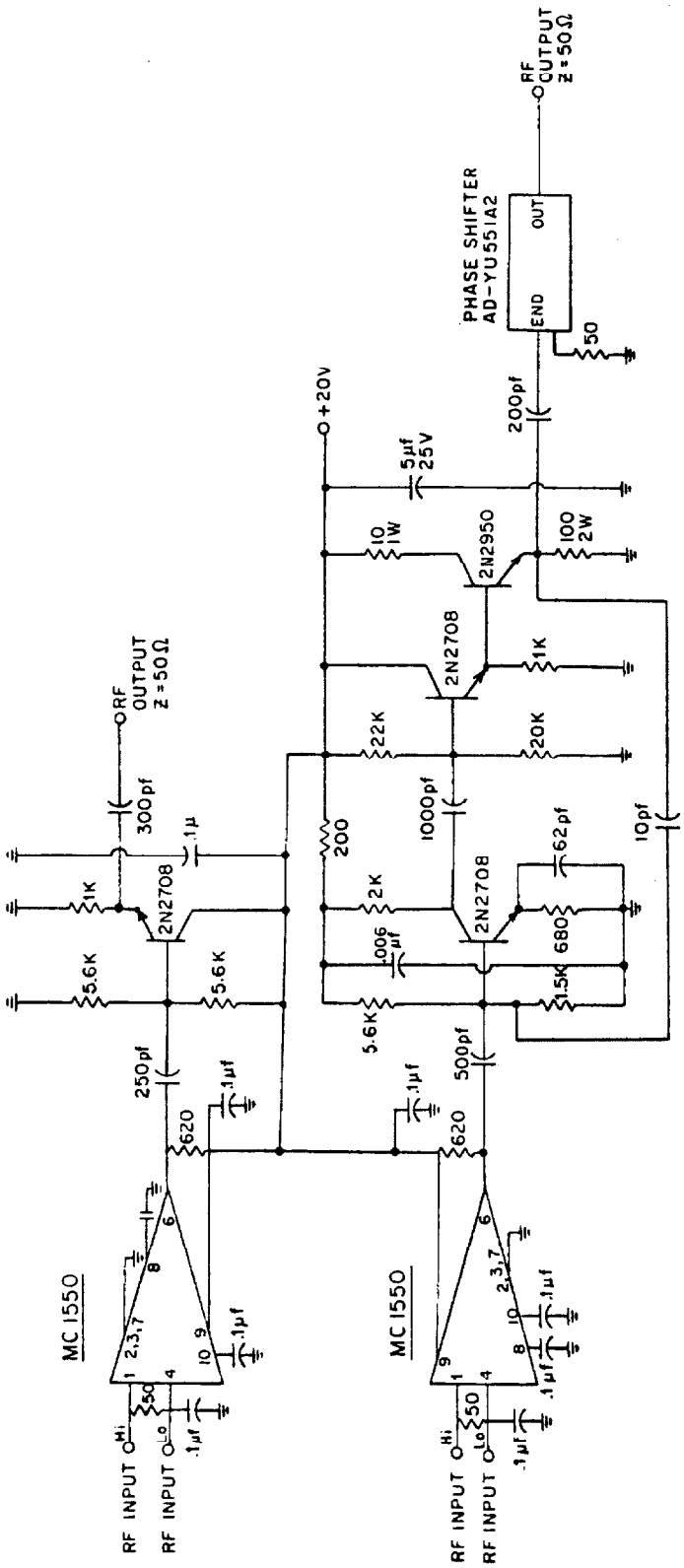
RF OUTPUT Z = 50Ω
PHASE SHIFTER AD-YU551A2
OUT
END
50
200pf
+20V
5µf 25V
10 1W
2N2950
100 2W
2N2708
1K
22K
20K
1000pf
10pf
200
2K
.006 µf
62pf
680
1.5K
5.6K
500pf
620
.1µf
MC 1550
RF INPUT Hi
RF INPUT Lo
300pf
1µ
250pf

an Ad-Yu 551A2, is capable of providing 0.0 - 0.5 μsec delay: i.e., more than 360° of phase shift for all fequencies used. The gain of the reference channel is controlled by a step-attenuator.

2.3. Transmitter

The unmodulated radio-frequency signal is controlled by an rf gate that consists of an integrated circuit amplifier (Motorola, MC1550) that is switched between cut-off and amplification by a negative gating pulse.

The power amplifier was designed by Clark and has been described in detail elsewhere.[1] The transmitter has a designed output of 5 kW and is capable of producing a circularly polarized rf field H_1 of about 50 gauss. Circuit diagrams of the transmitter are given in Figures 3 and 4.

2.4. Coils

The pulses of radio frequency are applied to the transmitter coil of a Varian 8 - 16 MHz wideline NMR probe (V4230B). The high power levels have necessitated the removal of the capcitors from the parallel LC circuit in the probe: the transmitter coil is connected directly to the UHF jack on the body of the probe. In order to minimize coupling, the transmitter and receiver coils are orthogonal and are separated by a Faraday shield. Although the decoupling is on the order of 40 dB, the transmitter pulses induce such strong signal in

FIGURE 3

Circuit Diagram of the Radio-Frequency Gate and the Initial Stages of the Transmitter.

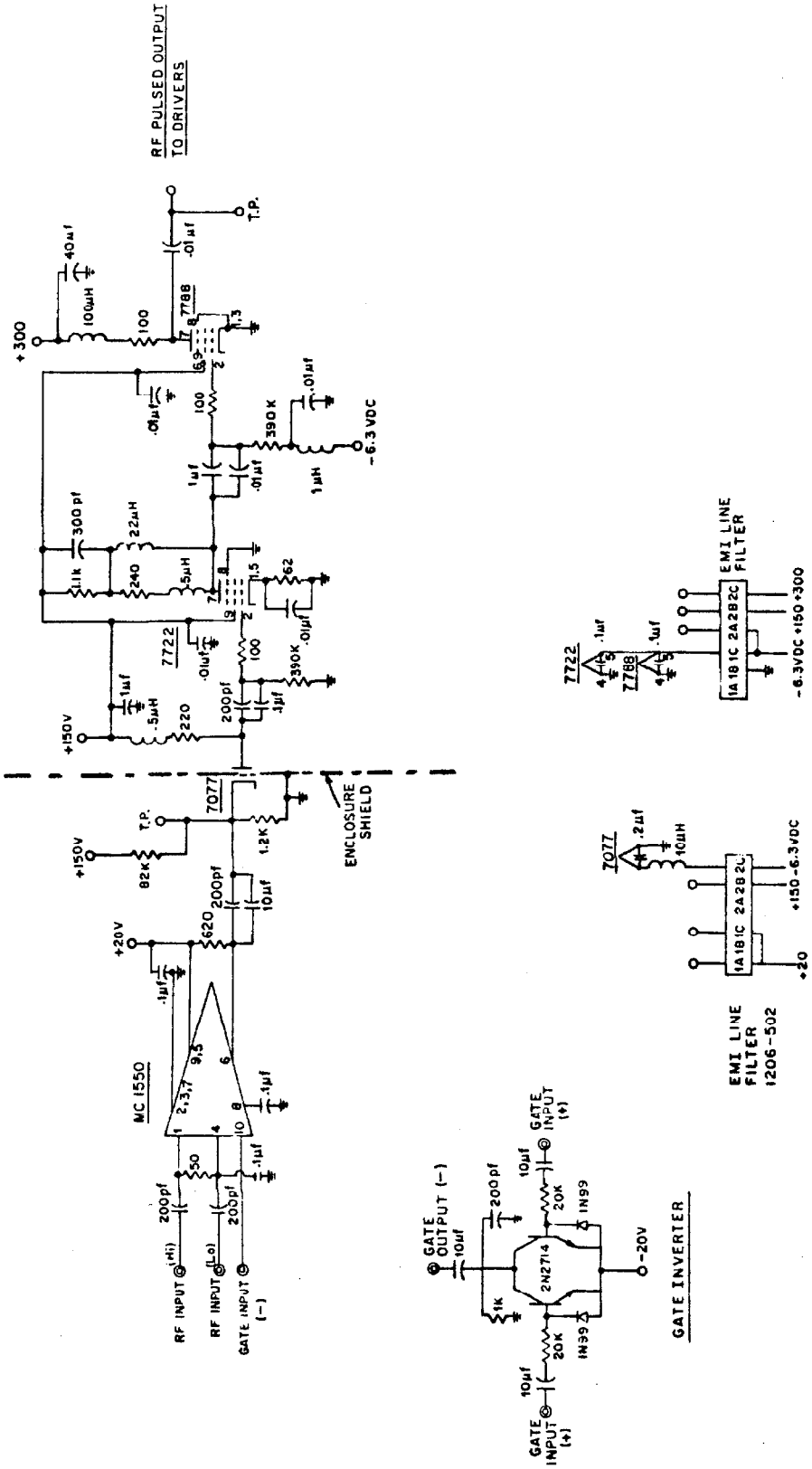
RF PULSED OUTPUT
TO DRIVERS
T.P.
+300
40µf
100µH
100
7788
.01µf
.1µf
.01µf
100
390K
-6.3 VDC
1µf
.01µf
1µH
300 pf
22µH
1.1k
240
.5µH
62
.01µf
7722
.01µf
100
390K
1µf
.5µH
220
200pf
.1µf
+150V
7077
ENCLOSURE
SHIELD
T.P.
+150V
82K
1.2K
200pf
10µf
+20V
620
.1µf
MC 1550
.1µf
50
200pf
200pf
RF INPUT (Hi)
RF INPUT (Lo)
GATE INPUT (-)
7722
7788
.1µf
.1µf
EMI LINE FILTER
1A1B1C 2A2B2C
-6.3VDC +150 +300
7077
.2µf
40µH
1A1B1C 2A2B2C
+150 -6.3VDC
+20
EMI LINE FILTER
1206-502
GATE OUTPUT (-)
10µf
1K
200 pf
2N2714
10µf
20K
1N99
GATE INPUT (+)
-20V
GATE INPUT (+)
10µf
20K
1N99
GATE INVERTER

FIGURE 4

Circuit Diagram of the Final Stages of the Transmitter

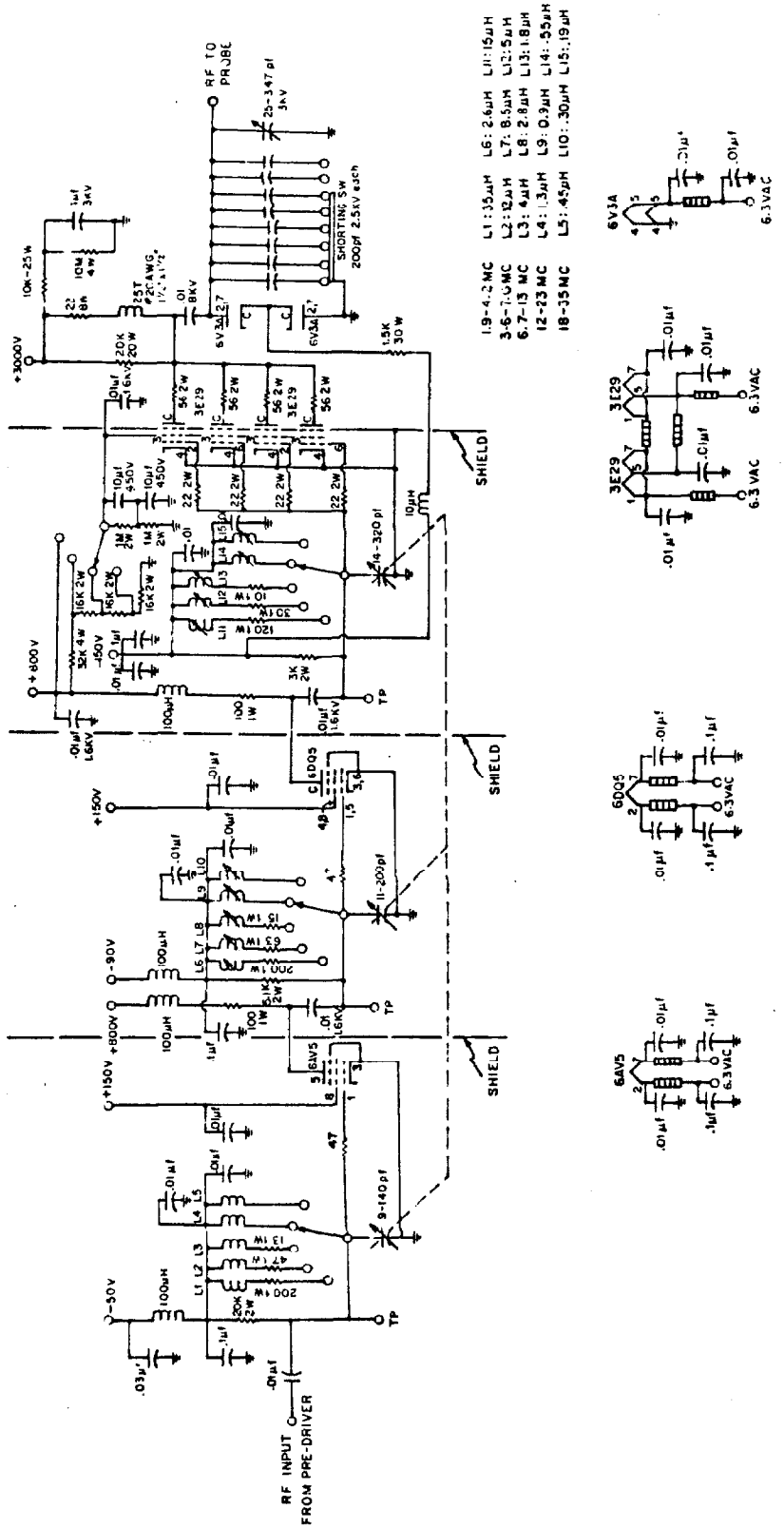
RF INPUT FROM PRE-DRIVER
RF TO PROBE
SHIELD
SHIELD
SHIELD
SHORTING SW
1.9-4.2 MC L1:35μH L6: 2.6μH L11:15μH
3.6-7.0 MC L2:12μH L7: 8.5μH L12:5μH
6.7-13 MC L3: 4μH L8: 2.8μH L13:1.8μH
12-23 MC L4: 1.3μH L9: 0.9μH L14:.55μH
18-35 MC L5: .45μH L10: .30μH L15:.19μH
6V3A
3E29
6DQ5
6AV5
6.3VAC

the receiver coil that the preamplifier and receiver are saturated for approximately 50 μsec following the pulse. Since the experiments described in this Thesis have $T_2^* \sim 5$ msec and $T_1 \gtrsim 1$ sec, saturation is not a problem.

2. 5. Preamplifier-Receiver

The preamplifier and the receiver were designed by Clark and have been described in detail elsewhere.[1] The preamplifier was built by Dr. A. S. Dubin.

2. 6. Digital Data Acquisition System

We utilize a data acquisition system that is similar to the one described by Stejskal;[2] the two systems differ only in the choice of instruments. For an "error function" free induction decay (cf., Section I. 4. 2), the detected output of the receiver is

$$V(t) \propto M_z(t_i) \exp(-t^2/T_2^{*2}) \tag{2}$$

A voltage-to-frequency converter (Vidar, 260-08) converts the amplitude modulated signal to a constant amplitude, frequency modulated pulse train

$$\nu(t) = \frac{V(t)}{V_{ref}} \times 10^6 \text{ Hz} \tag{3}$$

where $\nu(t) \leq 1$ MHz, and V_{ref} is an adjustable reference voltage that is internally supplied. The pulse train is sampled for a time t' by a gated counter (Hewlett Packard, 5245L with a 5262A Time Interval Unit). The counter output equals the number of pulses during the sampling period and is proportional to $M_z(t_i)$

$$N = \int_0^{t'} \nu(t)dt \propto M_z(t_i) \int_0^{t'} \exp(-t^2/T_2^{*2})dt$$
$$\propto M_z(t_i) \text{ erf } (t'/T_2^*) \tag{4}$$

For most of the experiments described in this thesis, $t' \sim 2$ msec. A second counter (TSI, 361-R/M2), gated on by the 180° pulse and gated off by the 90° pulse, measures the time interval t_i.

2.7. Pulse Sequence Unit for T_1 Experiments

A low frequency function generator (Hewlett Packard 202A) operating in the square wave mode controls the rate at which experiments are repeated. In order for the spin system to be in equilibrium at the start of an experiment, it is necessary that the repetition rate $\lesssim 1/5T_1$. The positive portion of the square wave triggers the waveform generator (Tektronix, 162) which controls the three pulse generators (Tektronix, 163). Upon initiation of an experiment, the waveform generator (a) immediately triggers PG 1 which produces the 180° control pulse, and (b) produces a ramp voltage. When, after a time delay t_i, the ramp voltage coincides with a reference level in

PG 2, the 90° control pulse is produced; at the same time, PG 3 is triggered producing the sampling pulse that gates the counter associated with the voltage-to-frequency converter.

2. 8. Power Supplies

The spectrometer utilizes six power supplies (+3000 Vdc, +800 Vdc, +150 Vdc, -150 Vdc, -6. 3 Vdc, and 6. 3 Vac). The power supplies are interlocked in such a manner that a component failure will shutdown the spectrometer. The interlocking diagram is given in Figure 5.

FIGURE 5

Circuit Diagram of the Power Supply Interlock

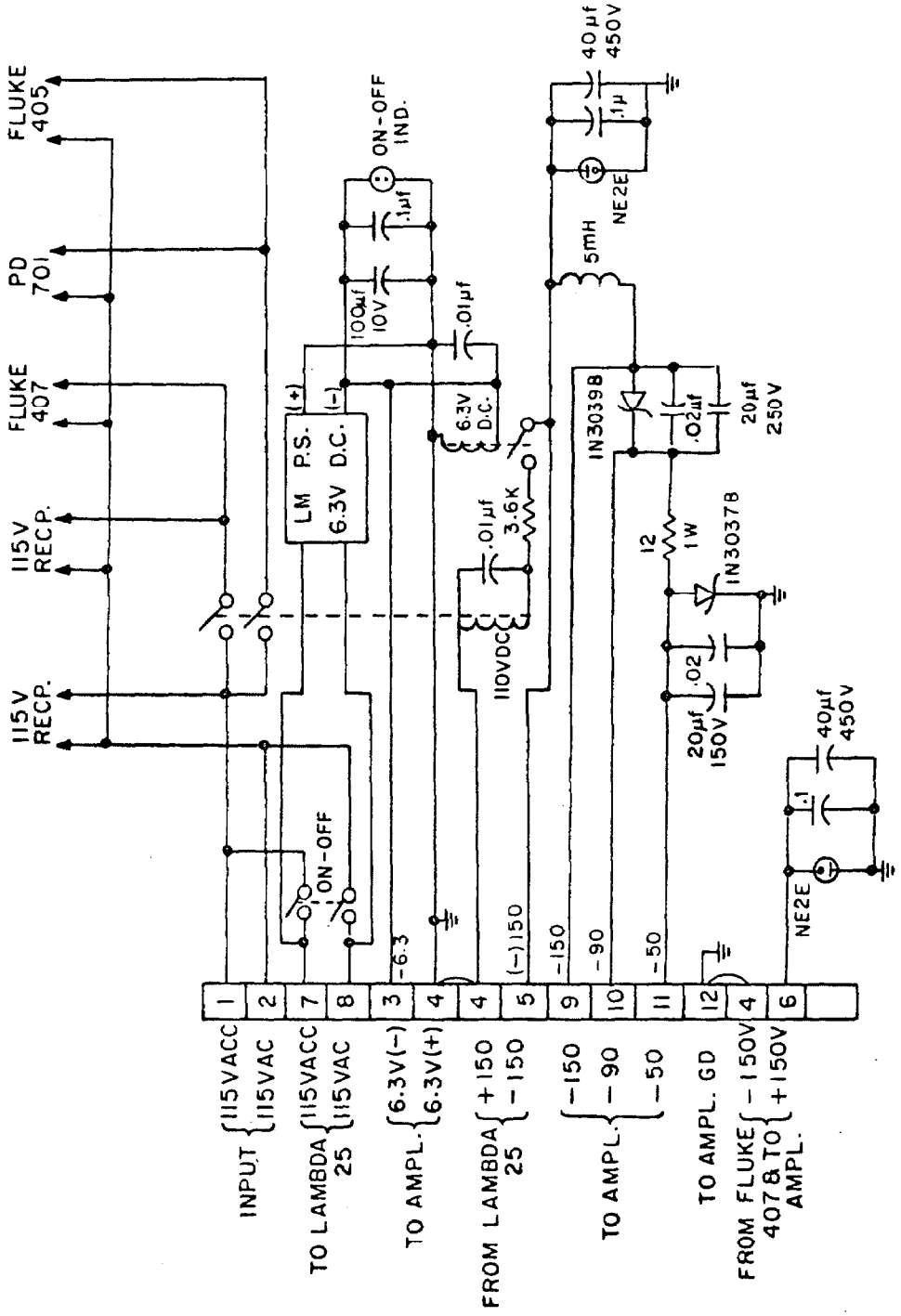
FLUKE 405
PD 701
FLUKE 407
115V RECP.
115V RECP.
ON-OFF
LM P.S.
6.3V D.C.
(+)
(-)
ON-OFF IND.
.1μf
100μf 10V
.01μf
6.3V D.C.
.01μf
3.6K
110VDC
40μf 450V
.1μ
NE2E
5mH
IN3039B
.02μf
20μf 250V
12
1W
IN3037B
.02
20μf 150V
.1
40μf 450V
NE2E
1 2 7 8 3 4 4 5 9 10 11 12 4 6
-6.3
(-)150
-150
-90
-50
INPUT 115VAC 115VAC
TO LAMBDA 25 115VAC 115VAC
TO AMPL. 6.3V(-) 6.3V(+)
FROM LAMBDA 25 +150 -150
TO AMPL. -150 -90 -50
TO AMPL. GD
FROM FLUKE 407 & TO AMPL. -150V +150V

REFERENCES

(1) W. G. Clark, Rev. Sci. Instr. 35, 316 (1964).

(2) E. O. Stejskal, Rev. Sci. Instr. 34, 971 (1963).

PROPOSITIONS

PROPOSITION I

It is proposed that depolarization of Rayleigh scattered light be used for the investigation of molecular xenon Xe_2.

Bernardes and Primakoff[1] have predicted that, except for helium, all the inert gases in their ground state electronic configurations will form stable diatomics. Several authors have subsequently invoked the existence of Xe_2 to account for experimental observations.

Carr and co-workers[2, 3] have used pulsed nuclear magnetic resonance techniques to study ^{129}Xe ($I = \frac{1}{2}$). They have observed a density dependent chemical shift (relative to ^{129}Xe at low density) and a rate of relaxation ($1/T_1$) that is several orders of magnitude more rapid than can be accounted for by standard relaxation theory. Both the chemical shift and ($1/T_1$) are proportional to the density over a wide range extending from low density gas well into the liquid phase. Torrey[4] has interpreted their results in the following way: during a molecular collision the charge cloud of the xenon atom is distorted. At the same time, the relative motion of the colliding atoms causes the distorted charge clouds of the collision complex to rotate. The rotation produces a fluctuating magnetic field at the nucleus and causes relaxation. Torrey's interpretation is also consistent with the chemical shift observations.

Shardanand[5] has measured the attenuation cross section at Lyman-α (1216Å) for xenon. The attenuation, which cannot be

attributed to atomic absorption, is anomalous because it does not obey Beer's law: the attenuation cross section increases linearly with the pressure. The observed attenuation is interpreted in terms of atomic scattering and molecular absorption:

$$\sigma_{eff} = \sigma_1 + Kn'\sigma_2 \qquad (1)$$

where σ_{eff} is the experimentally observed attenuation cross section; σ_1 and σ_2 are the cross sections for, respectively, atomic scattering and molecular absorption; n′ is the total concentration of monomers and dimers; and K is the equilibrium constant for the reaction

$$Xe + Xe \rightleftharpoons Xe_2 \qquad (2)$$

Shardanand points out that the dimerization of xenon will lead to a deviation in the perfect gas representation of atomic xenon gas. Thus he finds that he can relate the equilibrium constant K with the second virial coefficient B for xenon:

$$K = B = 2.2 \times 10^{-22} \text{ cm}^3/\text{molecule} \qquad (3)$$

From the temperature dependence of σ_{eff}, Shardanand has calculated that the heat of dissociation for Xe_2 is equal to 0.030 eV.

The basic disadvantage of the attenuation technique is that the intensity I of transmitted light depends strongly upon the pressure:

$$I = I_0 \exp\left[-p^2 N_L{}^2 K \sigma_2 \ell\right] \qquad (4)$$

where p is the pressure (atmospheres), N_L is Loschmidt's number, and ℓ is the optical path length. An attenuation study of xenon gas over a range of temperatures and pressures would require cells with different path lengths. Even then, experiments would have to be restricted to low pressures: for example, path lengths of the order of 10^{-2} cm would be required for studies at 10 atmospheres pressure. In other words, the critical region (P_c = 58.2 atmospheres) and the liquid state cannot be studied by the attenuation technique.

We propose that light scattering techniques would permit studies of xenon over a greater range of experimental conditions, including the critical region and the liquid state. Such studies would complement the attenuation studies at low pressures and, in addition, might provide information about the moment of inertia of Xe_2 and, therefore, the internuclear distance. We shall now discuss light scattering in order to show that such experiments are feasible.

The depolarization ratio ρ_0 for light scattered normal to the plane defined by the propagation and electric vectors of the polarized incident light is given by

$$\rho_0 = I_\perp / I_\parallel \qquad (5)$$

where $I_\perp$ and $I_\parallel$ are the intensities of the light polarized perpendicular and parallel to the electric vector of the incident light. For a two

component system consisting of monomers (Xe) and dimers (Xe_2), the depolarization ratio may be written

$$\rho_0 = \frac{n_1\sigma_{depol}^{(1)} + n_2\sigma_{depol}^{(2)}}{n_1\sigma_{pol}^{(1)} + n_2\sigma_{pol}^{(2)}} \tag{6}$$

where n_i is the concentration (molecules/cm^3) of i-mers. The cross section for polarized scattering by an i-mer is related to the autocorrelation function of the average value $\bar{\alpha}^{(i)}$ of the polarizability tensor $\underset{\sim}{\alpha}^{(i)}$:[6]

$$\sigma_{pol}^{(i)} = \int_{-\infty}^{\infty} \left\langle \bar{\alpha}^{(i)}(0) \cdot \bar{\alpha}^{(i)}(\tau) \right\rangle e^{-i\omega\tau} d\tau \tag{7}$$

The cross section for depolarized scattering by an i-mer is related to the autocorrelation function of the anisotropy $\beta^{(i)}$ of the polarizability tensor:[6]

$$\sigma_{depol}^{(i)} = \int_{-\infty}^{\infty} \left\langle \mathrm{Tr}\, \underset{\sim}{\beta}^{(i)}(0) \cdot \underset{\sim}{\beta}^{(i)}(\tau) \right\rangle e^{-i\omega\tau} d\tau \tag{8}$$

where

$$\underset{\sim}{\beta}^{(i)} = \underset{\sim}{\alpha}^{(i)} - \underset{\sim}{1}\,\bar{\alpha}^{(i)} \tag{9}$$

Atomic xenon is spherically symmetric; consequently, $\underset{\sim}{\beta}^{(1)} = \sigma_{depol}^{(1)} = 0$: viz., a spherically symmetric scattering center will not depolarize the incident light. Since Shardanand's equlibrium constant gives

$n_2 \approx 0.006\ n_1$ at 1 atmosphere and 20°C, we shall assume that we can neglect the contribution of Xe_2 to $I_{||}$. Thus Eq. (6) reduces to

$$\rho_0 = (n_2/n_1)\left(\sigma^{(2)}_{depol}/\sigma^{(1)}_{pol}\right) \tag{10}$$

$\sigma^{(1)}_{pol}$ may be evaluated as follows: since $\bar{\alpha}^{(1)}$ is a constant independent of the time τ

$$\left\langle \bar{\alpha}^{(1)}(0) \cdot \bar{\alpha}^{(1)}(\tau) \right\rangle = \left[\bar{\alpha}^{(1)}\right]^2 \tag{11}$$

Therefore

$$\sigma^{(1)}_{pol} = \left[\bar{\alpha}^{(1)}\right]^2 \int_{-\infty}^{\infty} e^{-i\omega\tau}\, d\tau = \left[\bar{\alpha}^{(1)}\right]^2 \delta(\omega) \tag{12}$$

since the integral is the Fourier representation of the Dirac delta function $\delta(\omega)$.

Although $\sigma^{(2)}_{depol}$ cannot be evaluated analytically, it may be simplified:

$$\sigma^{(2)}_{depol} = \frac{2}{3}\left(\alpha^{(2)}_{||} - \alpha^{(2)}_{\perp}\right)^2 \int_{-\infty}^{\infty} \left\langle P_2[\vec{u}(0) \cdot \vec{u}(\tau)] \right\rangle e^{-i\omega\tau}\, d\tau \tag{13}$$

where $\alpha^{(2)}_{||}$ and $\alpha^{(2)}_{\perp}$ are the components of $\underset{\sim}{\alpha}^{(2)}$ parallel and perpendicular to the bond axis, P_2 is the second Legendre polynomial, and $\vec{u}$ is a unit vector along the molecular symmetry axis.[6] Therefore, Eq. (10) reduces to

$$\rho_0 \sim \frac{n_2}{n_1} \left[\frac{\alpha_{\parallel}^{(2)} - \alpha_{\perp}^{(2)}}{\bar{\alpha}^{(1)}} \right]^2 \frac{\int_{-\infty}^{\infty} \left\langle P_2[\vec{u}(0) \cdot \vec{u}(\tau)] \right\rangle e^{-i\omega\tau} d\tau}{\delta(\omega)} \quad (14)$$

In order to estimate the magnitude of ρ_0, it will be assumed that $\langle P_2[\vec{u}(0)\cdot\vec{u}(\tau)]\rangle \sim \frac{1}{4}$ and that $\alpha_{\parallel}^{(2)} \sim 1.3\, \alpha_{\perp}^{(2)} \sim 1.3\, \bar{\alpha}^{(1)}$. Then, with $n_2/n_1 \sim 0.006\, p$ for low pressures, Eq. (14) gives

$$\rho_0 \sim 2 \times 10^{-4}\, P \quad (15)$$

Since the results of Bridge and Buckingham[7] suggest that measurements can be made for depolarization ratios $\rho_0 \gtrsim 10^{-3}$, depolarization of scattered light should be observable at xenon pressures $p \gtrsim 5$ atmospheres.

The normalized frequency distribution of the depolarized light intensity is given by[8]

$$I(\Delta\omega) = \frac{1}{1 + (\Delta\omega)^2 \tau_\alpha^2} \quad (16)$$

where $\Delta\omega$ is the frequency shift, relative to the frequency of the incident light, and τ_α is the correlation time associated with fluctuations of $\underset{\sim}{\alpha}$. The correlation time for a molecule undergoing dynamically coherent reorientation is[9]

$$\tau_\alpha = \frac{1}{2} \left[\frac{\pi I}{3kT} \right]^{\frac{1}{2}} \quad (17)$$

Therefore, the width of the distribution is related to the moment of inertia of Xe_2 and, consequently, to the internuclear distance.

REFERENCES

(1) N. Bernardes and H. Primakoff, J. Chem. Phys. 30, 691 (1959).

(2) R. L. Streever and H. Y. Carr, Phys. Rev. 121, 20 (1961).

(3) E. R. Hunt and H. Y. Carr, Bull. Am. Phys. Soc. 7, 293 (1962).

(4) H. C. Torrey, Phys. Rev. 130, 2306 (1964).

(5) Shardanand, Phys. Rev. 160, 67 (1967).

(6) R. G. Gordon, Advances in Magnetic Resonance, 3, 1 (1968).

(7) N. J. Bridge and A. D. Buckingham, J. Chem. Phys. 40, 2733 (1964).

(8) M. Leontovich, J. Phys. USSR 4, 449 (1941).

(9) W. A. Steele, J. Chem. Phys. 38, 2404 (1963); 38, 2411 (1963).

PROPOSITION II

A study of the temperature, density, and concentration dependence of the nuclear spin relaxation of gaseous $^{15}N_2$ is proposed. Such a study would provide information about the transfer of angular momentum between colliding molecules and would also serve as a test of the general validity of theories of relaxation which have been developed for H_2.

The rate at which a system of spin-$\frac{1}{2}$ nuclei approaches thermal equilibrium with its surroundings is governed by the fluctuating magnetic fields at the nuclear sites. (1) The local field at a nucleus, generated by the molecular rotational magnetic moment and by the dipole moments of other nuclei on the same molecule, is made time dependent by those collisions which cause molecular reorientation. Thus studies of nuclear spin relaxation can provide information about the anisotropic intermolecular interactions required to cause molecular reorientation during a collision.

The rate of relaxation of molecular hydrogen, the only gas which has been extensively studied, is given by

$$\frac{1}{T_1} = \frac{2}{3}\gamma^2 H'^2 J(J+1)\tau_c + \frac{6\gamma^2 H''^2 J(J+1)\tau_c}{(2J-1)(2J+3)} \qquad (1)$$

where $H' = 27$ gauss is the spin-rotational coupling constant and $H'' =$

34 gauss is the dipolar coupling constant.[1] Because of symmetry restrictions and the large rotational constant ($\theta_r = 86°K$), the $J = 1$ rotational state of H_2 is the only observable state with a significant population at temperatures $T \lesssim 300°K$. The correlation time τ_c, the mean time between Δm_J transitions within the $J = 1$ manifold, is related to the details of the collisional process.[2]

Bloom and Oppenheim[3] have proposed that, in the limit where transitions between J states may be neglected, Eq. (1) may be modified in order to account for the population of higher rotational states ($J = 3, 5, \cdots$):

$$(1/T_1) = \sum_{\text{odd } J} P_J (1/T_1)_J \qquad (2)$$

where $(1/T_1)_J$ is the rate of relaxation of a molecule in the Jth rotational state [Eq. (1)] and

$$P_J = \frac{(2J+1)\exp\left[-J(J+1)\theta_r/T\right]}{\sum_{\text{odd } J}(2J+1)\exp\left[-J(J+1)\theta_r/T\right]} \qquad (3)$$

is the probability that the J state is occupied. Since any ΔJ transitions will serve to shorten the correlation time τ_c, Eq. (2) represents an upper limit to the rate of relaxation.[3]

Although molecular hydrogen has received considerable theoretical[4] and experimental[5] attention, it is unique in that the intermolecular torques are very weak and the rotational levels are

very widely spaced. Therefore the techniques which are used for the interpretation of H_2 relaxation times may be of limited usefulness for heavier molecules.[6] We propose that a study of the nuclear spin relaxation of gaseous $^{15}N_2$ would provide a test of the validity of Eq. (2).

The parameters which are required to evaluate Eq. (2) for $^{15}N_2$ have been measured or are readily calculable: $H' = 50.97$ gauss,[7] $H'' = 1.19$ gauss, and $\theta_r = 2.68°K$. Since the spin-rotational contribution is dominant for all values of J, Eq. (2) may be written

$$\frac{1}{T_1} \approx \frac{2}{3} \gamma^2 H'^2 \tau_c \sum_{\text{odd } J} [P_J J(J+1)] \tag{4}$$

Replacing the summation by integration gives

$$(1/T_1) \approx \frac{2\gamma^2 H'^2 T \tau_c}{3\theta_r} \tag{5}$$

The correlation time τ_c is related to the mean time between collisions τ_{coll}:

$$\tau_c = W^{-1} \tau_{coll} \tag{6}$$

where W is the probability that a given collision will cause a Δm_J transition. τ_{coll} may be calculated from the results of the kinetic gas theory for hard spheres[8]

$$\tau_{coll} = \frac{1}{Na^2} \left[\frac{\mu}{8\pi kT} \right]^{\frac{1}{2}} \tag{7}$$

where N is the number density of molecules and a is the collision diameter. Thus Eq. (5) gives

$$\frac{1}{T_1} \approx \frac{2\gamma^2 H'^2 T^{\frac{1}{2}}}{3\theta_r} \times \frac{1}{Na^2}\left[\frac{\mu}{8\pi k}\right]^{\frac{1}{2}} W^{-1} \qquad (8)$$

which, for pure $^{15}N_2$, is

$$(1/T_1) = 17.3\, T^{\frac{1}{2}}/W\rho \qquad (9)$$

where ρ is the number density in amagat units.

Christensen[9] has reported the value of the transition probability per collision (W = 0.091) for H_2 at infinite dilution in N_2 at 29°C and 25.0 amagats. Since W is a measure of the ease with which H_2 and N_2 exchange angular momentum, the same value describes the transition probability per collision for N_2 at infinite dilution in H_2. With the assumption that there is no significant isotope effect, Eq. (8) gives

$$(1/T_1) \approx 46.4 \text{ sec}^{-1} \qquad (10)$$

for $^{15}N_2$ at infinite dilution in H_2 at 29°C and 25.0 amagats. Any significant shortening of $(1/T_1)$ would have to be ascribed to ΔJ transitions.

In summary, a study of the temperature, density, and concentration dependence of the nuclear spin relaxation of $^{15}N_2$ would

provide information about the probability per collision for a change of angular momentum and would also serve as a test of the general validity of theories which have been developed for H_2.

REFERENCES

(1) A. Abragam, The Principles of Nuclear Magnetism (Oxford University Press, London, 1961).

(2) M. Bloom, I. Oppenheim, M. Lipsicas, C. G. Wade, and C. F. Yarnell, J. Chem. Phys. 43, 1036 (1965).

(3) M. Bloom and I. Oppenheim, Can. J. Phys. 41, 1580 (1963).

(4) N. Bloembergen, E. M. Purcell, and R. V. Pound, Phys. Rev. 73, 679 (1948); G. T. Needler and W. Opechowski, Can. J. Phys. 39, 870 (1961).

(5) E. M. Purcell, R. V. Pound, and N. Bloembergen, Phys. Rev. 70, 986 (1946); M. Bloom, Physica 23, 237, 378 (1957); M. Lipsicas and M. Bloom, Can. J. Phys. 39, 881 (1961); D. L. Williams, Can. J. Phys. 40, 1027 (1962); C. S. Johnson and J. Waugh, J. Chem. Phys. 36, 2266 (1962).

(6) R. G. Gordon, J. Chem. Phys. 44, 228 (1966).

(7) M. R. Baker, C. H. Anderson, and N. F. Ramsey, Phys. Rev. 133, A1533 (1964); S. I. Chan, M. R. Baker, and N. F. Ramsey, Phys. Rev. 136, A1224 (1964).

(8) A. A. Frost and R. G. Pearson, Kinetics and Mechanism (John Wiley & Sons, Inc., New York, 1961), p. 60.

(9) C. R. Christensen, Ph. D. Thesis, California Institute of Technology, 1966 (unpublished), p. 50.

PROPOSITION III

The high-frequency contribution to dielectric absorption in aniline has been attributed both to internal rotation and to inversion. It is proposed that the question may be settled by nuclear spin relaxation techniques.

For a rigid dipolar molecule, the only mechanism for dielectric absorption at microwave frequencies consists of the rotational motion of the molecular dipole against the intermolecular force field. The situation is more complex for non-rigid molecules because the internal motions may also constitute an absorption mechanism. Since the observed dielectric behavior of a molecule may be related to the details of the reorientational processes, non-rigid molecules have been extensively investigated. (1)

Dielectric absorption and dispersion measurements at frequencies from 0.5 MHz to 150 GHz indicate that anisole (φOCH_3) has two relaxation times: the larger of the two ($\tau_M = 14.7 \times 10^{-12}$ sec) is due to end-over-end motion; the shorter relaxation time ($\tau_M = 3.2 \times 10^{-12}$ sec) corresponds to the rotational motion of the OCH_3 group about its bond to the benzene ring. An analysis of the relative contributions of the end-over-end and internal motions to the total orientation polarization suggests that the internal reorientation of the methoxy group is hindered by a potential barrier which could arise from some double-bond character over overlap of π-orbitals in the C-O

bond. [2, 3]

It has also been observed that aniline has two relaxation times. [2, 4] As is the case with anisole, the longer relaxation time ($\tau_M = 22.2 \times 10^{-12}$ sec) corresponds to overall molecular reorientation, and the shorter relaxation time ($\tau_M = 0.9 \times 10^{-12}$ sec), to an internal reorientation process. Although the internal reorientation has been attributed both to internal rotation[4] and to inversion, [2] Smyth has pointed out that there is no conclusive support for either interpretation. [3] It is proposed that a study of the temperature dependence of the rates of nuclear spin relaxation of the amine and ring protons of aniline would resolve this question.

Let us assume that internal reorientation occurs by means of nitrogen inversion. Since the effect of molecular vibrations on nuclear spin relaxation is completely negligible, [5] the relaxation of the amine protons will be controlled by the overall reorientation of the molecule. Consequently, the ratio T_1(ring)/T_1(amine) will be independent of the temperature.

Since the internal reorientation process is strongly temperature dependent ($\Delta H \approx 1$ kcal/mole), [6] an increase of temperature will increase the rate of internal reorientation. Since any internal rotation decreases the effectiveness of the intramolecular dipolar interaction, [7] the ratio T_1(ring)/T_1(amine) will decrease with increasing temperature if the internal reorientation occurs via internal rotation.

In summary, a study of the temperature dependence of T_1(ring)/T_1(amine) for aniline protons can resolve the question about the nature

of the internal reorientation: if internal reorientation occurs via inversion, the ratio will be independent of the temperature; if the internal reorientation occurs via internal rotation, the ratio will decrease with increasing temperature.

REFERENCES

(1) See, for example, C. P. Smyth, Ann. Rev. Phys. Chem. 17, 433 (1966).

(2) S. K. Garg and C. P. Smyth, J. Chem. Phys. 46, 373 (1967).

(3) C. P. Smyth, Advan. Mol. Relaxation Processes 1, 1 (1967).

(4) E. L. Grubb and C. P. Smyth, J. Am. Chem. Soc. 83, 4879 (1961).

(5) N. Bloembergen, E. M. Purcell, and R. V. Pound, Phys. Rev. 73, 679 (1948).

(6) Calculated from data in Reference 2.

(7) D. E. Woessner, J. Chem. Phys. 36, 1 (1962); 42, 1855 (1965).

PROPOSITION IV

An ion cyclotron resonance study of the ion-molecule reactions of a model planetary atmosphere is proposed.

According to the hypotheses put forward by Oparin[1] and Haldane,[2] life originated from ordinary chemical reactions by a slow evolutionary process. Oparin postulated that the Earth had a reducing atmosphere of methane, ammonia, water, and hydrogen from which various organic compounds might be formed. Haldane suggested that the organic matter accumulated in the oceans thereby forming a "primordial soup" which gradually gave rise to replicating systems.

The synthesis of biologically significant molecules under conditions simulating those of the primitive Earth was established by Miller.[3] He exposed a mixture of methane, ammonia, water, and hydrogen to an electrical discharge and obtained amino acids and such organic compounds as urea and formic acid. Subsequent investigators have verified Miller's results and have extended the scope of the original work.[4] It has been observed that, as long as the model atmosphere is reducing, a variety of initial conditions will lead to hydrogen cyanide and formaldehyde which are apparently essential precursors of the more complex organic molecules.[5] There have been numerous attempts to synthesize organic compounds under the oxidizing conditions of the present atmosphere: all have been unsuccessful.[6] It has also been observed that the production of organic

molecules in a reducing atmosphere is independent of the source of energy (vacuum UV radiation, electrical discharges, heat, and high-energy radiation).[7]

Lederberg has commented that, to date, biology has been an earth-bound science whereas physics and chemistry have a universality.[8]

> This disparity in the domains of the physical versus the biological sciences attenuates most of our efforts to construct a theoretical biology as a cognate of theoretical physics and chemistry. For the most part, biological science has been a rationalization of particular facts, and we have had all too limited a basis for the construction and testing of meaningful axioms to support a theory of life ...
>
> .....
>
> From this standpoint, the overriding objective of exobiological research is to compare the over-all patterns of chemical evolution of the planets ...

As part of an effort to contribute to an understanding of the chemical evolution of the planets, it is proposed that the ion-molecule reactions of the Jovian atmosphere be studied by ion cyclotron resonance techniques. Why Jupiter? Jupiter, the nearest planet with a reducing atmosphere, might be regarded as a representation of the primitive Earth. Sagan[9] has pointed out that the conditions on Jupiter are similar to those used in abiogenesis experiments such as Miller's.[3] Furthermore, if organic molecules are being generated, their spectral ines might be detectable by observational spectroscopy. Indeed, lines of unknown origin have been detected in high-resolution spectra of Jupiter.[10] An anomalous enhancement of 8-14 micron radiation has been observed to take place in eclipsed regions as

Jupiter is crossed by the shadow of its satellite.[11] It has been suggested that this phenomena may be due to the production of ethylene in the ionosphere.[12] A study of the ion-molecule chemistry of a simulated Jovian atmosphere might shed light on such questions.

The upper Jovian atmosphere is generally considered to consist of H_2, He, CH_4, and NH_3 in varying abundances. Lasker[13] has suggested that the composition is 74% H_2, 24% He, 2% CH_4, and ~0.3% NH_3. The ion chemistry of methane has been extensively studied and it has been shown that polymers, ethane, ethylene, and other hydrocarbons are obtained by irradiating solid or gaseous methane.[14] The qualitative nature of the yield appears to be relatively independent of the nature of the radiation as long as it is sufficiently energetic to ionize methane (13.1 eV, $\lambda = 946$Å). The effects of high concentrations of H_2 and NH_3 are not known. Hydrogen might saturate the hydrocarbons; ammonia, with an ionization potential of 10.5 eV, might neutralize such species as CH_4^+ by electron transfer. Although electric discharge studies involving anhydrous methane and ammonia lead to the formation of acetylene and hydrogen cyanide,[7] whether or not such molecules can be generated in a reasonable facsimile of the Jovian atmosphere remains an open question.

Because ion cyclotron resonance techniques are uniquely suited for studies of complex ion-molecule reactions,[15] it is reasonable that these techniques be applied to studies of the chemistry of the Jovian atmosphere.

REFERENCES

(1) A. I. Oparin, Life, Its Nature, Origin, and Development (Oliver and Boyd, London, 1961).

(2) J. B. S. Haldane, Rationalist Annual, 142 (1928).

(3) S. L. Miller, J. Am. Chem. Soc. 77, 2351 (1955).

(4) See, for example, E. A. Shneour and E. A. Ottesen, Extra-terrestial Life: An Anthology and Bibliography (National Academy of Sciences, Washington, D. C., 1966).

(5) S. L. Miller and H. C. Urey, Science 130, 245 (1959).

(6) See, for example, W. M. Garrison, D. C. Morrison, J. G. Hamilton, A. A. Benson, and Melvin Calvin, Science 114, 416 (1951).

(7) C. Ponnamperuma, Icarus 5, 450 (1966).

(8) J. Lederberg, Science 132, 393 (1960).

(9) I. S. Shklovskii and C. Sagan, Intelligent Life in the Universe (Holden-Day, Inc., San Francisco, 1966), p. 328.

(10) H. Spinrad and L. M. Trafton, Icarus 2, 19 (1962).

(11) B. C. Murray, R. L. Wildey, and J. A. Westphal, Astrophys. J. 139, 986 (1964).

(12) W. C. Saslaw and R. L. Wildey, Icarus 7, 85 (1967).

(13) B. M. Lasker, Astrophys. J. 138, 709 (1963).

(14) S. Wexler and N. Jesse, J. Phys. Chem. 84, 3425 (1962); L. W. Sieck and R. H. Johnson, J. Phys. Chem. 67, 2281 (1963); D. R. Davis and W. F. Libby, Science 144, 991 (1964).

(15) J. L. Beauchamp, Ph. D. Thesis, Harvard University, 1967 (unpublished); J. L. Beauchamp, J. Chem. Phys. 46, 1231 (1967); J. D. Baldeschwieler, Science 159, 263 (1968).

PROPOSITION V

It has been observed that focused, coherent radiation causes a degradation of hydrocarbons. The mechanism of the degradation and the nature of any intermediates are not known. An experiment is proposed which will indicate whether or not ionic intermediates are involved.

The physical conditions existing at the focal point of a focused, pulsed laser have been the subject of some speculation.[1-3] Since the beam can be focused on a very small area, extremely high power densities and electric field strengths are attainable. The exposure of a chemical to such severe conditions should lead to extensive degradation.

To date, there have been only a few attempts to study the products formed by laser degradation. Wiley and Veeravagu have degraded solid aromatic hydrocarbons with a 6943Å ruby laser operating in the normal (burst) mode.[4] Degradation was extensive. The gaseous products, analyzed by gas chromatographic and mass spectrometric techniques, consisted primarily of methane and acetylene with small amounts of C_2 and C_4 unsaturated hydrocarbons; there was no analysis for hydrogen. Wiley and Reich[5] have "photolyzed" gaseous methane, ethane, ethylene, cyclopropane, and butane. Extensive degradation was observed and carbon was formed. The principal products were methane and acetylene. Lane and Valance

have "photolyzed" propane with a Q-switched neodymium laser (1.06 μ).[6] Their results indicate that methane, acetylene, and molecular hydrogen are the principal products; formation of carbon was not observed. They have ruled out localized heating and/or sparking as degradation mechanisms; the possibility of multi-photon absorption or scission in the intense electric fields remains.

The nature of the intermediates involved in the degradation cannot be ascertained through the use of either radical[7] or charge[8] scavengers since foreign species would also be expected to undergo degradation.

In order to determine whether or not ionization is involved, the following experiment is proposed. An ion cyclotron resonance spectrometer,[9] set to a specific (e/m) ratio, may be used to moniter the ions, if any, that are formed during a laser pulse. The mass spectrum of the ions can be obtained in a stepwise fashion. Since the possibility that multiply charged ions are formed cannot be ruled out, the "photolysis" of a low molecular weight hydrocarbon such as ethane is proposed.

Such an experiment, while only a small part of what is obviously a very detailed study, would be of invaluable assistance in the interpretation of the results.

REFERENCES

(1) C. H. Townes, Biophys. J. 2, 325 (1962).

(2) J. Berkowitz and W. A. Chupka, J. Chem. Phys. 40, 2735 (1964).

(3) A. L. Shawlow, Science, 149, 13 (1965).

(4) R. H. Wiley and P. Veeravagu, J. Phys. Chem. 72, 2417 (1968).

(5) R. H. Wiley and E. Reich, presented at the American Chemical Society Meeting (Division of Physical Chemistry, Abstract 211), Atlantic City, September, 1968.

(6) A. L. Lane and W. Valance, private communication.

(7) J. G. Calvert and J. N. Pitts, Jr., Photochemistry (John Wiley & Sons, Inc., New York, 1966) p. 597.

(8) G. G. Meisels, "Formation and Reactions of Ions in Ethylene Radiolysis," in Ion-Molecule Reactions in the Gas Phase (American Chemical Society, Washington, D. C., 1966) p. 243.

(9) J. D. Baldeschwieler, Science, 159, 263 (1968).